SCUOLA DI DOTTORATO
UNIVERSITÀ DEGLI STUDI DI MILANO-BICOCCA

Department of Medicine and Surgery

PhD Program in Experimental Neuroscience - Cycle XXXIII

GENDER, AGE AND METABOLIC DYSFUNCTION AS RISK FACTOR FOR NEUROINFLAMMATORY DISEASES

PhD candidate: Murtaj Valentina

Registration number: 835088

Tutor: Prof. Moresco Rosa Maria

Coordinator: Prof. Moresco Rosa Maria

ACADEMIC YEAR 2019/2020

To my mother, my grandmother

and all the beautiful women in my family

ABSTRACT

The high prevalence of metabolic and cognitive disorders represents one of the major issues of health systems. Recent findings indicate that obesity may affect brain functions, however the effect of a high-fat diet (HFD) on the central nervous system is not fully understood. The aim of this study is the evaluation of the influence of HFD on neuroinflammation and regional brain function in a mouse model of Insulin Resistance (IR) focusing on sex-dependent differences induced by peripheral metabolic impairment.

C57BL/6J male and female mice were fed with standard chow or HFD (45%/60%) for 35 weeks. Animals were monitored weekly for body weight, haemato-chemical analysis (circulating glucose, total cholesterol, ALT, and AST), and glucose tolerance test (GTT). Positron Emission Tomography (PET) imaging studies were performed longitudinally using [^{18}F]-FDG and [^{18}F]-VC701 as radiotracers, to measure respectively glucose consumption and microglia/macrophages activation within the brain. Magnetic Resonance Imaging (MRI) and Magnetic Resonance Spectroscopy (MRS) was used to measure the effects of diet on hepatic lipid content and peri abdominal fat accumulation. Finally, post-mortem transcriptome analysis was applied to the anterior cortex to reveal potential modification in gene expression.

HFD induced a significant increase in body weight, glucose tolerance and haemato-chemical parameter in a sex dependent manner. HFD diet increased peri abdominal fat accumulation in male and lipid content in the liver as revealed at MR spectroscopy. This last effect was particularly evident in females. PET [^{18}F]-FDG showed a relative increase in glucose metabolism in the anterior region of the brain including the olfactory bulbs in both male and female mice while an increase in the anterior cortex was found in males mice fed with 60% HFD. Moreover, correlation analysis between glucose uptake and different metabolic biomarkers revealed, mainly in male mice, regional brain metabolic modifications associated with BMI values and haemato-chemical parameters. [^{18}F]-VC701-PET showed a general trend toward an increase of tracer uptake all over the brain after diet consumption in both male and female HFD mice. Anterior cortex transcriptome analysis showed a common de-regulation of genes related to nervous system development but also sex-specific modifications.

Our finding suggests that HFD induced obesity in adult mice causes a general metabolic impairment not confined in the periphery but involving also selected brain regions. The increased binding of the

activated microglia associated with TSPO radioligand suggests that obesity can induce a diffuse neuro-inflammatory reaction in mice's brains. PET imaging technique allowed to identify the presence of metabolic derangement and the neuro-inflammatory response of mice brain induced by HFD. This finding is relevant since our model reproduces the peripheral metabolic modification typical of IR and type 2 diabetes.

ABSTRACT (ITALIANO)

L'elevata prevalenza di disturbi metabolici e cognitivi rappresenta uno dei maggiori problemi della salute umana. Recenti scoperte indicano che l'obesità può influenzare le funzioni cerebrali, tuttavia l'effetto di una dieta ricca di grassi sul sistema nervoso centrale non è ancora completamente compreso. Lo scopo di questo studio è la valutazione dell'influenza della dieta grassa sulla neuro infiammazione e sulla funzione cerebrale regionale in un modello murino di insulino-resistenza, con particolare attenzione alle differenze dipendenti dal sesso.

I topi maschi e femmine C57BL/6J sono stati nutriti con dieta standard o dieta grassa (due tenori: 45% / 60% di grassi) per 35 settimane. Gli animali sono stati monitorati settimanalmente per analizzare le variazioni di peso corporeo, analisi ematochimiche (glucosio circolante, colesterolo totale, ALT e AST) e test di tolleranza al glucosio. Gli studi di imaging con tomografia a emissione di positroni (PET) sono stati eseguiti longitudinalmente utilizzando [^{18}F] -FDG e [^{18}F] -VC701 come radio-traccianti, per misurare rispettivamente il consumo di glucosio e l'attivazione di microglia / macrofagi all'interno del cervello. La risonanza magnetica (RM) e la spettroscopia a risonanza magnetica (SRM) sono state utilizzate per misurare gli effetti della dieta sul contenuto lipidico epatico e sull'accumulo di grasso peri addominale. Infine, l'analisi della trascrittomica post-mortem è stata applicata alla corteccia anteriore al fine di rivelare potenziali modifiche nell'espressione genica.

La dieta grassa introduce in modo significativo un aumento del peso corporeo, della tolleranza al glucosio e dei parametri ematochimici che variano in base al sesso. Anche l'accumulo di grasso peri addominale nel maschio e il contenuto di lipidi nel fegato, come rivelato alla spettroscopia RM, sono stati osservati in tale modello. Quest'ultimo effetto è stato particolarmente evidente nelle femmine. La PET [^{18}F]-FDG ha mostrato un aumento relativo del metabolismo del glucosio nella regione anteriore del cervello, inclusi i bulbi olfattivi sia nei topi maschi che in quelli femmine, mentre l'aumento osservato nella corteccia anteriore è stato riscontrato solamente nei topi maschi alimentati con il 60% di dieta grassa. Inoltre, l'analisi della correlazione tra l'assorbimento del glucosio cerebrale e i diversi biomarcatori metabolici ha rivelato, principalmente nei topi maschi, modificazioni metaboliche cerebrali regionali associate a valori di BMI e parametri ematochimici. Lo studio PET condotto con il tracciante [^{18}F]-VC701 ha mostrato una tendenza generale verso un aumento dell'assorbimento del tracciante in tutto il cervello dopo il consumo di dieta grassa nei topi

maschi e femmine. L'analisi della trascrittomica nella corteccia anteriore ha mostrato una comune de-regolazione dei geni associati allo sviluppo del sistema nervoso, ma anche modificazioni specifiche legate al sesso.

Il nostro studio suggerisce che l'obesità indotta da regime alimentare di dieta grassa nei topi adulti, causa un deterioramento metabolico generale non confinato alla periferia ma che coinvolge anche regioni cerebrali selezionate. L'aumento del segnale del tracciante per la proteina TSPO suggerisce che l'obesità può indurre una reazione neuro-infiammatoria diffusa nel cervello dei topi di entrambi i sessi. La tecnica di imaging PET è stata usata per identificare la presenza di squilibrio metabolico e risposta neuro-infiammatoria del cervello di topo sotto regime alimentare di dieta grassa. Questo dato è rilevante poiché il nostro modello riproduce le alterazioni metaboliche periferiche tipiche della sindrome di insulino resistenza e del diabete di tipo 2.

Abbreviation

AD-Alzheimer's disease

ADP-Adenosine Diphosphate

ALT- Alanine Aminotransferase

AMPK-Adenosine Monophosphate-activated Protein Kinase

AMY-Amygdala

AKT-Protein Kinase B

ANOVA- Analysis of Variance

ARC-Arcuate Nucleus

AST- Aspartate Aminotransferase

ATP-Adenosine Triphosphate

BBB-Blood Brain Barrier

BDNF-Brain Derived Neurotrophic Factor

BMI-Body Mass Index

BOLD-Blood-Oxygen Level Dependent

BS-Brainstem

CD-Cluster of Differentiation

CG-Cingulate Cortex

CNS-Central Nervous System

CRP-C-Reactive Protein

CRB-Cerebellum

CTX- Cortex

CVD-Cardiovascular Disease

DA-Dopamine

DAMP- Damage/Danger Associated Molecular Patterns

DAVID-Database for Annotation, Visualization, and Integrated Discovery

DEGs- Differentially Expressed Genes

dlPFC-dorsolateral Prefrontal Cortex

DM-Diabetes Mellitus

DNL-De Novo Lipogenesis

Era-Estrogen Receptor alpha

ER-Endoplasmic Reticulum

FAO-Fatty Acid Oxidation

FDG-Fluorodeoxyglucose

FFA-Free Fatty Acid

fMRI-Functional Magnetic Resonance Imaging

FS-Fat Suppression

FTO-Fat mass and obesity associated

GFAP-Glial Fibrillary Acid Protein

GLP-1-Glucagon-like peptide 1

GLUT-Glucose Transporter type

GO-Gene Ontology

GWAS- Genome-Wide Association Studies

HDL-High Density Lipoprotein

HFD-high fat diet

HIF-Hypoxia inducible transcription factor

HIPP-Hippocampus

HLC-Hepatic Lipid Content

HPA axis-Hypothalamic Pituitary Adrenal axis

H&E-Hematoxylin and Eosin

HYP-Hypothalamus

Iba-1-Ionized Calcium-Binding Adapter molecule 1

IFG-Inferior Frontal Gyrus

IFN-Interferon

IGF-1- Insulin Growth-Factor 1

IKKβ/NF-κB- Inhibitor of κB Kinase β/Nuclear Factor-κB

IL-1β-Interleukin 1 beta

IL-6- Interleukin 6

IL-4-Interleukin 4

IR-Insulin resistance

Jnk- c-Jun N-terminal Kinase

KEEG- Kyoto Encyclopaedia of Genes and Genomes

LDL-Low Density Lipoprotein

LPS-Lipopolysaccharide

MAPK-Mitogen Activated Protein

MCR-Melanocortin receptor

MetS- Metabolic Syndrome

MMe-Metabolic Macrophages

MRI- Magnetic Resonance Imaging

MRS-Magnetic Resonance Spectroscopy

NAc-Nucleus Accumbens

NAFLD-Non-Alcoholic Fatty Liver Disease

NASH-Nonalcoholic Steatohepatitis

NIRKO-Neuron Specific insulin receptor knockout

NFS-Non-Fat Suppression

NGF- Nerve Growth-Factor

OGTT- Oral Glucose Tolerance Test

OLF.B-Olfactory Bulb

OPC-Orbitofrontal Cortex

PAMP- Pathogen Associated Molecular Patterns

PCA-Principal Component Analysis

PCSK1- Prohormone Convertase 1

PFC-Prefrontal Cortex

PIK3- Phosphoinositide 3-Kinase

PET-Positron Emission Tomography

PM-Perfect Match

POMC- Proopiomelanocortin

PUFA-Polyunsaturated Fatty Acid

RIN-RNA Integrity Number

RMA-Robust Multichip Analysis

ROI-Region of Interest

RT-PCR-Real Time Polymerase Chain Reaction

SFA-Saturated Fatty Acids

SNP-Single Nucleotide Polymorphism

STD-Standard Diet

STR-Striatum

STZ-Streptozotocin

SUV-Standardized Uptake Value

TNF-α-Tumor Necrosis factor alpha

TLR-Toll Like Receptors

T2D-type 2 Diabetes

THA-Thalamus

TREM2- Triggering Receptor Expressed on Myeloid cells 2

TSPO-Translocator protein

VEGF- Vascular Endothelial Growth Factor

VLDL-Very Low-Density Lipoproteins

VTA-Ventral Tegmental Area

ZFD-Zucker Diabetic Fatty rats

List of figures

List of tables

CONTENTS

1. INTRODUCTION

1.1. Obesity and associated metabolic syndrome

According to the World Health Organization (WHO), obesity represents an emerging and critical health and social problem. It is linked with increased morbidity for cardiovascular disease, type 2 diabetes (T2D), certain forms of cancer and it has been associated with psychiatric and neurological disorders. Weight gain is associated with the so-called metabolic syndrome (MetS) characterized by Insulin Resistance (IR), hyperglycaemia, hyperinsulinemia, modification of immune cell metabolism and low-grade systemic inflammation affecting different organs (Klöting and Blüher, 2014; Cho et al., 2018).

Obesity arises when energy intake, principally stored as triglycerides, exceeds energy expenditure and diet, developmental stage, age, physical activity, and genes represent risk factors (Delrue and Michaud, 2004).

WHO criteria for MetS diagnosis required different markers including IR, hyperglycaemia, hypertension, high serum triglycerides, reduced serum high-density lipoprotein (HDL) cholesterol or microalbuminuria, body-mass index (BMI) and fasting serum insulin (Nilsson et al., 2019). Clinical criteria are reported in table 1, according to the US National Heart, Lung and Blood Institute and American Heart Association Consensus Statement (Chobanian et al., 2003). Among all components associated with MetS, lifestyle including unhealthy high palatable diet and poor physical activity play an important role in determining the worsening of the physiological features that leads to obesity (Blanquet et al., 2019).

Table 1 Clinical Diagnosis of Metabolic Syndrome

Risk Factors	**Defining Level**
Abdominal obesity, given as waist circumference	
○ Men	>102 cm
○ women	>88 cm
Triglycerides	150 mg/dL
HDL cholesterol	
○ men	>40 mg/dL
○ women	>50 mg/dL
Blood pressure	130/85 mm Hg
Fasting glucose	110 /dL

1.2. Pathophysiology of metabolic syndrome

The exact aetiology of MetS is multifactorial, including inflammation, lipotoxicity, and modified metabolism, oxidative and cellular stress. Intra-abdominal fat accumulation associated with increase in waist circumference acts as pivotal components in pathology. In fact, excessive fat accumulation leads to adipose tissue dysfunction that, in turns, leads to impairments in adipokines release and increased free fatty acid (FFA) release (Sherling et al., 2017).

1.3. Insulin resistance

MetS is also called insulin resistance syndrome, which has been defined as a defect in insulin actions resulting in hyperinsulinemia, characterized by the disturbed maintenance of proper eu-glycaemia (Eckel et al., 2005).

Insulin hormone is secreted by the β cells of the pancreatic islet of Langerhans, and acts via glycoprotein receptors located in the main target tissues of the liver, skeletal muscle, and adipocytes. Insulin binds to its extracellular insulin receptor, transmitting a signal across the plasma membrane and activating the tyrosine kinase domain of the intracellular subunit. Protein kinase B, also called AKT is a key downstream effector of this process. It phosphorylates and inactivates glycogen synthase kinase 3, allowing glycogen synthesis and finally promoting glucose storage as glycogen (Saltiel and Kahn, 2001; Lizcano and Alessi, 2002).

Insulin-dependent glucose cellular uptake is stimulated by glucose transporter protein type 4 (GLUT4) migration to the cell surface, in which glucose can be either stored as glycogen or metabolized to produce adenosine triphosphate (ATP). GLUT4 is highly expressed in skeletal muscle and adipose tissue. Insulin inhibits gluconeogenesis and glycogenolysis and stimulates genetic transcription of enzymes involved in glycolytic and fatty acid synthetic pathways (Bryant et al., 2002).

Obesity and adipose deposition favour the development of IR, release of FFA and lipotoxicity underlying insulin desensitization, systemic inflammation, mitochondrial dysfunction and oxidative stress (Sripetchwandee et al., 2018).

Insulin activity mediates the hepatic gluconeogenesis maintaining normal glucose metabolism. HFD promotes insulin resistance and this results in the suppression of liver gluconeogenesis and hyperglycaemia (Eckel et al., 2005; Hatting et al., 2018).

Several studies suggest that insulin influences not only peripheral organs such as liver, muscle, and adipose tissue but also the brain. In the brain, glucose transport depends on GLUT3 highly expressed by neurons, and GLUT1 mainly present in glial and endothelial cells. Nevertheless, high levels of GLUT4 has been described in the hippocampus where insulin may exert its activity (McEwen and Reagan, 2004; McNay and Pearson-Leary, 2020). Moreover, it has been shown that insulin is involved in the regulation of feeding behaviour and monitoring energy storage, acting through insulin receptors localized on neurons. Indeed, knockout of the neuron specific insulin receptor (NIRKO mouse) promotes diet-induced obesity and triggers IR and hypertriglyceridemia (Brüning et al., 2000). On the contrary, other studies showed that insulin modulates cognitive functions in the hippocampal region, reward and in general memory functions. For this reason, insulin nasal delivery is currently used in clinical trials as potential therapy for early Alzheimer's disease (AD) (Craft et al., 2012). Moreover, Glucagon-like peptide 1 (GLP-1) an Incretin hormone, which acts as a glucose metabolism controller has been shown to alleviate learning and memory deficit in AD and improve motor and cognitive function in Parkinson's disease. Its neuroprotective effect is probably related to the glucose metabolism and insulin sensitivity (Bae and Song, 2017; Kim et al., 2017).

1.4. Adipose tissue dysfunctions and systemic inflammation

Adipose tissue is specialized in storage of lipid droplets mainly as triacylglycerols that are released as fatty acids and glycerol in case of lipolysis. Adipocytes are also involved in the synthesis of fatty acid from the excessive circulating glucose mechanism called de novo lipogenesis (DNL). Enragement of lipid droplet occurs upon excessive availability of nutrients resulting in larger fat depots and body weight gain (Vegiopoulos et al., 2017).

Two main mechanism arises in the expansion of adipose tissue: hypertrophy, which is the increase in size of pre-existing adipocyte and hyperplasia, a new adipocyte formation derived from the differentiation of resident precursors preadipocytes cells and contribute to adipose tissue expansion (Ghaben and Scherer, 2019). Dysfunctional adipocyte fails to respond to the extracellular signals, like insulin which provides differentiation signal to preadipocytes maturation, and acquire a pro-inflammatory phenotype leading to fibrosis and necrosis enhancing inflammatory response and macrophages infiltrations (Melo et al., 2019). Chronic, low-grade inflammation is one of the hallmarks of diet induced MetS. Preadipocytes adopt a macrophage-like inflammatory phenotype with increased expression of proinflammatory cytokines and decreased adipogenic capacity in

response to inflammatory stimuli (Isakson et al., 2009). In addition, immune cells play an important role in phenotypic alterations in obesity. In lean insulin-sensitive adipose tissue, anti-inflammatory regulatory T-cells and M2 alternatively activated macrophages contribute to tissue repair processes and resolution of inflammation. Contrary, adipose tissue expansion is associated with a decrease in $CD4^+$ helper and T-cells, infiltration of $CD8^+$ cytotoxic T-cells and macrophage polarization towards an M1-proinflammatory phenotype. The production of mediators such as tumor necrosis factor (TNF)-α, interleukin (IL)-6 lead to insulin resistance and MetS. Moreover, hypoxia facilitate the proinflammatory responses of obese adipose tissue leading to the activation of hypoxia-inducible transcription factors (HIF)-1, which in turn trigger the expression of key angiogenic factors vascular endothelial growth factor (VEGF) contributing further to angiogenesis and adipocyte pathological state (Ouchi et al., 2011; Cildir et al., 2013; Briançon-Marjollet et al., 2014). Inflammatory and deleterious mechanisms of dysfunctional adipose tissue is shown in figure 1.

Figure 1

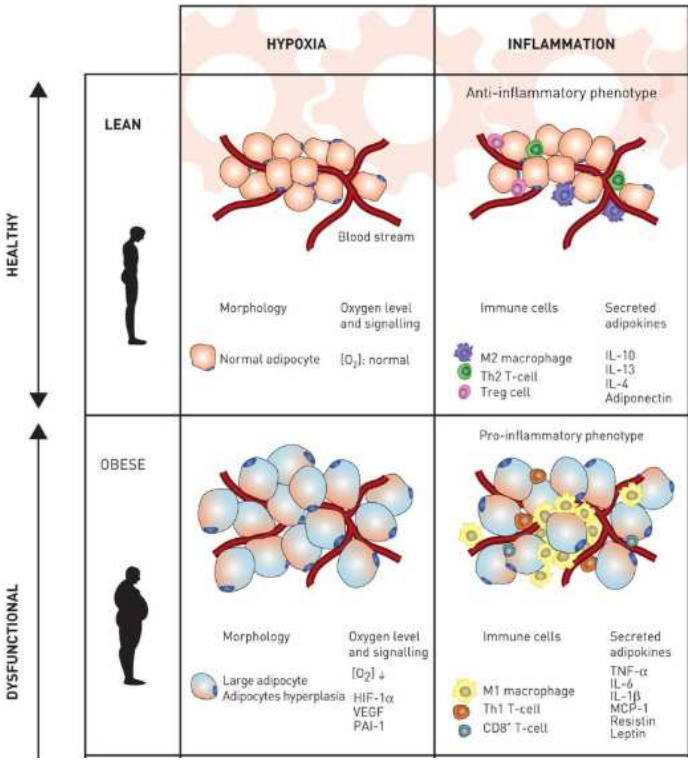

Figure 1 Inflammatory mechanism occurring during metabolic syndrome. Adapted from (Ryan et al., 2019)

1.5. High fat diet and free fatty acid

Obesity is driven by an unpaired balance between energy intake and consumption. Modification in macronutrients composition of the food contributes to developing MetS. Indeed, HFDs, high sugar and processed food are responsible for the development of obesity that favour MetS and T2D (van Dam and Seidell, 2007). As stated before, increased FFA and proinflammatory factors promote IR, reduce glucose uptake in peripheral tissue thanks to a deregulation of glucose homeostasis and decrease of GLUT4 translocation to plasma membrane, typical of obesity (Greenberg and Obin, 2006). In recently published preclinical data, researchers found that excessive fat content represents the only responsible factor involved in increased energy intake and adiposity, after comparing 29 types of diet in different mouse strains (Hu et al., 2018). FFA includes mono-, poly-, unsaturated and saturated subtypes of fatty acid that differ for length chain or presence/number of double bonds. Diets enriched with saturated fatty acids (SFAs) lead to a greater accumulation of fat and lower satiety in comparison with diets enriched in polyunsaturated fatty acids (PUFAs). Moreover, higher levels of circulating SFA increase inflammatory gene expression in adipose tissue reducing insulin sensitivity and increasing in triglyceride content (Rosqvist et al., 2014).

Literature evidence suggests that modern Western diet which is characterized by reduced intake of n-3 PUFA, high saturated FAs and n-6 PUFA consumption, may contribute to mechanism linking diet and mental health (O'Neil et al., 2014). HFD and sedentary lifestyle represents an important AD risk factor, due to its association with high FFAs plasma level, IR and chronic low-grade inflammation which is common in neurodegenerative diseases. In fact, AD and risk to develop dementia or impaired cognitive function has been linked to the higher body SFAs level and cholesterol intake sustained with low level of PUFAs (De Felice, 2013). Furthermore, it has been shown that cognitive functions outcomes are improved in aged populations that follow diet regimen enriched with PUFAs (Ortega et al., 1997; Barberger-Gateau et al., 2011). In figure 2 is reported the % change in total mortality in relation with increase in different types of FFA.

Figure 2

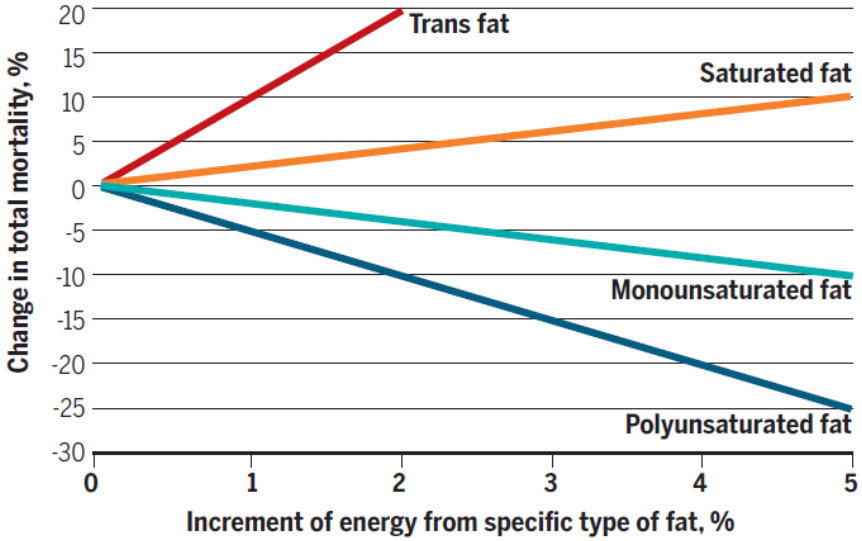

Figure 2 Change in total mortality (%) in relation to increased intake of different types of free fatty acid. Data are based on 126,233 men and women followed for up to 32 years, as described in (Wang et al., 2016).

In the case of a "low carbohydrate and high fat diet" total energy is reduced for carbohydrate and increased for fat (≥40% of energy). This regimen reached in fat induce typical MetS characteristics including IR and risk to develop T2D. As consequence, postprandial glucose blood concentration and insulin increase, glucagon secretion decreases, and metabolism did not shift on fat oxidation, whit final outcomes of increasing oxidative stress and inflammatory response, while low-fat diets may favourably influence body weight, adiposity, and glycaemic homeostasis (Cahill, 2006; Newman and Verdin, 2017). Central adiposity, high circulating concentrations of triglycerides, low levels of HDL cholesterol, high blood pressure, glucose intolerance, fatty and chronic inflammation comprises a constellation of clinical risk factors associated with insulin resistance that predispose to diabetes and cardiovascular diseases (Lee and Sanders, 2012).

It should be mentioned that, not all diets or caloric sources have similar metabolic effects on different populations. From literature, no evidence reported the best specific carbohydrate-to-fat ratio. However, attention to diet quality in terms of processed food, reduction of sugar and fat excess and refined grains could help to prevent MetS (Gardner et al., 2018).

1.6. How does metabolic syndrome affect the human body?

1.6.1. Liver disease

Particularly critical organ which is strongly associated with the various feature of MetS involve liver, as it regulates body metabolism, orchestrates the synthesis of new fatty acids, export them with subsequent redistribution to other tissues, as well as their utilization as energy substrates in which lipids play a major role in hepatic insulin resistance and hyperglycaemia (Perry et al., 2014). The most common liver disease in Western countries include non-alcoholic fatty liver disease (NAFLD), a hepatic manifestation of MetS, frequently associated with obesity, dyslipidaemia, IR and T2D. It is the major chronic liver diseases, with a prevalence of 30% in the general population, 42-70% in diabetic patients and 80% amongst obese people (Van Herck et al., 2017; Weinstein et al., 2018). NAFLD hallmarks include hepatic steatosis, inflammation, hepatocyte damage and fibrosis demonstrating the potential progressive nature of the pathology. In fact, such disease also included non-alcoholic steatohepatitis (NASH) in which hepatocyte results damaged with higher presence of fibrosis as extracellular matrix deposits. Moreover, fibrosis predicts the outcomes of liver-related mortality depending on its stage (Tsochatzis et al., 2009). The dysfunction of one or more liver physiological pathways may contribute to the retention of fat within the liver parenchyma and develop NAFLD. Hepatic fat accumulation is caused by an imbalance between lipid acquisition and disposal controlled through different pathways including uptake of circulating lipids, DNL, fatty acid oxidation (FAO), and export of lipids in very low-density lipoproteins (VLDL) (Ipsen et al., 2018).
The gold standard of the disease diagnosis is represented by liver biopsy, which can define NAFLD, even though it is an invasive and expensive procedure. Nowadays, new non-invasive screening tools have been proposed and relevance is attributable to multi-echo magnetic resonance (MR) imaging, which measures the amount of liver mobile proton density, due to fat deposition. It represents, together with MR spectroscopy, the most promising and sensitive non-invasive technique to assess liver fat accumulation in patients at risk of developing NAFLD pathology (Mancini et al., 2018).

Figure 3

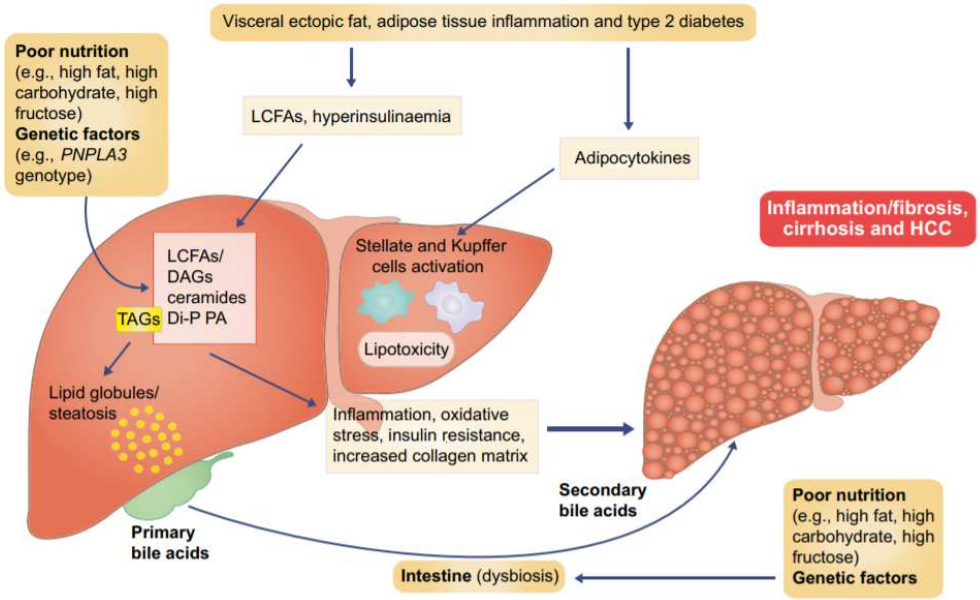

Figure 3 Metabolic syndrome affecting the liver. The influences of fat accumulation, adipose tissue inflammation, type 2 diabetes, and diet to promote the development of progressive liver disease in NAFLD. Adapted from (Byrne and Targher, 2015).

1.6.2. Cardiovascular disease

Heart and related cardiovascular diseases (CVD) are highly associated with obesity, as the major risk to develop hypertension, heart failure and coronary heart disease (Kachur et al., 2017).

As stated before, adipose tissue plays a substantial role in the pathogenesis and complication of obesity, in which adipocytes act as endocrine organs increasing leptin level, hormone that controls food intake and energy expenditure. Moreover, C-reactive protein (CRP) is associated with leptin resistance with the results of increased appetite and energy metabolism. Additionally, an increase in inflammatory response occurred in association with IR, obesity, and CVD (Enriori et al., 2006; Lavie et al., 2008; Litwin, 2008). Pathophysiology of CVD induced under obese condition is due to the increases in total blood volume and cardiac output with a consequence of higher arterial pressure (Messerli et al., 1982). BMI, as MetS hallmark, is also associated with the risk of CVD development such as angina, myocardial infarction, heart failure and death (Petrie et al., 2018). In addition, IR plays a role in endothelial dysfunction, in which phosphoinositide 3-kinase (PI3K) pathways activated by insulin promote the nitric oxide production, which induces vasodilatation and has anti-proliferative effect on vascular smooth muscle cells. On the other hand, insulin also activates Ras-mitogen activated protein kinase (MAPK) pathways, promoting vasoconstriction and proliferation of vascular smooth muscle cells. In IR condition, this PI3K pathway results impaired and

the imbalance of the signalling of these pathways leads to endothelial dysfunction, a key factor of the pathogenesis of CDV (Schulman and Zhou, 2009).

1.6.3. Central Nervous System and neuroinflammatory responses

MetS is characterized by presence of multiple morbidities and multi-organ damages. As previously stated, accumulating evidence links obesity to the central nervous system (CNS) dysfunctions favouring neurological disorders other than CVD. Obesity-driven dysfunction is associated with visceral adiposity, excessive dietary fat consumption and modified hypothalamic control of energy homeostasis (O'Brien et al., 2017). In fact, hypothalamic inflammation denotes an early CNS response to the high level of FFA concentration with microgliosis and astrocytosis and damage of myelin integrity microstructure. Microglial cells have been proposed as sensor cells of the diet that induce hypothalamic inflammation. Its toll like receptor 4 (TLR4) recognize long-chain fatty acid and promote cytokines production such as TNF-α, interleukin 1β (IL1-β), and IL-6, stress pathways endoplasmic reticulum (ER) activation, and subsequent activation of the c-Jun N-terminal kinase (Jnk) and inhibitor of κB kinase β/nuclear factor-κB (IKKβ/NF-κB). This results in activation of pro-inflammatory pathways followed by hypothalamic gliosis which could compromise the neural circuitry governing satiety control (De Souza et al., 2005; Milanski et al., 2009). Neuroinflammatory responses on hypothalamic arcuate nucleus level is described in the figure 4. ER and oxidative stress are induced by multiple intracellular responses subsequently induced by overnutrition, which increase mitochondrial respiration, leading to elevated cytosolic protein synthesis and unfolded protein response. In addition, this persistent ER stress results in proinflammatory activation of NF-κB and JNK signalling (Hotamisligil, 2010).

Figure 4

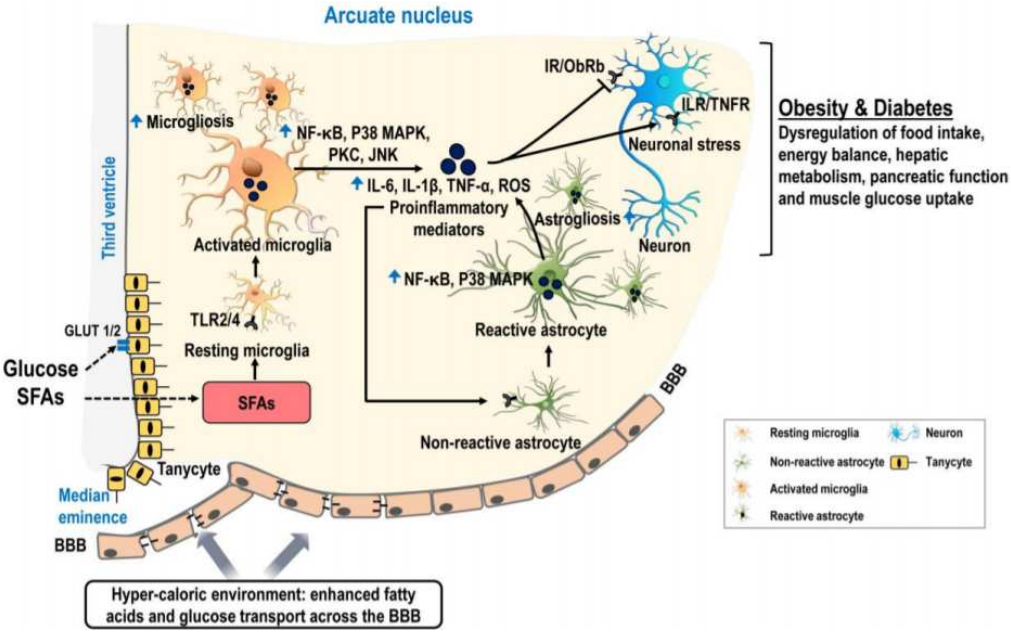

Figure 4 Neuroinflammatory responses on hypothalamic arcuate nucleus. Glial cells in the hypothalamus act together to induce hypothalamic inflammation and metabolic dysregulation in the pathophysiology of obesity and diabetes. BBB, blood–brain barrier; GLUT1/2, glucose transporter 1/2; IL-1β, interleukin-1β; IL-6, interleukin 6; ILR, interleukin receptor; IR, insulin receptor; MAPK, mitogen-activated protein kinase; NF-κB, nuclear factor-kappa B; ObRb, leptin receptor b; ROS, reactive oxygen species; SFA, saturated fatty acid; TLR2/4, toll-like receptor 2/4; TNFR, tumor necrosis factor receptor; TNF-α, tumor necrosis factor-α Adapted from (Rahman et al., 2018).

Under HFD, Blood Brain barrier (BBB) increased its permeability, due to a reactive glial cytokines production and circulating adipokines that leads to hippocampal injury. From the HFD regimen, FFA and triglycerides are also responsible for the hippocampal damage and impaired functions. Indeed, increased BBB permeability allows proinflammatory factors to reach the hippocampal region and initiate a vicious circle of neuroinflammation, promoting subsequent neurodegeneration (Lindqvist et al., 2006). In fact, unrestricted entry of chemokines, cytokines, FFA, triglyceride and immune cells potentiate hippocampal damage and atrophy, finally leading to cognitive dysfunction. Moreover, several studies reported modification in grey matter volume and cortical thickness in obese population (Buckman et al., 2014; Nota et al., 2020).

HFD accompanied by FFA entry into the brain, provokes important effects on brain myeloid cells, resulting in drastic metabolic consequences, in which microglial cells play a pivotal role. Microglia, a specialized macrophages-like cell in the CNS derived from yolk sac, are considered immune cells with important inflammatory response. This glial cell is also vital for the proper shaping of the brain, homeostasis surveillance and function as a neuroprotective component of the innate immune

response (Bachiller et al., 2018). In vitro studies, utilizing palmitate as a stimulus, have been used for the elucidation of the molecular pathways involved in the microglial response to HFD, as long chain SFA are involved in HFD induced hypothalamic inflammation which involve canonical and non-canonical mechanism. As stated before, TLRs is the largely immune signalling response as pattern recognition receptors which activates pro-inflammatory transcription upon recognition of specific pathogen- and damage/danger- associated molecular patterns (PAMPs; DAMPs), even if SFA are not considered as PAMPs or DAMPs (Takeuchi and Akira, 2010). Indeed, it has been shown that SFAs treatment in vitro induce the NLRP3-inflammasome activation and TLR4 activity triggering immune cell activation (Lee et al., 2001; Huang et al., 2012).

Lipid metabolism may play a central role in macrophages phenotype and its function in obesity, especially for the data related to immunometabolism. In fact, macrophages acquire a specific phenotype that is remarkably different from the classical pro-inflammatory M1 phenotype (stimulated by lipopolysaccharide (LPS)) or the anti-inflammatory M2 phenotype (activated by interleukin IL-4). SFA, insulin or glucose stimulation of macrophages lead to so-called “metabolic macrophages” (MMe), a specific phenotype associated with the cytokines production but with different sets of surface molecules. Lipid metabolism programs seem to play an essential role in determining the macrophages polarization and activation for the MMe. It has been observed that SFA are essential agent of MMe activation upon production of IL-1β cytokines, whose expression surface markers has been isolated from MMe obese mice (Kratz et al., 2014). From the mechanistic point of view, SFA inserts into phospholipid layer after internalization accompanied by changes in the membrane saturation degree that result in altered lipid composition leading to ER stress with final IL-1β production (Robblee et al., 2016).

1.6.4. Obesity affect cognitive functions

Synaptic plasticity is one of the key brain functions that results impaired in obesity. IR accompanied by the inflammatory state is associated with the increased risk of cognitive decline, impaired spatial learning, and mood disorder, increasing signs of depression and anxiety-like behaviour in which specific brain region has a role in performing specific cognitive tasks (Whitmer et al., 2008; McNay et al., 2010). Literature showed that the brain could be susceptible to chronic inflammation under consumption in HFD regimen leading to changes in neuronal connectivity with consequent cognitive alterations (Vinuesa et al., 2019). Moreover, different preclinical studies reported impaired and

reduced learning and memory functions in rodents under HFD (Tan and Norhaizan, 2019). Other studies demonstrate that HFD mice treated only for one day showed rapid reduction in episodic memory tasks, demonstrating cognitive dysfunction as an early event (McLean et al., 2018). IR seems to be the effector of HFD-induced cognitive decline. In fact, animals study reported altered lipid composition and energy metabolism due to the hypercaloric diet which leads to elevation in fasting glucose, impaired spatial learning ability and synaptic plasticity (Stranahan et al., 2008). Similar results were also observed in human study in which Western diets, enriched with refined sugar and saturated fatty acid, induced memory impairment in healthy subjects (Jena et al., 2018). Again, cognitive decline seems to be an early event upon HFD regimen. Holloway and colleagues demonstrate that 7 days upon HFD reduced attention and reaction time in sedentary adult males (Holloway et al., 2011). Mittal et al., reported poor cognitive performance caused by high triglyceride level and Okereke et al., found that increased uptake of SFA lead to impaired prospective memory, cognitive function including memory speed and flexibility in young adults (Okereke et al., 2012; Mittal and Katare, 2016). Other important brain functions impaired by the HFD regimen regard the regulation of energy homeostasis, energy expenditure and food intake. These functions are regulated by hypothalamic region, especially in appetite and satiety signalling although other brain regions are involved. The hypothalamus is responsible for plenty of physiological functions, including water balance, metabolism and feeding, in the memory aspects of cognition, learning, and attention (Najam et al., 2019). Once again, microglial activation is widely described, and it is induced by the elevated presence of SFA leading to alterations in hypothalamic neurons, at the earliest stage of obesity. In figure 5 is reported the comparison of glial fibrillary acid protein (GFAP-astrocyte activation)/ionized calcium-binding adapter molecule 1 (IBA-1-microgliosis) staining between normal diet (Chow) and HFD in male rodents fed for 7 days. It is well noticeable the greater amount of activated glial cells that reflect neuroinflammation into the hypothalamic region (Thaler et al., 2012).

Figure 5

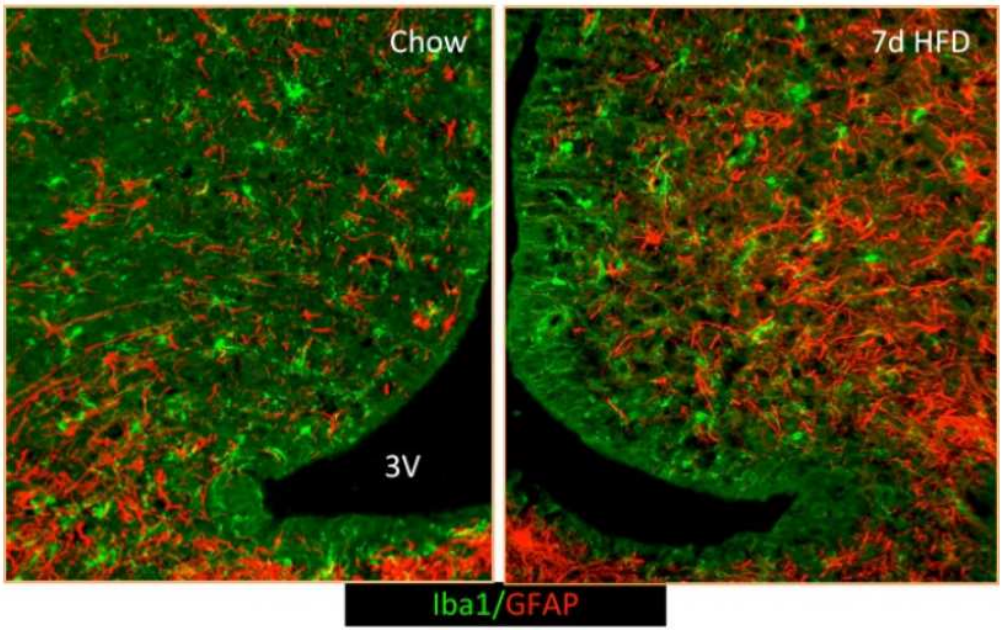

Figure 5 Hypothalamic inflammation in HFD in male rodents. Inflammatory activation of surrounding astrocytes (GFAP) and microglia (IBA-1). Adopted from (Thaler et al., 2012)

As for hypothalamus, also other brain regions such as the hippocampus, prefrontal cortex, limbic system could be subject to inflammatory pathways that could further conduct to cognitive deficit, due to continued metabolic disturbances. It should also be considered a brain mechanism of hedonic control of appetite and food intake which is related to the cognitive, reward and emotional factors. Cortico-limbic brain regions including the nucleus accumbens, striatal caudate nucleus, hippocampus, amygdala and orbitofrontal cortex are key components of the hedonic pathway involved in the food consumption (Lee and Dixon, 2017).

Brain functions are influenced also by the effect of HFD on gut microbiota. New evidence has linked HFD with alteration in the intestinal microbiota and in the regulation of the gut-brain axis, that may influence the mood and cognitive function associated with obesity (Portune et al., 2016). In brief, the gut-brain axis is characterized by a complex bidirectional communication system between the gut and the brain, mediated by immunological, hormonal, and neural signals. The system is composed by the autonomous and enteric nervous system that connects the gut to the brain via vagal and spinal fibres in which hypothalamic pituitary adrenal (HPA)-axis, immune system and neurotransmission play important roles. Moreover, HPA-axis is part of the limbic system that regulates stress response, immune function, emotion and mood (Tsigos and Chrousos, 2002; Foster et al., 2017). Gut infection can affect CNS leading to anxiety like behaviour in mice as demonstrated

by studies with LPS. It is known that chronic infection with *Trichuris muris*, decreased brain-derived neurotrophic factor (BDNF) expression in the hippocampus, accompanied by a mild increase of TNF-α and interferon (IFN) as well as kynurenine in plasma, leading to anxiety (Bercik et al., 2010). Stress is also prevailing in obese subject, as literature showed that there is positive association between stress, weight gain and adiposity, especially in individuals with higher value of BMI thus reinforcing modification of eating behaviour (Torres and Nowson, 2007). In figure 6 is reported the gut-brain axis mechanism that is linked to cognitive and mood dysfunction in an obesity state.

Summarizing, intestinal microbiota alteration within all the bidirectional communication involved may contribute to rise in neuroinflammation and dysregulation of CNS system and homeostasis, finally influencing mental impairment and cognitive dysfunction (Agustí et al., 2018).

Figure 6

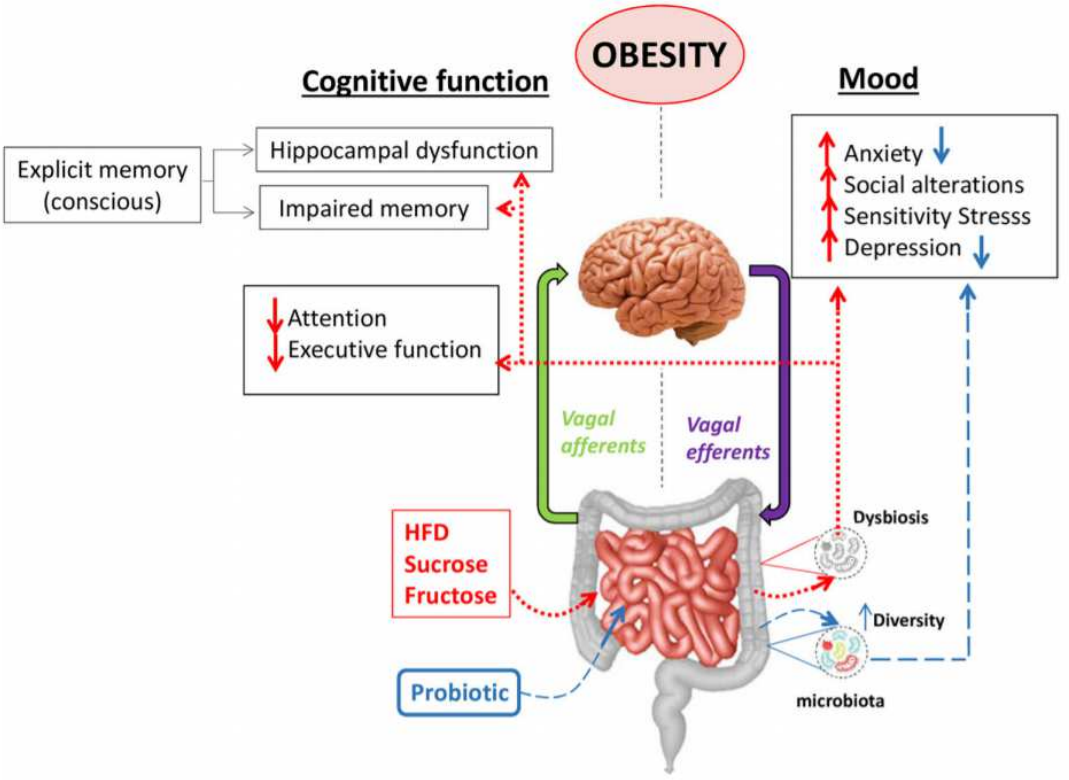

Figure 6 Neurological consequences of obesity Increased caloric intake and decreased energy expenditure result in a net energy overload, leading to adipose tissue expansion (hyperplasia and hypertrophy). Sustained caloric excess in visceral adipose tissue activates resident macrophages, contributing to adipose tissue dysfunction and metabolic inflammation. From (Agustí et al., 2018)

1.7. Neuroimaging approach to study brain metabolism

Obesity and MetS are associated with brain damage, thereby, over the last decades, brain functional imaging techniques have been widely used to investigate neural mechanisms underlying behavioural and cognitive processes in such pathologies. The two main techniques used include MRI and PET imaging (Guzzardi and Iozzo, 2019).

The application of a magnetic field is on the base of canonical MRI sequences, in which radiofrequency pulse results in the alignment of nuclear spins (hydrogen nuclei in water) in the human body tissue under examination. Spins then return in the original orientation, generate a signal that is detected by a coil placed around the tissue of interest, and produce a final image, depending on the spin time relaxation. Using tissue water protons, MRI can produce high-resolution images of tissue anatomy and metabolic information can be obtained to visualize changes in perfusion or in blood oxygenation, for example in the brain (Raichle, 2001). In fact, functional MRI (fMRI) is an indirect measure of brain activity obtained through different magnetic properties of oxygenated and deoxygenated haemoglobin, called blood-oxygen- level dependent contrast (BOLD). This particular sequence of fMRI performed during resting state, allows to measure intrinsic brain activity and to reconstruct neural network and connectivity in absence of particular sensory or cognitive stimuli (Amaro and Barker, 2006). Magnetic Resonance Spectroscopy (MRS) is additional useful modalities to detect tissue metabolism by recording tissue defined voxel making in relation to spatial information with spectral information. 1H-NMR spectra are the most used modalities that could provide a cellular metabolism profile at a particular time point (Gadian and Radda, 1981).

Positron emission tomography (PET) is a nuclear imaging minimally invasive technique using short-lived positron emitting radioisotopes to label molecules of interest (e.g., specific receptors, metabolic substrates, perfusion markers), to directly measure a biochemical process in individual organs or regions of interest. The radiotracer is administered to the subject and after certain time of uptake, PET exam is performed in which emitted positrons annihilate when combined with an electron in the body tissue, generating two 511 keV photons in opposite directions, which are collected by detectors arranged around the area of interest. Each parallel couple of photons is used to generate the image and then processed, to obtain the final image using a different algorithm of reconstruction. The radiolabelled glucose analogue [^{18}F]-FDG is the most commonly used PET tracer

to quantify regional brain glucose metabolism, which reflects neural activity (Iozzo et al., 2012). The figure 7 recapitulate the two main neuroimaging techniques used to study metabolic and structural changes within the obese brain.

Figure 7

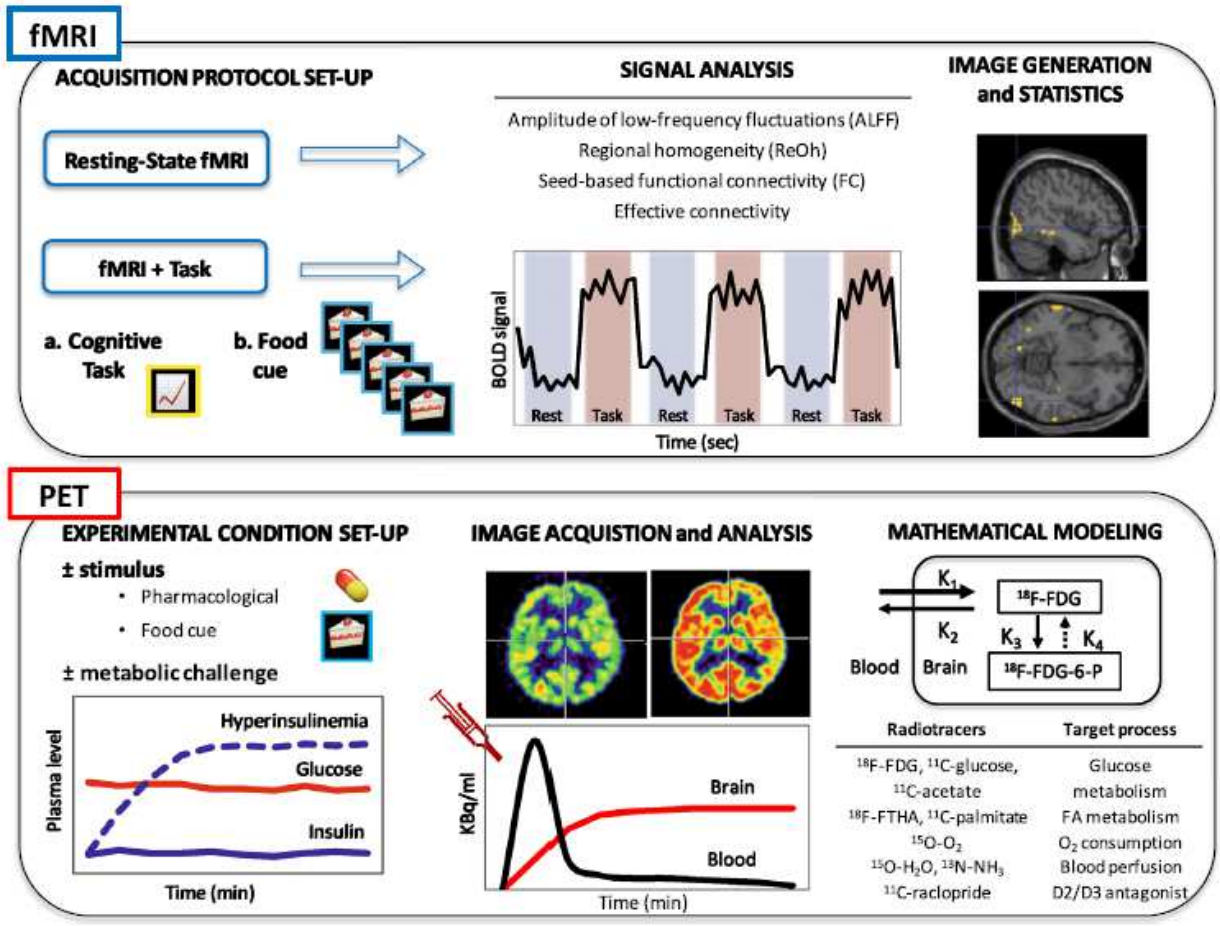

Figure 7 Neuroimaging techniques used for brain evaluation in metabolic syndrome and obesity state Adapted from (Guzzardi and Iozzo, 2019)

The main energy substrate for the brain is represented by glucose. Glucose metabolism contributes not only for regional brain function but also to regulate peripheral glucose level, feeding behaviour, rewarding system and appetite control. As glucose uptake mainly reflects cerebral energy requirement, aging, neurodegenerative processes and systemic metabolism influence brain metabolism at regional levels (Liistro et al., 2010; Hirvonen et al., 2011). Studies reported changes in brain metabolism under obese condition both in human and in rodent. High cerebral metabolic

rates occur in obese and glucose-intolerant subjects, during fasted or homeostatic stimuli, in region involved in food reward (Wang et al., 2004, 2009a; Guzzardi et al., 2018). Summarizing, PET imaging using glucose analogue as radiotracer is useful to study either in humans or in animal models the modulation and alteration of glucose brain metabolism in MetS and obesity.

Several brain function can be measured by using in vivo PET Imaging, applying different selected radiopharmaceuticals addressed to specific target (metabolism, hypoxia, inflammation, specific ligands, or receptors). Neuroinflammation are, among those, an important marker for several brain pathology, such as PD, AD, brain injury, ischemia, cognitive dysfunction, psychiatric disorders, Multiple Sclerosis and others (Cavaliere et al., 2020).

The 18 kDa translocator protein (TSPO) are expressed in brain parenchyma located in outer mitochondrial membrane of several cell type and results altered during neuroinflammatory process, thus has been used for the in vivo PET Imaging in which many tracers have been developed. Activated astrocyte and microglial cell seems to be the main target (Tournier et al., 2020).

Nowadays in obesity, TSPO PET has been applied to study brown and white adipose tissue in clinical and preclinical studies, in which thermoneutral condition and mitochondrial expression has been addressed (Ran et al., 2018, 28; Hartimath et al., 2019). Only one study involves the TSPO PET to brain inflammation in a mouse model of AD associated with HFD condition. Published data from Barron A.M. et all., reported that combination of obesity with β-amyloid infusion led to neuroinflammatory response and several inflammatory markers upregulation, in which poor learning and memory performance results as outcome (Barron et al., 2016). Altogether, literature indicate that more studies are necessary to explore brain inflammatory response during obesity and MetS. In vivo TSPO PET tool could be helpful to investigate neuroinflammatory response in both preclinical and clinical obese condition also related to other brain pathology.

1.8. Brain circuits involved in obesity

Brain studies performed using neuroimaging techniques have provided several evidence in brain circuits involvement and modulation during MetS and obesity state. Four main circuits that are reported in figure 8 have been proposed (Volkow et al., 2008, 2011).

- reward-saliency
- motivation-drive
- learning-memory
- inhibitory-control circuit

Figure 8

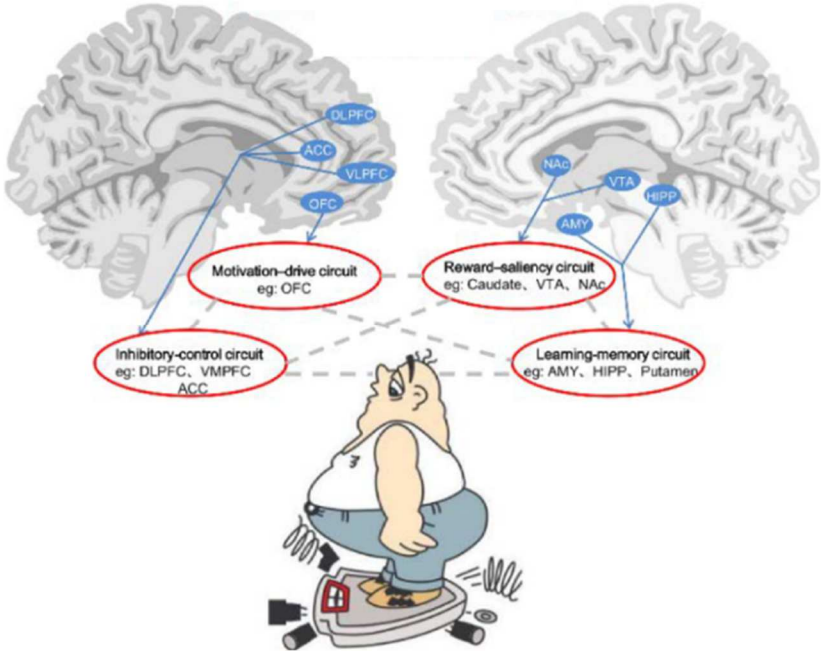

Figure 8 Brain circuitry of obesity Adopted from (Zhang et al., 2014).

Reward-saliency circuit

Reward circuits in obese subject induces compensatory overeating to reach sufficient reward, in which high palatable food consumption activate several brain regions encoding pleasantness to food. These regions include midbrain, insula, dorsal striatum, subcallosal cingulate and prefrontal cortex (PFC). Food pleasantness and satiety diminishes when chronic exposure to high palatable food occurs (Lenard and Berthoud, 2008). In this mechanism, dopamine (DA) neurotransmitters play a crucial role as involved in reward processing, motivation and positive behaviour reinforcement (Abizaid et al., 2006; Wang et al., 2009). Moreover, DA projection from ventral tegmental area (VTA) target striatal Nucleus Accumbens (NAc) for the feeding reinforcement encoding, influencing food ingestion and rating meal pleasantness based on the magnitude of the DA release (Salamone et al., 1997; Rothemund et al., 2007). Indeed, study from literature reported a decreased DA receptors

availability in the striatal region in morbidly obese subject that showed a higher level of metabolism in the somatosensory region, which is known to directly impact DA activity (Bassareo and Di Chiara, 1999; Schwartz et al., 2000). Authors have also shown a correlation between dopamine D_2 receptors availability and BMI value in which lower levels of dopamine receptors were correlated with high BMI (> 40) (Haltia et al., 2007). Summarizing, D2 receptors availability is crucial for the risk of overeating in obese individuals.

Motivation-drive circuit

Motivation and food consumption implicate activity of more frontal regions including orbitofrontal cortex (OFC), PFC and cingulate cortex (CG). In obese patients, it was observed an increase in activation of prefrontal region upon meal exposure compared to lean individuals (Gautier et al., 2000; Rolls, 2004). As OFC a region essential for modulation of flexible control of behaviour such as behavioural inhibition, self-control and emotional regulation, it has been shown its involvement in eating disorders and bulimia nervosa (Szalay et al., 2012; Rudebeck and Murray, 2014). Several evidence support also the role of OFC in behavioural compulsion to obtain reward even when it disappears, like drug addiction, in which the subject cannot stop abuse even when drug is no longer a pleasure (Carnell et al., 2012).

Learning and memory circuit

Memory are particularly important in obese brain as it can produce an intense desire for food and trigger addictive behaviour. Memory system is implied in several mechanism that include conditioned incentive learning (mediated in part by the NAc and the amygdala (AMY)), habit learning (mediated in part by the striatal caudate and putamen nuclei), and declarative memory (mediated in part by the hippocampus (HIPP)). All these circuits seem to be altered upon drug or food addiction (White, 1996). Furthermore, overeating generates reinforcing and motivational salience in absence of food, and it is a consequence of conditioned learning induced by exaggerated stimulation. Learning habits concern a sequence of behaviour that are automatic in response to an appropriate stimulus while declarative memory in the ability to learn to bring back episodic information in relationship to food intake (Volkow et al., 2003). Abnormalities in emotional and memory circuits implicating AMY and HIPP has been found in obese individuals when compared to

lean subject in which brain response has been investigated using multimodal neuroimaging techniques. Studies from obese patients using fMRI, reported delayed inhibition in the hypothalamus response, which is correlated to the impaired satiety signal generated from homeostatic region. At the same time, higher signals are enhanced from emotion/memory and sensory/motor region in these subjects (Carnell et al., 2012). The table 2 above reports the implicated brain region during MetS and obesity with the inevitable disrupted functions.

Table 2 Disrupted brain functions implicated in addiction and obesity (modified from (Volkow and O'Brien, 2007).

Implicated brain region	Disrupted functions
prefrontal cortex	Impaired inhibitory control
anterior cingulate gyrus	to drug intake in addiction
lateral orbitofrontal cortex	to food intake in obesity
nucleus accumbens	Enhanced reward
ventral pallidum	to drugs in addiction
hypothalamus	to food in obesity
amygdala	Conditioning/habits
hippocampus	to drugs and drug cues in addiction
dorsal striatum	to food and food cues in obesity
medial orbitofrontal cortex	Enhanced motivation/drive
mesencephalic dopamine nuclei	to consume drugs in addiction
dorsal striatum	to consume food in obesity
amygdala	Emotional reactivity
ventral cingulate gyrus	

Inhibitory-control circuit

Inhibitory-control circuits act in controlling executive function, goal-directed behaviour, and response inhibition whose main region involved is represented by frontal area including dorsolateral PFC (dlPFC) and inferior frontal gyrus (IFG). This circuit seems to be significantly activated in subjects that desire to consume high palatable unhealthy food. The prefrontal region involved, in healthy individuals, acts as inhibition of the desire to consume food. This mechanism is implied in the self-control of choosing between healthy and unhealthy food (Hare et al., 2009; Hollmann et al., 2012). Briefly, the brain's top-down control system modulates the subjective evaluation of food and individual difference in food intake regulation may be a consequence of structural difference or connectivity in such areas. Indeed, obese people has been associated with decreased activity in prefrontal region (Le et al., 2006, 2007). dlPFC are also involved in the reward pathways as they integrate information and act as inhibitory control of DA release from reward signalling (NAc and

ventral tegmental area (VTA)), leading to overconsumption of palatable food (Bhurosy and Jeewon, 2014).

Despite these four main brain circuits, as previously stated, there are other regions involved in feeding behaviour including the hypothalamus, which regulates appetite and energy homeostasis, though the activity of the arcuate nucleus (ARC) (Myers and Olson, 2012). Hormonal and nutritional metabolic signals are integrated in the ARC from the periphery that generate a feedback response. These circuits are also associated with the mesolimbic reward circuit, thus to the VTA and NAc which control the hedonic aspect of food intake, as stated before (Roh and Kim, 2016). The hyperactive association between hypothalamus and cortico-striatal region seems to derange the homeostatic control of food intake. Furthermore, it has been shown that obese individuals showed increase in PFC activation upon fasting state and lower activation in the hypothalamus when asked to choose between healthy and unhealthy food (Harding et al., 2018).

To conclude, recent publication indicates a progress in understanding obesity from neural circuits point of view. Published results indicate that high palatable food consumption is a major cause in obesity, which causes dysregulation of different brain circuit mechanisms that regulate food intake and consumption including also feeding behaviour. This topic pushed researchers to apply a functional connectivity approach based on neuroimaging techniques, to study the perturbation in brain region activity during obesity in order to understand how to apply new therapeutic strategies based on specific region activity or a network (Gluck et al., 2017; Clarke et al., 2018).

1.9. Preclinical research of metabolic syndrome: animal models

Most of the preclinical research on obesity and MetS are performed on small rodents, such as mice and rats. There are several animal models based on mutation or manipulation of different genes involved in obesity or IR, or that include animals exposed to an obesogenic environment as high fat diet consumptions. The leptin-deficient ob/ob mouse, db/db mouse and the Zucker rat represent the most common animal model of diabetes and obesity. Several animal models have been described (Lutz and Woods, 2012). Animal models based on deficiency in the leptin receptor pathway include Lep^{ob}/Lep^{ob} mouse, a spontaneous mutation leading to a marked obesity state in mice. Leptin is mainly synthetized in white adipocytes and its secretion reflects the triglyceride storage. Leptin deficiency has also been observed in rare cases of human obesity (O'Rahilly, 2009). The diabetic mouse (db/db) is characterized by more marked hyperglycaemia, hyperphagia and

reduced energy expenditure leading to marked early-onset obesity (Chua et al., 1996). The obese Zucker (fa/fa or 'fatty' rat) and the Koletsky rat carry the extracellular domain of the leptin receptor mutated forms. Glucose tolerance is impaired, and fertility is reduced. Zucker Diabetic Fatty (ZDF) rats were derived from a sub-strain of obese Zucker fatty rats that displayed early dysregulation of glucose metabolism. ZDF rats develop early diabetes in concomitant with HFD regimen, and the main feature regard the alteration of expression of the glucose transporter GLUT4 in muscle (Zierath et al., 1998). Animal models in which there is a deficit downstream of the brain leptin receptor include POMC-KO mouse. Proopiomelanocortin (POMC) expressing neuron are direct leptin target in the hypothalamic ARC and it is a precursor of α-melanocyte-stimulating hormone, a potential neuropeptide that reduces eating and increases energy expenditure by melanocortin 3 and 4 receptor (MCR) activation in hypothalamus. Transgenic mice KO for POMC shows overeating and marked obesity. MCR4 KO models exhibit energy homeostasis dysregulation, hyperphagia and morbid obesity as consequence of disrupted control of food intake (Huszar et al., 1997; Challis et al., 2004). Another genetically induced model of obesity comprises the GLUT4 glucose transporter subtypes in which animals develop a massive increase in the number of fat cells. Melanin concentrating hormone mouse model in which eating, and body weight is increased but obesity is developed late in life and other models (Lutz and Woods, 2012).

Another method to induce obesity and MetS is the exposure to a high fat or high-energy diet. Sprague Dawley rats and C57Bl/6J mice share many characteristics with the common form of human obesity, when exposed to HFD (Patterson et al., 2010). Cafeteria-diet induced obesity include varied palatable food which mimic human Western diet. Consequences include hyperphagia and overeating due to the increased average meal size and frequency (Pérez et al., 1999). HFD exposure often leads to obesity. Specifically, diet is reached in high caloric density that contribute to higher total energy intake which rapidly reduce insulin and leptin action leading to IR and typical MetS hallmark. Fat composition in which saturated FA has the most deleterious role are responsible for the development of obesity related diseases. This type of diet acts on intracellular signalling pathways of hypothalamic neurons and in other brain areas (Hariri and Thibault, 2010; Clegg et al., 2011).

Finally, there are also surgical or chemical models of obesity. Surgical methods to induce obesity are obtained upon lesions of hypothalamic ventromedial nucleus, paraventricular and arcuate

nucleus. This leads to adiposity, increase in body weight, higher circulating insulin and reduced glucagon and IR (Nemeroff et al., 1978; King, 2006).

Finally, the chemical model includes streptozotocin (STZ) administration which has been used to study Diabetes Mellitus (DM) in rodents. STZ is applied to induce toxic effects on insulin produced by pancreatic cells which enter in the cell through GLUT2 glucose transporter and causes DNA alkylation and eventual pancreatic β cell death contributing to cytotoxicity (Deeds et al., 2011).

1.10. Gene regulation of complex disease

The aetiology of obesity and MetS is multifactorial, including intricate interaction between genetic, neuroendocrine regulation, environmental factors such as sedentarism or unhealthy dietary habits. In the last 50 years, an increase in prevalence of common obesity (multifactorial) has occurred while a small proportion of obesity cases result from monogenic alteration. The common obesity is probably due to the interplay between environmental changes and individual genetic susceptibility. Strong genetic impact in common obesity has been establish from evidence reported in studies including derived from family, twin and adoption in ethnically diverse population involving BMI confirming genetic role (Allison et al., 1996; Pietiläinen et al., 1999; Katzmarzyk et al., 2000; Koeppen-Schomerus et al., 2001; Fesinmeyer et al., 2013). Single gene mutation induces monogenic form of obesity including syndromic type which is accompanied by cognitive delay, dysmorphic features, and organ-specific abnormalities or non-syndromic (Kaur et al., 2017). Prader-Willi syndrome is the well characterized obesity syndrome form due to the imprinting defect in the region on chromosome 15q11-13. Other forms include Fragile X syndrome, Bardet-Biedl syndrome and Albright's hereditary osteodystrophy (Bonnefond et al., 2013; Pigeyre et al., 2016).

Regarding non-syndromic monogenic form of obesity, genes are mainly involved in the regulation of energy haemostasis mediated by leptin-melanocortin pathway (Ingelsson and McCarthy, 2018). Leptin stimulates POMC neurons which produces alpha-melanocyte-stimulating hormone (a-MSH) binding to MC4R that act on energy balance and mutation occurring in MC4R result in increased food intake and body mass (Farooqi et al., 2003). SIM1, a transcription factor involved in the development of the paraventricular and supraoptic nuclei of the hypothalamus seems to be involved in severe obesity in humans when loss of function mutation occurs as it is involved in signalling of MC4R (Goshu et al., 2002).

Finally, obesity accompanied by glucocorticoid deficiency, hypogonadotropic hypogonadism, and postprandial hypoglycaemia occurs when mutation occurred when enzymes such as prohormone convertase 1 (PCSK1) processed melanocortin peptides (Pritchard et al., 2002).

Genome-Wide Association Studies (GWAS) contribute to relevant new information about genetics of obesity. The interplay between multiple loci occurs in common multifactorial obesity, a polygenic form and GWAS has led to the discovery of novel genetic factors associated with obesity, e.g., an association of single nucleotide polymorphisms (SNPs) in the fat mass and obesity associated (FTO) gene region with BMI and risk of obesity was identified in populations from different countries, making FTO the first locus associated with adiposity (Frayling et al., 2007). Recent finding has reported several obesities carry genes involved in neural circuits of appetite and satiety regulation (BDNF, MC4R, NEGR) insulin secretion and action (TCF7L2, IRS1), adipogenesis and energy and lipid metabolism (FTO, RPTOR, MAP2K5) (Kilpeläinen et al., 2011; Locke et al., 2015). Epigenetic, as a gene regulatory system, is also involved in the mechanism of obesity in which several modifications have been shown including DNA methylation (Wu Ct and Morris, 2001; Keller et al., 2017). Four mechanisms of epigenetics contribution have been proposed: as downstream effectors of environmental signals; through abnormal global epigenetic state driving obesogenic expression patterns; through facilitating developmental programming and through transgenerational epigenetic inheritance (Youngson and Morris, 2013). Diet and nutrition seem to be able to influence genome inducing epigenetic reprogramming. In fact, several food components produce epigenetic changes in health individuals and response to diet. Epigenetic mechanism is influenced by bioactive food composition that can inhibit enzymes that catalyse DNA methylation or histone modification altering the availability of substrate, necessary for enzymatic activity (Haggarty, 2013). Summarizing, GWAS within epigenetic DNA methylation study could provide a potential novel genotype-epigenotype interaction within disease-associated loci in order to deeply understand common complex diseases like obesity and MetS (Bell et al., 2010).

While several studies from genetic point of view have been performed regarding the main organs affected by the MetS and obesity, only few studies focused on brain functions and brain transcripts of specific regions including hippocampus, hypothalamus and prefrontal cortex. Preclinical research using female mice treated with Western Diet reported 2.412 differentially expressed hippocampal genes with the majority involving in the regulation of cell signalling proteins and their transcription

factors, differential expression of miRNAs, and a lesser proportion of non-protein coding RNAs when compared to control mice. Another study demonstrates that obesity-induced microglia activation is associated with hippocampal-dependent learning and memory deficit, decreased synaptic density, and dysregulation of genes involved in synaptic plasticity. Transcriptomic investigation performed on Prader-Willi syndrome revealed an upregulated gene involved in the hunger signal and downregulation of POMC neurons activated by feeding. Finally, the prefrontal cortex was also studied in a preclinical model of obesity as associated with higher cognitive functions. Results obtained from HFD adolescence male mice showed marked impairment of prefrontal cognitive activity including epigenetic processes involving microRNAs (Bochukova et al., 2018; Labouesse et al., 2018; Nuthikattu et al., 2019; Valcarcel-Ares et al., 2019; Yang et al., 2019).

To conclude, further brain analysis at transcriptional and epigenetic level are needed to elucidate different mechanisms and pathways involved in obesity and related diseases

1.11. Sex difference during insulin resistance and metabolic syndrome

Nowadays, unfortunately, there is limited comprehension of the molecular and physiological peculiarity of sex difference in several disease. An inadequate number of preclinical and clinical publication include both, males, and females into the research investigation, which could be of useful to facilitate precision medicine and sex-specific therapeutic approach. Males represent the “appropriate and preferred” gender, as females, due to the modulated sex hormones during fertile period, are belief to generate high variability data (Della Torre and Maggi, 2017).

In MetS and obesity, male and female results differentially affected showing sex-specific hallmarks, often age dependent. In fact, females are more susceptible to gain weight in the post-menopausal period accompanied by secondary complications. On the other hand, neonatal overnutrition cause, in pre-pubertal male and female, an excessive gain weight with no hypothalamic inflammation while in later adulthood, only male exhibit hypothalamic inflammation accompanied by gliosis (Argente-Arizón et al., 2018). Indeed, puberty is a period that includes development, changes in body composition and fat distribution, influenced also by hormones (Loomba-Albrecht and Styne, 2009; Rogol, 2010). In both, male and female, sexual hormones influence the MetS mechanism leading to obesity and related pathology in different ways. Androgens are highly expressed in male while lower in females and regulate plenty of mechanisms associated with the risk to develop obesity. On the

contrary, estrogen is highly expressed in women during the fertile period of life until menopause, and lower expressed in males. In fact, energy metabolism and body composition are regulated upon balance between these two hormones. In females, body weight and visceral fat deposition increase upon high androgens level, while in male a negative correlation between obesity degree, waist circumference, increased BMI and testosterone available has been found (Kelly and Jones, 2015; Kautzky-Willer et al., 2016).

In both humans and rodents, male, appear to be more susceptible and more prone to develop MetS and obesity than premenopausal females. Among several MetS hallmark, body fat distribution and composition, control of metabolism and low-grade inflammatory state may result different according to the sex and age at organ level, both in humans and in rodents (Freire-Regatillo et al., 2020).

Figure 9

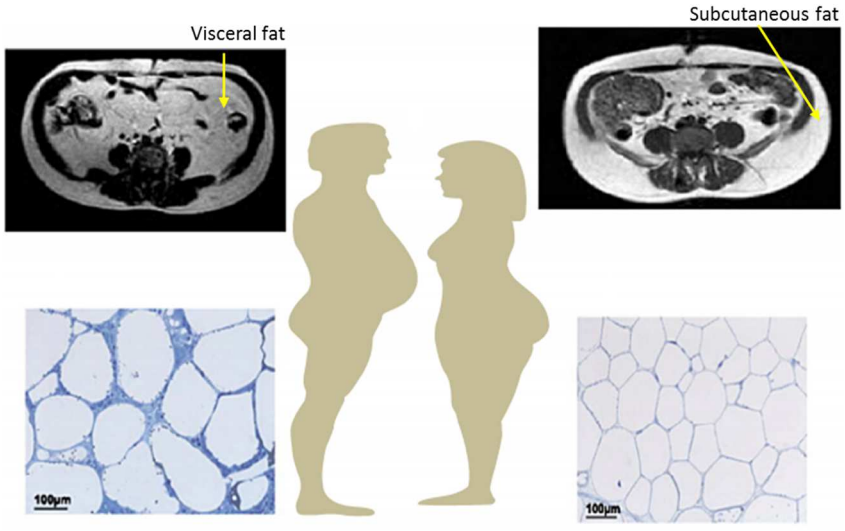

Figure 9 Sex difference in body fat distribution. *Adopted from* (Palmer and Clegg, 2015)

Adipose tissue contributes to metabolic homeostasis as well as represent triglyceride storage, in which cells secrete a variety of molecules involved in different signalling pathways. Male and female exhibit differences in the amount, and distribution of fat cells. In particular, pre-menopausal females have higher total body fat content with a tendency to distribute it more subcutaneously while man fat deposition is mainly visceral. Subcutaneous accumulation of fat in females represents an energetic strategy but also to protect from MetS. After menopause, fat deposition shifts from subcutaneous to visceral, as normally occurs in man, accompanied by more susceptibility to risk in

MetS and obesity related disorder (Palmer and Clegg, 2015). This sex differences during obesity are largely linked to hormones. In females, estrogen regulates fatty acid metabolism, fat distribution, appetite and energy expenditure. In post-menopausal women, with a decrease in circulating hormone, this protective effect of estrogen disappears (Gambacciani et al., 1997; Clegg et al., 2007). Preclinical research is in line with these results showing increased energy expenditure in rodents upon activation of estrogen receptors in the hypothalamus (Xu et al., 2011). In these findings, estrogen receptors α (ERa) are implicated as modulated fat distribution between the depots. In CNS, estrogen receptors are expressed in the ventromedial nucleus of hypothalamus and are involved in the decision of adipose tissue distribution. Studies demonstrate that disruption of ERa in such hypothalamic nuclei lead to visceral fat accumulation in females and that CNS administration of estrogens as therapy radically reduces visceral adiposity. Indeed, other research showed that depletion of ERa from adipocyte increases adiposity in the visceral depot in both male and female mice, indicating that estrogen modulates fat distribution (Lindberg et al., 2002).

Concluding, fertile female mice seems to be protected from obesity and MetS as show more neural projection to subcutaneous depot and a higher number of ERa receptors expressing neuron projection compared to male which projection goes mainly to visceral one (Xu et al., 2011; Adler et al., 2012).

An interesting sex dimorphism is present in liver metabolism. It has been demonstrated that during short fasting conditions, male mice activate lipogenic and gluconeogenic pathways to preserve amino acid reserves while female mice use amino acids as fuel font maintaining hepatic lipid synthesis (Della Torre et al., 2018). The risk to develop liver diseases such as NAFLD has been shown to be higher in men while in women it has become more common after menopause, suggesting a strong influence and protection of estrogen hormones (Park et al., 2006; Long et al., 2018). This has been confirmed by a multicentre clinical trial showing that NAFLD and hepatic fibrosis are associated with a worse outcome with a higher incidence of hepatocellular carcinoma during aging and in male (Vilar-Gomez et al., 2018). Premenopausal woman with sever hepatocyte injury and inflammation showed less fibrosis compared to man and to postmenopausal subjects (Yang et al., 2017). Moreover, as ERs are highly expressed during pre-menopause, it has been demonstrated that females regulate liver function and the nutrition availability to preserve fertility (Maggi and Della Torre, 2018).

Insulin resistance, one of MetS hallmark, has been shown to be present in both sexes during obesity and T2D, however in general in women insulin sensitivity is higher as well as the development of resistance in case of obesity (Nuutila et al., 1995; Tura et al., 2018). Increased insulin secretion and sensitivity in women could be related to the GLP-1. In fact, in normal conditions, woman show a 20% increase in serum GLP-1 at OGTT test compared with man, but this response disappear in prediabetes state or in T2D patient with no sex dependent effect (Færch et al., 2015).

Finally, sex differences were also found in the inflammatory reaction that occur in MetS and obesity both in periphery (e.g. adipose tissue and liver) and brain (e.g. hypothalamus). Adipose tissue dysfunction is characterized by high leptin production, low adiponectin production, cellular hypoxia, accumulation of non-esterified fatty acids in adipocytes, and deposition of excess extracellular matrix components like collagens and elastin which promote immune response (Khan et al., 2009; Divoux et al., 2010). Gender dimorphism is determined by two factors, sex hormones as stated before and X-chromosome genes modulation which favour female to have stronger immune system. In fact, X-chromosome dependent differences in innate immune systems lead to modification of several genes including these for TLR7 and TRL8. In females such genes are strongly expressed and only occasionally lead them more susceptible to some auto-immune diseases (Berghöfer et al., 2006; Pisitkun et al., 2006). Anti-inflammatory effects are exerted also by estradiol. Indeed, this hormone can reduce the production of IL-6, IL-1β and TNF-α by macrophages (Kramer et al., 2004).

As stated, also in brain the inflammatory reaction present in MetS and obesity is sex dependent. In fact, preclinical research focused on the hypothalamus, indicates sex difference within microglial activation, macrophages response and in cytokines production. Such differences were found more pronounced in male HFD mice rather than in females which shows higher levels of the anti-inflammatory IL-10 cytokines (Lainez et al., 2018). Sex dimorphism in response to HFD regards also cognitive function and synaptic activity. Indeed, impairment of learning and cognitive function has been shown in different preclinical models of obesity indicating male as more vulnerable to learning and synaptic plasticity impairment. One hypothesis is that this higher vulnerability is associated with a worst IR present in obese male mice. In fact, insulin has a positive role in maintaining synaptic plasticity and memory (Park, 2001; Stockhorst et al., 2004; Martin et al., 2008). This is also supported

by the effect of intranasal administration of insulin that is able to improve cognition in early AD patients (Reger et al., 2008).

Overall, male appear to be more vulnerable to develop MetS and obesity due to the higher prevalence of increased body weight, metabolic alteration, increased visceral adiposity, pronounced immune response and brain deficits such as learning and synaptic impairment upon HFD regimen or wrong lifestyle. On the contrary, females seem to be protected both by hormones such as estrogen and by X-chromosomes genes mechanism during premenopausal lifetime. However, data on the brain are limited and mainly focused on the hypothalamus.

2. AIM

Aged and demented population represent the highly relevance for delirium appearance. Neuro-inflammation involved in aging is one of the most supported by the literature. Microglial cells are activated by local and systemic inflammation and become primed (hyper-responsive) to small stimuli with aging, which can potentially cause damage and neuronal death. When an acute inflammatory stimulation occurs peripherally in a vulnerable individual, microglial cells become over activated and inflammatory mediators overexpressed in the CNS. There are also several risk factors that could facilitate neurodegeneration development, including gender, lifestyle, and presence of genetic polymorphism. Obese state is associated with chronic-low grade inflammation in which exposure to free fatty acids initiates inflammatory signalling leading to immune cell infiltration contributing to inflammation state.

In this 3 year of PhD Program in Experimental Neuroscience, I focused my attention on sex difference involved in neuroinflammatory response during aging and in metabolic syndrome. Aging mechanism underlying neuroinflammatory response has been investigated during the first year and has been published as the original article in *Frontiers in Aging Neuroscience* (Murtaj et al., 2019). This study showed sex and age dependent differences in brain neuroinflammatory response to a LPS peripheral challenge as revealed by microglial and astrocyte activation, cytokines, and microglia regulator levels. The published study is annexed to the thesis (in annex 1).

Here I present a second potential risk factor for brain health and neuroinflammation that is represented by obesity. As for the LPS challenge, the studies were conducted in both male and female mice. Sex difference of metabolic syndrome were evaluated upon prolonged HFD intake on the brain and periphery to understand the effect of enhanced caloric intake on brain biology. To this aim, we characterized mouse model of HFD induces obesity using longitudinal multimodal imaging approach including MRI and PET with selected radioligands for neuroinflammation measuring microglial/macrophages activation and glucose metabolism measuring regional brain function and connectivity. To associate the effect on the brain with the severity of metabolic impairment, PET findings were correlated with the haemato-chemical profile of HDF and normal fed mice.

3. MATERIALS AND METHODS

3.1. Animals and diet

Five weeks old, male and female C57Bl/6J mice were purchased from Charles River. Animals were maintained and handled in compliance with our institutional guidelines for the care and use of experimental animals (IACUC) and the national law for animals used in research (Prot. N. 6B2B3.44 D.lsg. 116/1992 and N. 29/2018-PR D.lsg. 26/2014). Mice were housed in the San Raffaele Hospital animal facility, maintained in a 12/12-hour light/dark cycle with access ad libitum to food and water. Following one week of acclimation, mice were randomly assigned to one of the following diet regimens: *Standard Diet* (STD), containing 10% of calories derived from fat (D12450B, Research Diets Inc); *45% High Fat Diet* (45HFD), containing 45% of calories derived from fat (D12451, Research Diets Inc.) and *60% High Fat Diet* (60HFD), containing 60% of calories derived from fat (D12492, Research Inc.). Specific diet composition is reported in table 3. This diet was selected based on the low tenor of cholesterol content in which fatty acids are mainly composed of lard that contain less non saturated fatty acid than butter.

Table 3 High Fat Diet and Standard diet composition

FAT	%	% saturated	% monounsaturated	% polyunsaturated	main ingredient
STD	10%	23%	30%	47%	wheat
45HFD	45%	31%	36%	33%	lard
60HFD	60%	32%	36%	32%	lard

3.2. Experimental design

A total number of 132 mice were used in this study (72 male and 60 female mice). Separate animal groups were dedicated to experiments that investigate different biological questions. First imaging pilot experiments were performed using 6 male mice per group considering only STD and 45HFD for a shorter period (8 weeks) to standardize the methods, a second experiments were performed using 15 male and 15 female mice (5 per group per diet, STD, 45HFD and 60HFD) in which Optical Imaging were done in order to investigate potential systemic inflammation. Data from these experiments were not reported due to not relevant results obtained.

From the 30 males and 30 females dedicated to longitudinal PET study, 8 mice per diet/sex performed [^{18}F]-FDG PET acquisition at 7 and 12 weeks from diet while 4 mice performed acquisition at 31 weeks. Some animals were excluded due to the death. [^{18}F]-VC701 PET study was performed on 6 mice per diet and sex for the 7 and 12 weeks as time point while lately, 3 mice per diet/sex performed imaging study at 31 weeks from diet. From 15 males and 15 females dedicated to MRI studies, 4 mice per diet/sex performed the study. All sample size used in the Imaging study were reported in the table 4. Mice of each experimental task were monitored weekly for body weight and BMI were calculated measuring the body length from the tip of the muzzle to the attachment of the tail and expressed as g/cm^2. Caloric and energy intake were also calculated, measuring food every day, in terms of gram/day and kcal/day. At the end of the imaging study, all animals were sacrificed for further investigation (blood chemistry, immunohistochemistry, transcriptomic and western blot analysis). In specific at sacrifice:

-**Serum level** (from blood sample)

14 weeks: 5 mice per diet/gender from MRI groups + 5 mice per diet/gender from PET groups

35 weeks: 5 mice per diet/gender from PET groups

-**Immunohistochemistry** (liver sample)

14 weeks: 5 mice per diet/gender from MRI groups

-**Transcriptomic** (half-anterior cortex)

35 weeks: 5 mice per diet/gender from PET groups

-**Western Blot** (half-anterior cortex)

35 weeks: 5 mice per diet/gender from PET groups

Table 4 All sample size of each imaging study

	Experimental group	PET Imaging						MRI Imaging	
		FDG PET			VC701 PET				
		7 weeks	12weeks	31 weeks	7 weeks	12weeks	31 weeks	4 weeks	12weeks
Male	60% HFD	8	8	3	6	6	3	4	4
	45% HFD	8	8	4	6	6	3	4	4
	STD	8	7	4	6	6	3	4	4
Female	60% HFD	8	8	4	6	6	3	4	4
	45% HFD	8	8	4	6	6	3	4	4
	STD	8	8	4	6	6	3	4	4

Figure 10

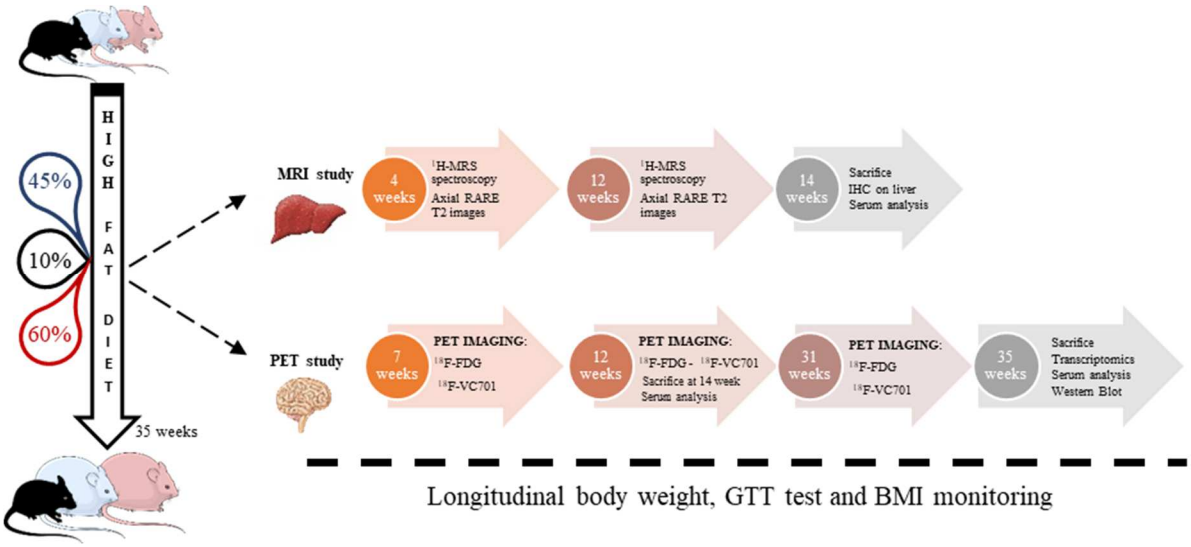

Figure 10 Experiment design of the study Male and female mice undergo two type of HFD for 35 weeks and separate animal group performed imaging study using PET and MRI techniques

3.3. Metabolic evaluation

Mice were monitored for basal glycaemia and for Glucose Tolerance Test (GTT). Basal glycaemia was measured in fasted animals in which blood glucose concentrations were collected from the tail vein with a glucometer (StatStrip Xpress®2, Nova Biomedical, MA, USA). For GTT test, mice were injected intraperitoneally with a glucose solution (2g/kg/bw, dissolved in saline) in the morning, after basal glycaemia measurement. Blood glucose level, collected from the tail vein, was taken through glucometer at 0, 15, 30, 45, 60 and 120 min after glucose injection. Both measurements, basal glycaemia and GTT test were performed longitudinally at 4, 7, 12 and 31 weeks of high fat diet regimen. MRI groups of animals (5 per diet and gender) performed two time points of metabolic evaluation, at 4 and 7 weeks after diet regimen while PET group of animals (5 per diet and gender) performed metabolic evaluation at 12 and 31 weeks of diet.

3.4. Blood sampling and blood chemistry analysis

From each animal blood samples were collected and put into the Eppendorf tubes. The blood samples were clotted for 30 min after blood sampling; afterwards, the tubes were centrifuged at recommended speed (1300 RCF) for 10 min. The obtained serum was collected and stored at -80°C for further analysis. On serum samples, the concentrations of total cholesterol (mg/dL), high density lipoprotein (HDL, mg/ dL), low density lipoprotein (LDL, mg/ dL), aspartate aminotransferase (AST;

UI/L), alanine aminotransferase (ALT; UI/L), albumin (g/dL) were determined by LAM Service (Laboratory of Murine Analyses) in San Raffaele Scientific Institute, which uses certified instruments and kits, performed analyses. During each session, internal quality control was done for each single test. Serum levels of different components were analysed by a spectrophotometry system (ILab ARIES, Werfen Instrumentation Laboratory S.p.A., Milan, IT) according to the manufacturer's protocol. Data from serum were collected at two different time points, 14 and 35 weeks of diet. After 14 weeks of diet, serum was collected at sacrifice from the MRI experimental group (n=30; 15 male and 15 females, 5 per type of diet) and from the PET Imaging experimental group that undergo on diet regimen until 14 weeks (n=30, 15 male and 15 females, 5 per type of diet). At the late time point (35 weeks of diet), serum was collected only from the second PET imaging experimental group (n=30, 15 male and 15 females, 5 per type of diet). Same sample was discarded from the analysis due to haemolysis. Sample size analysed at each time point for each diet group of study is reported on table 5.

Table 5 Sample size per group of diet analysed for blood chemistry analysis

Serum collection	**MRI study**			**PET study**			**Sample size**
Male	STD	45HFD	60HFD	STD	45HFD	60HFD	Total n per group
14 weeks	5	5	5	5	5	5	10/group
35 weeks				5	5	5	5/group
Female	STD	45HFD	60HFD	STD	45HFD	60HFD	Total n per group
14 weeks	5	5	5	5	5	5	10/group
35 weeks				5	5	5	5/group

3.5. MRI study

Magnetic Resonance Imaging (MRI) were performed on a dedicated group of animals that undergo on diet regimen for 14 weeks (n=30, 15 males and 15 females, 4 per diet group) in which liver region were investigated to obtain information regarding hepatic steatosis and fibrosis. Animals performed a two-time point of analysis, an early time point at 4 weeks and a late one at 12 weeks of diet regimen, based on the literature articles (Soares et al., 2018).

All MRI studies were performed in a 7T preclinical scanner (Bruker, BioSpec 70/30 USR, Paravision 6.0.1), equipped with 450/675 mTm gradients (slew-rate: 3400-4500T/m/s; rise time 140µs) and a circular polarized mouse body volume coil with an inner diameter of 40 mm. All mice underwent

imaging under inhalational anaesthesia (Isoflurane, 3% for induction and 2% for maintenance in 2L/minute oxygen); lying prone on a dedicate temperature control apparatus to prevent hypothermia, having breathing rate and body temperature continuously monitored (SA Instruments, Inc. Stony Brook, NT, USA).

Sample sizes that undergo MRI study were 24 animals, 12 male and 12 females, 4 per group of diet. Two studies were performed. First, axial 2D High Resolution (HR) Rapid Acquisition with Relaxation Enhancement (RARE) T2 images was obtained. Images with fat suppression (FS) or without fat suppression (NFS) (repetition time (TS)=3000 ms; echo time (TE)=40ms; rare factors=8: field of view (FOV)=230 x 20 mm; matrix=224 x 192 (resolution= 0.143 x 0.104)) were acquired to measure liver and intra-abdominal adipose tissue volumes. Enough slices were acquired to allow imaging of the liver and kidney region. Liver volume was calculated by manual contour of the RARE T2 sequence. Axial RARE T2 images with FS and NFS were used to measure intra-abdominal fat volume, using MIPAV 8.0.2 (NIH, MA, USA). Three adjacent slices per animal were selected from a slice in which renal pelvises had approximately the same dimensions, both in FS and NFS images. Segmentation was performed by subtracting FS from NFS images. Multispectral Fuzzy C-means clustering algorithm was applied on the resulting whole images to perform “hard and fuzzy segmentation”. Fat tissue volume quantification was finally calculated using the Paint Grow tool on each slice.

Secondly, MRI spectroscopy (^{1}H-MRS) was performed in order to extract the Hepatic Lipid Content (HLC). Multi-slice gradient echo images (TR=3000ms, Echos=20, TE=from 6.78 to 135.63ms, matrix =128x128 (resolution=0.250 x 0.156mm), FOV=320 * 20mm) were used for liver identification and definition of a (3x3x3) mm^3 volume of interest for proton magnetic resonance spectroscopy (^{1}H-MRS). MR spectra were acquired with Point Resolved Spectroscopy (PRESS) technique (TS=2500MS, TE=16.6, spectral width=4504.50 Hz), reconstructed with Topspin program (PV6.0, Bruker BioSpin) and analysed using Mnova program (Mestrelab Research S.L.). From water suppression spectra, the integral of each peak was determined in order to extract HLC, as previously described (Soares et al., 2018).

3.6. Immunohistochemistry

From the MRI group of animals (5 per type of diet and gender), liver samples were collected and weighed after 14 weeks of diet regimen. Right anterior liver lobe was collected, fixed in formalin,

paraffin embedded and four/five sections per animal was stained with hematoxylin and eosin (H&E) in order to visualize the steatosis into the liver parenchyma.

3.7. Brain PET Imaging

Positron Emission Tomography was used to image brain glucose metabolism and neuroinflammation. Dedicated groups of animals were acquired longitudinally during the period of diet regimen (7, 12 and 31 weeks of diet). Glucose metabolism was measured with [^{18}F]-FDG whereas brain inflammation with the TSPO agent, [^{18}F]-VC701 previously used in our laboratory to measure neuroinflammation in mice (Di Grigoli et al., 2015; Belloli et al., 2018).

PET imaging study was repeated twice: first longitudinal experiment includes 7 and 12 weeks as time point in which 3 animals for [^{18}F]-VC701 and 4 animals for [^{18}F]-FDG per group of diet and gender were acquired. The second longitudinal experiments include 7, 12 and 35 weeks as time point and again 3 animals for [^{18}F]-VC701 and 4 animals for [^{18}F]-FDG per group of diet and gender performed the acquisition. In the analysis of PET data, animals were pooled together for the 7- and 12 weeks as time point. PET acquisition was performed using the YAP(S)-PET II small animal tomograph (ISE S.r.l., Pisa, Italy) in three-dimensional mode and all the images were reconstructed using the expectation maximization (EM) algorithm. [^{18}F]-FDG radiopharmaceuticals were prepared for clinical use (European Pharmacopoeia VIII Edition) while [^{18}F]-VC701, a radio ligand that bind Translocator Protein (TSPO) was prepared as previously described (Di Grigoli et al., 2015).

For [^{18}F]-FDG radiotracer, animals were injected with 4.31±0.05 MBq of activity and acquired 60 min after injection while for [^{18}F]-VC701 animals were injected with 4.80±0.22 MBq of activity and acquired 120 min after dose administration. During dynamic acquisition (scan duration: 30 min; 6 frames of 5 min), animals were maintained under light gas anaesthesia (isoflurane 2% in air). Data were corrected for the physical decay of fluorine 18 (t1/2: 109.8 min). PET images were manually co-registered to a software MRI brain template and radioactivity average value were extrapolate applying PMOD software mouse region of interest (ROIs) brain template (Ma et al., 2005).

Quantification analysis was performed using PMOD 2.7 software (Zurich, Switzerland). For each ROI, radiotracer uptake was expressed as SUV (Standardized Uptake Value). For each animal, regional [^{18}F]-FDG data were normalized for the mean whole brain uptake values. This method is used for clinical studies to reduce single subject variability of [^{18}F]-FDG uptake in the brain. For the same reason, regional uptake values of [^{18}F]-VC701 were normalized to that measured in muscle. In the

case of [^{18}F]-VC701, muscle was selected as HFD induced general increase of [^{18}F]-VC701 uptake all over the brain whereas radioactivity concentration in muscles was not influenced by diet.

3.8. Brain metabolic connectivity: an explorative analysis

Correlations between ROIs of different [^{18}F]-FDG brain regions were done separately in STD control group, 45HFD and 60HFD group as population study in which male and female mice were pooled together. Sample size for the 12 weeks of diet correlations included 15 mice for STD: 16 for 45HFD and 60HFD. Sample size for the 31 weeks of diet correlations included 8 for STD and 45HFD while 7 mice for 60HFD. Pearson's correlation was performed using a p value threshold of 99% as confident interval (statistical significance obtained when $p \leq 0.01$) in order to avoid false positive results based on the assumptions that regions that are functionally associated are metabolically correlated (Horwitz et al., 1984). Subsequently, *r coefficient* was transformed to *z score* using Fisher's transformation and used for the evaluation of the *z test.* Z tests were used to define significant correlation straight from the HFDs to the STD control group, with the p value threshold of 99% as a confidence interval (statistical significance obtained when $p \leq 0.01$). Comparisons include HFD vs STD and 45HFD vs 60HDS at both time points.

3.9. Transcriptomic analysis of mice anterior cortex

Transcriptome analysis was performed on the half-anterior cortex of the male and female mice sacrificed at 35 weeks from diet, derived from the PET group of animals. Brains were rapidly removed, and the anterior cortex was collected, snap-frozen in liquid nitrogen, and stored at −80°C. Samples were stabilized in RNA Later Ice (Thermo Fisher), -20°C ON, and then disrupted and homogenized in RLT buffer (350uL) using TissueLyser (Qiagen). Total RNA was extracted following the Qiagen RNeasy Plus Micro kit procedure. The RNA concentration and purity were assessed by spectrophotometer (Nanodrop): 260/280 and 260/230 ratios were evaluated. Total RNA integrity was assessed by Agilent Biopanalyzer and the RNA Integrity Number (RIN) was calculated. The quality of each sample was assured by a RIN≥6 and visual confirmation of clear, distinct 28s and 18s rRNA peaks. An aliquot (10ng) of RNA was used for the preparation of targets for Clariom™ S Mouse arrays, according to the IVT Pico Reagent kit (Thermo Fisher). The Clariom™ S Mouse arrays were purchased from *Thermo Fisher Scientific* (Massachussetts, USA) and contain >22,100 genes, >150,300 transcripts, >221,900 total probes with several probes targeting genes >221,300. The

staining, washing and scanning of the arrays were conducted using a Fluidics 450 station, Command Console Software and GeneChip® Scanner 3000 7G, generating .CEL files for each array (*Thermo Fisher Scientific*, USA). The images were scanned by Thermo Fisher GeneChip Command Console (AGCC) and analyzed with the Thermo Fisher GeneChip Expression Console. The quality control of the scanned data was first estimated by confirming the order of the signal intensities of the Poly-A and Hybridization controls using Expression Console Software (*Thermo Fisher Scientific*, USA). Raw expression values were imported as Thermo Fisher .CEL files into TAC 4.0 software (*Thermo Fisher Scientific*, USA). This software allows analysing and normalizing the data, through workflows that include the Pre-processing, Differentially Expressed Genes (DEGs) Finding and Clustering modules.

Transcriptome analysis in male mice was performed by analysing 14 samples (5 STD, 4 45HFD and 5 60HFD). Since great variability was observed, we performed principal component analysis (PCA) analysis to select concordant Biological replicates corresponding to 2 biological samples for the group's STD and 45HFD and 4 samples for the group 60HFD creating 8 .CEL files. DEGs analysis was performed by using a Fold change equal to 2 and a p-Value of 0.05. A Robust Multichip Analysis (RMA) quantification method (Irizarry et al., 2003) was used as a probe set summarization algorithm for log transformation with base 2 (log2) and Quantile normalization method was chosen to evaluate the preliminary data quality in the Pre-processing module, which functions as a data quality control through the Thermo Fisher Expression Console Software. The mean signal intensities of all genes were obtained using 2 chips for STD AND 45FHFD and 4 chips for 60HFD group. After normalization, the differentially expressed genes satisfying the conditions of the fold change cut-off 2 and a One-Way analysis of variance (ANOVA) p-value<0.05 from all the genes probed in the array, were selected as DEGs.

For the experiment conducted on female animals, a total of 15 .CEL files (5 STD, 5 45HFD and 5 60HFD) were uploaded and normalized in PM (perfect match)-only conditions as a PM intensity adjustment. A Robust Multichip Analysis (RMA) quantification method (Irizarry et al., 2003) was used as a probe set summarization algorithm for log transformation with base 2 (log2) and Quantile normalization method was chosen to evaluate the preliminary data quality in the Pre-processing module, which functions as a data quality control through the Thermo Fisher Expression Console Software. PCA analysis was again used to select the most concordant biological replicates within each experimental group. The mean signal intensities of all genes were obtained using 3 chips for

STD and 45HFD and 3 chips for 60HFD group. After normalization, the differentially expressed genes satisfying the conditions of the fold change cut-off 2 and a One-Way Analysis of variance (ANOVA) p-value<0.05 from all of the genes probed in the array, were selected as DEGs.

The list of DEGs from both male and female were analysed for ontology enrichment using Database for Annotation, Visualization and Integrated Discovery (DAVID; http://david.abcc.ncifcrf.gov/) and the Enrichr web site (https://maayanlab.cloud/Enrichr/) (Irizarry et al., 2003).

3.10. Western blot analysis of anterior cortex

Western Blot analysis was performed on the other half anterior cortex in males and females, collected from PET animal groups after 35 weeks from HFD in all experimental groups, as described in the transcriptomic analysis sections. Brain tissue was tested for the evaluation of serine-threonine kinase (AKT) and for ionized calcium-binding adapter molecule 1 (Iba-1).

For the AKT evaluation, after thawing the anterior cortex of each mouse (male n= 5 60HFD; 4 45HFD; 5 STD: female n= 5 60HFD; 5 45HFD; 4 STD) were separately homogenized, using the TissueLyser II' from QIAGEN. Tissues were homogenized twice for 10 min each in a lysis buffer containing 290 mM sucrose, Tris 0.5M pH 6.8 and 3% SDS, 10 ug /ul of proteases inhibitors leupeptin, bestatin, pepstatin A, and aprotinin the phosphatase inhibitor sodium orthovanadate 1mM, Na F 10 mM and Tetrasodium Pyrophosphate 10 mM. After each lysis, the homogenates were centrifuged at 10000xg at 10°C, the supernatant recovered and diluted to a concentration of ~1 mg/mL with assay buffer. Protein concentrations were measured using the Pierce™ BCA Protein Assay Kit. Antibodies (Abs) used for anti-human AKT1 mouse IgG1 (Invitrogen), anti-human pSer473-AKT1 rabbit IgG (Thermo Fisher Scientific) and anti-GAPDH Ab (sc 25778, Santa Cruz Biotechnology, Dallas, Texas, USA) and anti Iba1 (WAKO 016.20001).

SDS-PAGE and blotting were carried out by standard procedures. In brief, 5-10 mg of proteins obtained from lysed tissues were loaded, separated trough SDS-polyacrylamide gel electrophoresis using 7.5 % acrylamide and electrophoresis-mediated transferred to nitrocellulose membranes with 0.45 mm pores (Schleicher and Schull ll, Dassel, Germany). The blots were blocked overnight in 4% non-fat milk in Tris-buffered saline, washed in a buffer containing 4% non-fat milk and 0.3% Tween20 in Tris-buffered saline, and incubated for 2 h with the primary antibody at the following concentration: AKT and pAKT 1:1000, GAPDH 1:4000. Primary Abs were then incubated for 1h with the appropriate secondary antibody (anti-rabbit Ly-Cor IRDye800RD) and after several washes,

membranes were dried overnight in the dark, at room temperature (RT). The infrared (IR) signal was measured using an Odyssey CLx - Infrared Imaging System. The Western blot bands of AKT/pAKT signal intensity was quantified using iStudio software normalizing to the GAPDH content and then to the optical density of STD control value (1) as previously described (Pistillo et al., 2016). For IBA-1 evaluation in anterior cortex, tissues from mice fed with HFD and STD were homogenate in 290mM sucrose; 62.5mM Tris HCl; 3% (w/V) SDS supplemented with protease and phosphatase inhibitors using TissueLyserII (Qiagen Cat No./ID: 85300) 3' at 30Hz 2 times. Protein concentration was calculated using PierceTM BCA Protein Assay Kit (ThermoFisher Cat No. 23227). 10ug of proteins were separated using pre-cast 4–15% CriterionTM TGX Stain-FreeTM gel supplied by Bio-Rad and transferred onto nitrocellulose using Nitrocellulose Transfer Kit (Bio-Rad Cat No. #170-4270). After protein transfer, the membrane was treated with a 5% BSA blocking buffer followed by overnight incubation @4°C with primary antibodies. Proteins of interest were detected with HRP-conjugated secondary antibody and visualized with Clarity Western ECL substrate (Bio-Rad Cat No. #1705061). The Stain-Free gel technology was used for normalizing bands intensities on total protein loading (Gürtler et al., 2013).

Statistical analysis was obtained applying Kruskal–Wallis test followed by Dunn's post hoc test with p-value≤0.05, as cut-off. Data were expressed as mean values ± S.E.M. of 3-4 separate experiments performed in duplicate for each antibody.

3.11. Statistical analysis

To evaluate the diet effect in brain and periphery (PET, MRI, GTT and haemato-chemistry), statistical evaluation was performed using One Way analysis of variance (ANOVA) when comparing the three group of diet regimen while Two Way ANOVA were used for comparison of two variables including the diet regimen and gender and or time point. All tests were followed by Tukey's multiple comparisons. Statistically significant difference was accepted when p≤0.05. PET [^{18}F]-FDG / [^{18}F]-VC701 tracer uptake values were correlated with BMI, and haemato-chemistry values including glycaemia, using a Pearson's or Spearman's r correlation analysis. Data were summarized into the heat map and expressed as r coefficient in which r = ± 0.7 were applied as significant cut off. All statistical evaluation was performed using Prism 7.04 (GraphPad Software Inc., CA, USA). Statistical analysis for [^{18}F]-FDG roi-roi metabolic connectivity and for Western Blot analysis has been previously described in a dedicated paragraph.

4. RESULTS

4.1. Characterization of the High Fat Diet induced-obesity mouse model

Animals that undergo HFD or STD regimen were monitored weekly for different parameters, including body weight gain, caloric and energy intake, BMI and glycaemia. Sex difference were investigated among groups. All measurements were performed longitudinally from the beginning of the diet treatment until sacrifice, at 7-, 12-, 31- weeks from diet.

Animals fed with the two different HFD (45% and 60%) showed a progressive increase in body weight in comparison to those fed with STD. Figure 11 showed male and female body weight increased in which a clear difference among sex could be appreciated (fig.11A/B). Male 60HFD mice exhibit higher and earlier body weight increased in comparison to STD diet starting from the 7th week of diet regimen that is maintained until sacrifice. 45HFD male mice showed statistically significant increase in body weight from the 10th week of diet regimen maintaining it until sacrifice. Instead, female HFD mice, in comparison to male HFD mice, gain much lower body weight during the period of diet regimen. 60HFD female body weight was like 60HFD male mice, becoming significant at 7th weeks after diet in comparison to STD. Otherwise, 45HFD female mice start to increase significantly their body weight in comparison to STD lately, around the 20th week of diet regimen.

Energy intake was calculated measuring every day a certain amount of food (5g/mouse) with measurement of the excess the day after. Caloric intake was also calculated, multiplying the gram per day eaten by the mice per kcal/g of the specific diet regimen (*STD* 3.4 kcal/gr; *45HFD* 4.73 kcal/gr; *60HFD* 5.24 kcal/gr). Data reported on the figure 11 C (male); D (female) showed almost the same results. Energy intake was similar between male and female mice. HFD mice showed lower energy intake in comparison to STD for both genders. Caloric intake, instead, showed higher value for both male and female in comparison to STD diet.

As clinical practice used to define BMI to evaluate the grade of obesity, measurements were done also in all animals that undergo diet regimen. Male mice exhibit significant higher BMI value for all experimental groups longitudinally including also control mice (STD). Significance was reached for all groups at 35 weeks compared to 7- and 12-weeks post diet (fig.11 E). This result indicates that physiologically male mice increase their BMI as their body weight. However, when compared HFD

to STD group, only 60HFD male mice showed a significant increase of BMI after 35 weeks, as indicated in Figure 12A. 45HFD follows a trend of increase in BMI compared to STD even if not reaching statistical significance. On the contrary, female mice did not show physiological increase in BMI value (fig.11 E). Again, only 60HFD female mice showed significantly increased BMI at 31 weeks compared to STD and to 45HFD females (fig.12 B).

Figure 11

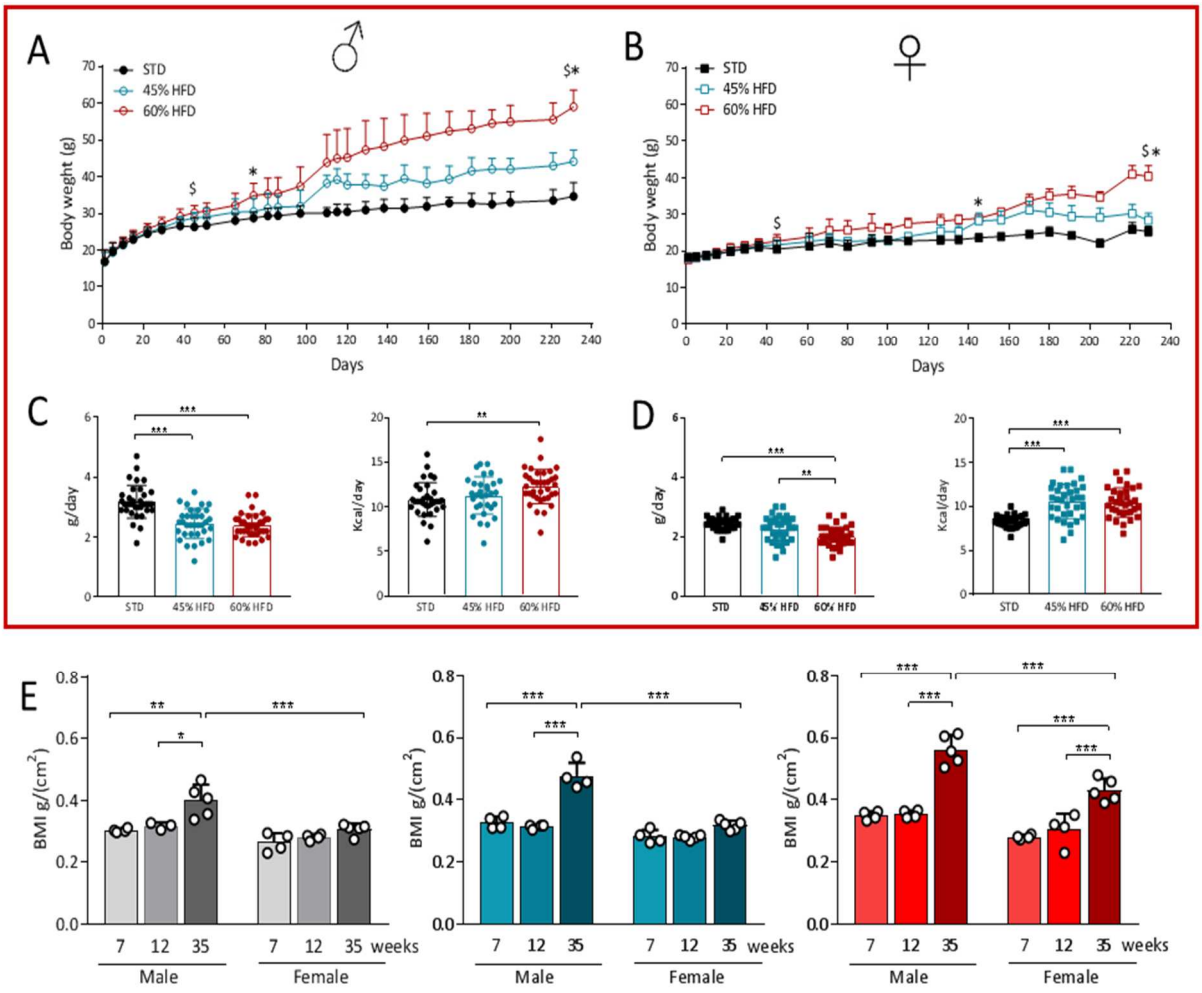

Figure 11 A High Fat Diet mouse model characterization and gender difference. A Increase male body weight. B increase female body weight, (* 60HFD vs STD maintained until sacrifice, $ 45HFD vs STD maintained until sacrifice). C energy (g/day) and caloric (Kcal/day) intake in male. D energy (g/day) and caloric (Kcal/day) intake in females. E longitudinal BMI (g/mm2) evaluation in male and female STD (grey), 45HFD (green) and 60HFD (red bars) mice after 7, 12 and 35 weeks from diet. Data are expressed as mean ± SD; * 60HFD vs STD, $ 45HFD vs STD

Taken together, these results indicate that 60HFD was able to induce a massive increase in BMI in male and in female mice while 45HFD in females showed a similar trend found in the control group.

Finally, figure 12 C/D showed mice body pictures taken before sacrifice at 35 weeks from the diet start and it is appreciable the increase in mass volume on 60HFD male and female animals compared to control groups.

Figure 12

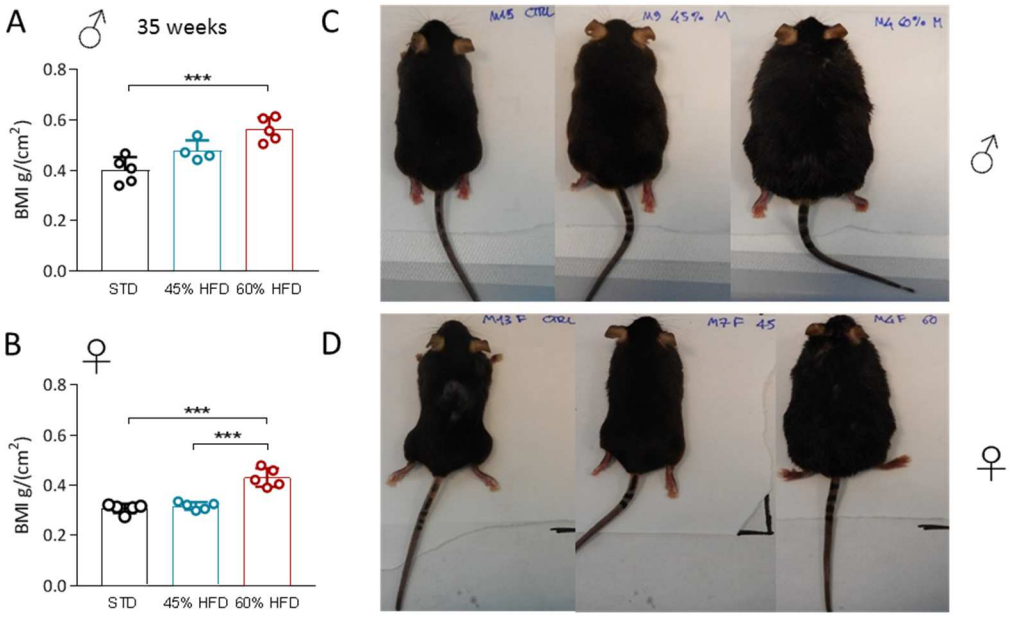

Figure 12 High Fat Diet mouse model characterization and gender difference. BMI evaluation in male (A) and female (B) at 35 weeks of diet. Animal picture captured at sacrifice after 35 weeks of diet, C. From left to right: male STD; 45HFD; 60HFD. D from left to right: female STD; 45HFD; 60HFD. Data are expressed as mean ± SD; * 60HFD vs STD, $ 45HFD vs STD

Basal glycaemia and Glucose Tolerance Test (GTT) were also investigated to confirm Insulin Resistance that represent a typical metabolic dysfunction hallmark. Prior to glucose i.p. administration, fasting basal glycaemia was measured from the tip of the tail vein longitudinally at 7- 12- and 31 weeks from diet. As expected, an age dependent trend toward an increase in basal glycaemia was observed in both sexes. This increase was found more pronounced in male mice in which both HFDs induce an increase in blood glucose concentration in fasting animals (fig.13A). 45HFD female mice behave as STD mice in which a slight glucose concentration was found at 31 weeks compared to the earliest time point. Even if not statistically significant, 60HFD female mice showed gradual increases in basal glucose level (fig13B).

Figure 13

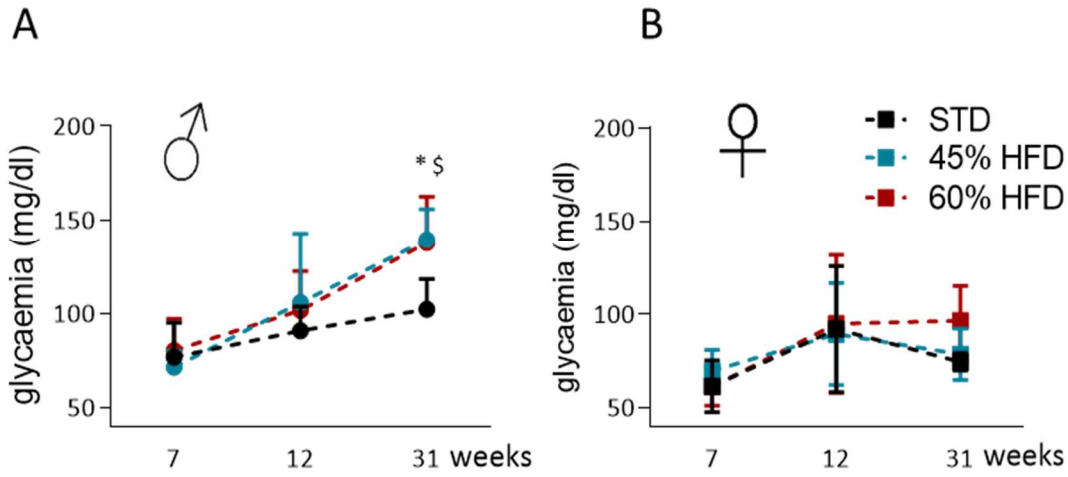

Figure 13 Fasting basal glycaemia. A male basal glycaemia measured during fasting condition at -7, -14, -31 weeks post diet; B female basal glycaemia measured during fasting condition at -7, -14, -31 weeks post diet. Data are expressed as mean ± SD; * 60HFD vs STD, $ 45HFD vs STD

GTT was performed at different time points (4-, 7-, 12- and 31 weeks post diet) to investigate the appearance of IR hallmark and blood glucose concentration was measured at different times after glucose administration (15, 30, 45, 60 and 120 min post injection). In male, glucose tolerance occurred earlier, starting after 4 weeks of diet (fig.14A). The female GT was present only after 12 weeks of diet (fig.14B). At 35 weeks GTT curve of HFD mice showed a significant increase of glucose concentration when compared to STD from 15 to 120 minutes after glucose load. In females, a similar effect of both HFD regimens was observed, but the load of glucose-affected glycaemia only lasted until 60 minutes. Taken together these results indicated that both HFD were able to increase mice BMI and glucose tolerance, effects that were more evident and earlier in males than in females. This data indicates a clear gender difference and timing dependent affecting metabolic dysfunction.

Figure 14

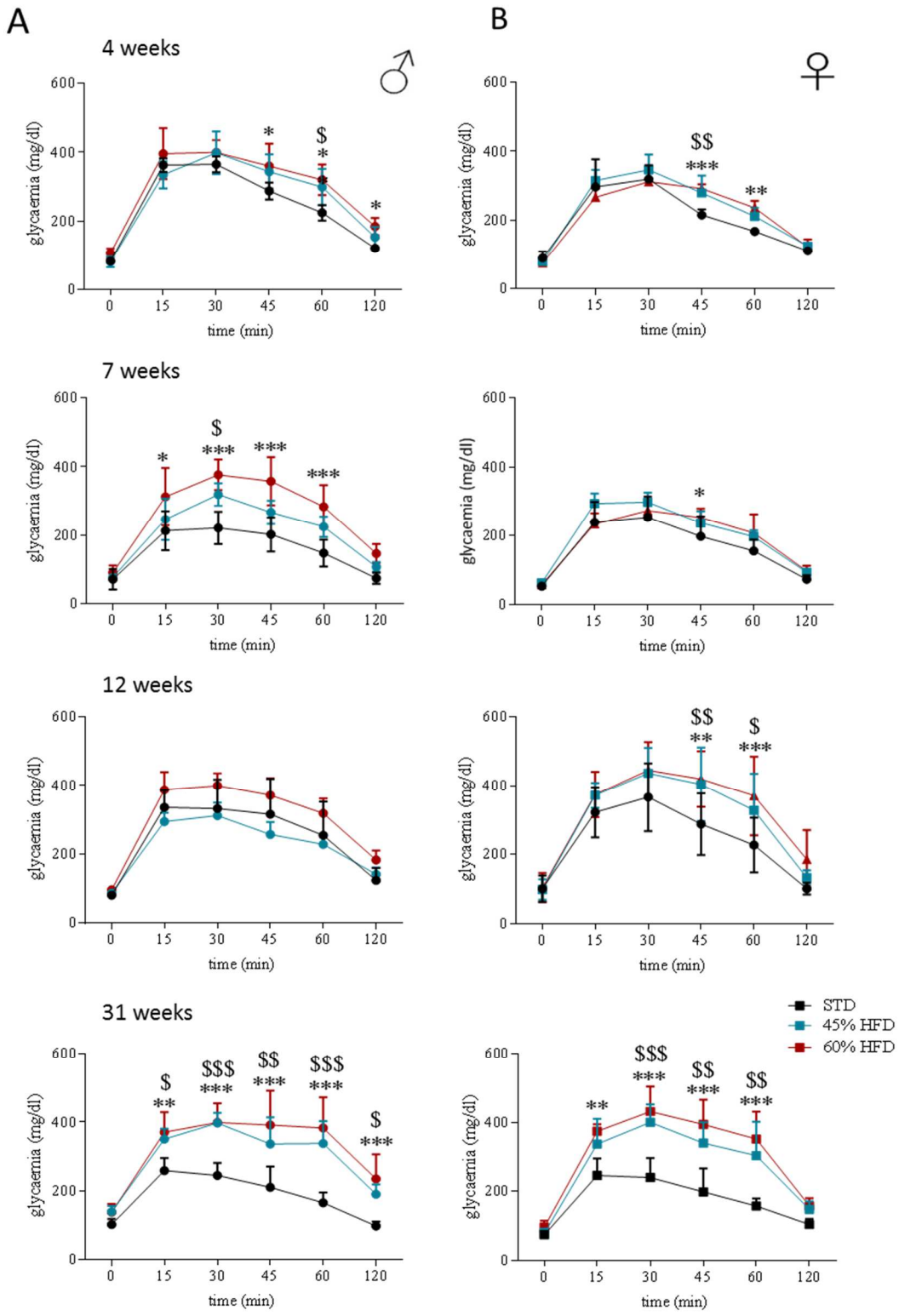

Figure 14 Longitudinal Glucose Tolerance Test. A GTT at 4, 7, 12 and 31 weeks from diet in male mice. B GTT at 4, 7, 12 and 31 weeks from diet in female mice; data are expressed as mean ± SD; * 60HFD vs STD, $ 45HFD vs STD

Finally, serum analysis on lipid profile was added on model characterization to investigate biochemical compounds involved in metabolic dysfunction. Compounds included total cholesterol, HDL, LDL for lipid evaluation and AST, ALT and Albumin liver process. From two different groups of animals that undergo PET and MR imaging, blood was collected at time of sacrifice and analysed in two different time points: 14- and 35-weeks of diet for both male and female. Sample size of the first time point includes 5 animals per group derived from MRI group plus 5 mice per group derived from PET imaging group for a total sample size of 10 mice per group of study including gender variable. Regarding 35 weeks post diet as of lately time point, 5 animals per group were included in the analysis derived from the PET group that undergo the longer longitudinal study. However, some samples were discarded due to the haemolysis of the sample analysed.

Data obtained for the two time points regarding total cholesterol and its lipoproteins (HDL and LDL) for both male and female HFD mice were shown in figure 15. Total cholesterol was found to significantly increase for both sexes. 60HFD male mice showed higher total cholesterol after 14 weeks of diet while both HFD groups exhibited higher total cholesterol compared to STD after 35 weeks of diet. Female mice, instead, showed lower cholesterol value compared to male mice but both HFDs were able to increase in significant ways compared to STD in both time-point of analysis (fig. 15A). Serum level of a cholesterol lipoprotein HDL also called “the good cholesterol” for its beneficial factor of lowering blood lipid level, was found similar between gender and experimental group. In all animals, it was found an increase in HDL level on HFD mice at the two time point of analysis, as reported in figure 15 B. An increase, as expected, was also reported regarding LDL cholesterol lipoprotein but with high heterogeneity. 45HFD male and female mice showed significant increase of LDL level after 35 weeks while no difference was found at early time point due to the high variability (fig.15C).

Figure 15

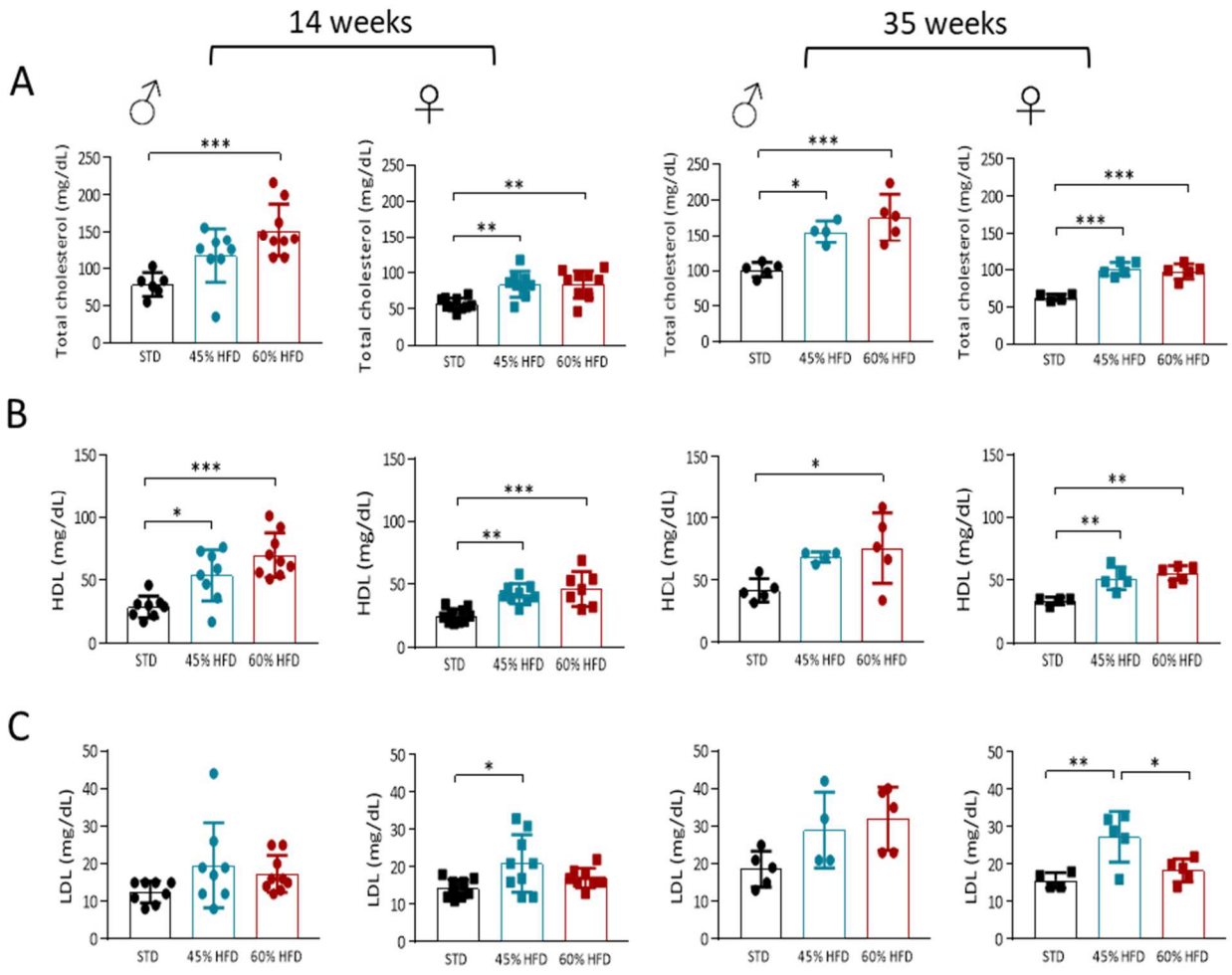

Figure 15 Longitudinal serum level analysis of different metabolic parameters. A Total Cholesterol. B High Dense Lipoprotein (HDL).C Low Dense Lipoproteins (LDL) at 14 and 35 weeks of diet in male (left) and female (right) animals; data are expressed as mean ± SD

Liver functionality was also assessed across the serum of AST/ALT enzyme and albumin protein level. Early time point of analysis showed lower levels of hepatic serum enzymes in both experimental groups without significant changes while on late time point (35 weeks) a trend over an increase was detectable in all HFD groups despite gender variables. Statistical difference was found only for female 60HFD animals for ALT enzyme (fig.16B). No significant differences were detectable on albumin level even if an increase occurred in 35 weeks when compared to 14 weeks of diet (fig.16C). Nevertheless, despite high intergroup variability, these results indicate a change in liver processes upon HFD regimen both in male and female animals.

Figure 16

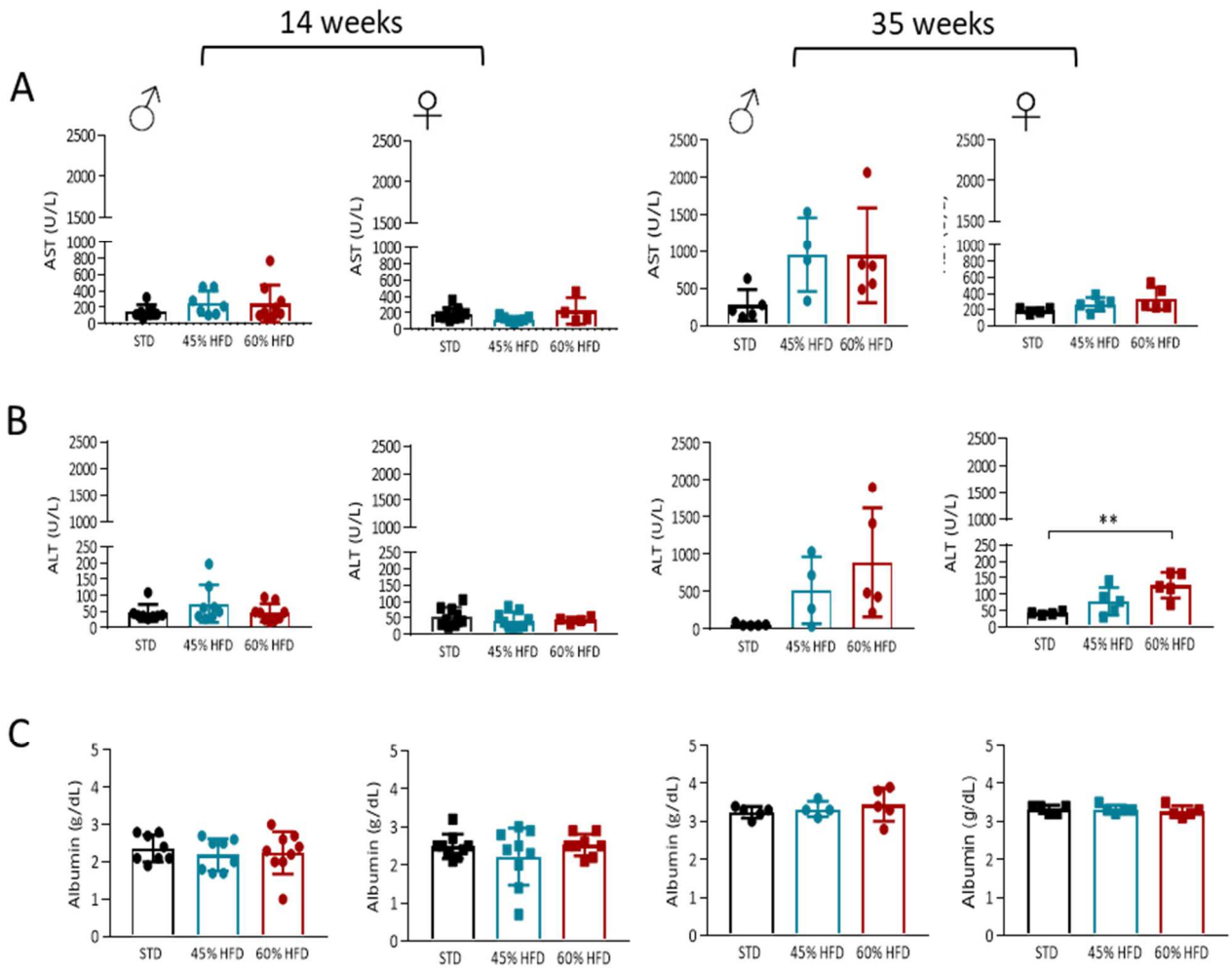

Figure 16 Longitudinal serum level analysis of different metabolic parameters. A Aspartate transaminase enzyme (AST). B Alanine transaminase enzyme (ALT). C Albumin (Alb) at 14 and 35 weeks of diet in male (left) and female (right) animals; data are expressed as mean ± SD

4.2. Liver dysfunction assessment of HFD model

Different body regions are affected during metabolic dysfunction. Among this, the liver region represents the major contributor in body metabolism in which lipid intermediates are involved in molecular mechanisms that lead to hepatic insulin resistance and hyperglycaemia (Perry et al., 2014). To this topic, hepatic lipid content was characterized using MR spectroscopy to confirm alteration occurring during HFD. 1H-NMR spectroscopy was performed on a dedicated animal at two time points, 4 and 12 weeks after diet consumption. The two-time point was selected based on previous publication with two biological questions: time point of raising of lipid content and gender difference response (Soares et al., 2018). Results obtained indicate a slight increase in total hepatic lipid content (%HLC) for both sexes at 4 weeks of diet while significant increases were detected after 12 weeks in all the experimental groups of study (fig.17B/C). Along with these results, male mice exhibit progressive increase in %HLC as the increase in diet composition. On the contrary, 45HFD female mice showed greater enriched lipid components compared to the STD group and to 45HFD at an early time point. Longitudinal analysis on male mice showed significant higher lipid content on 60HFD mice at 14 weeks when compared to the 12 weeks of diet.

Figure 17

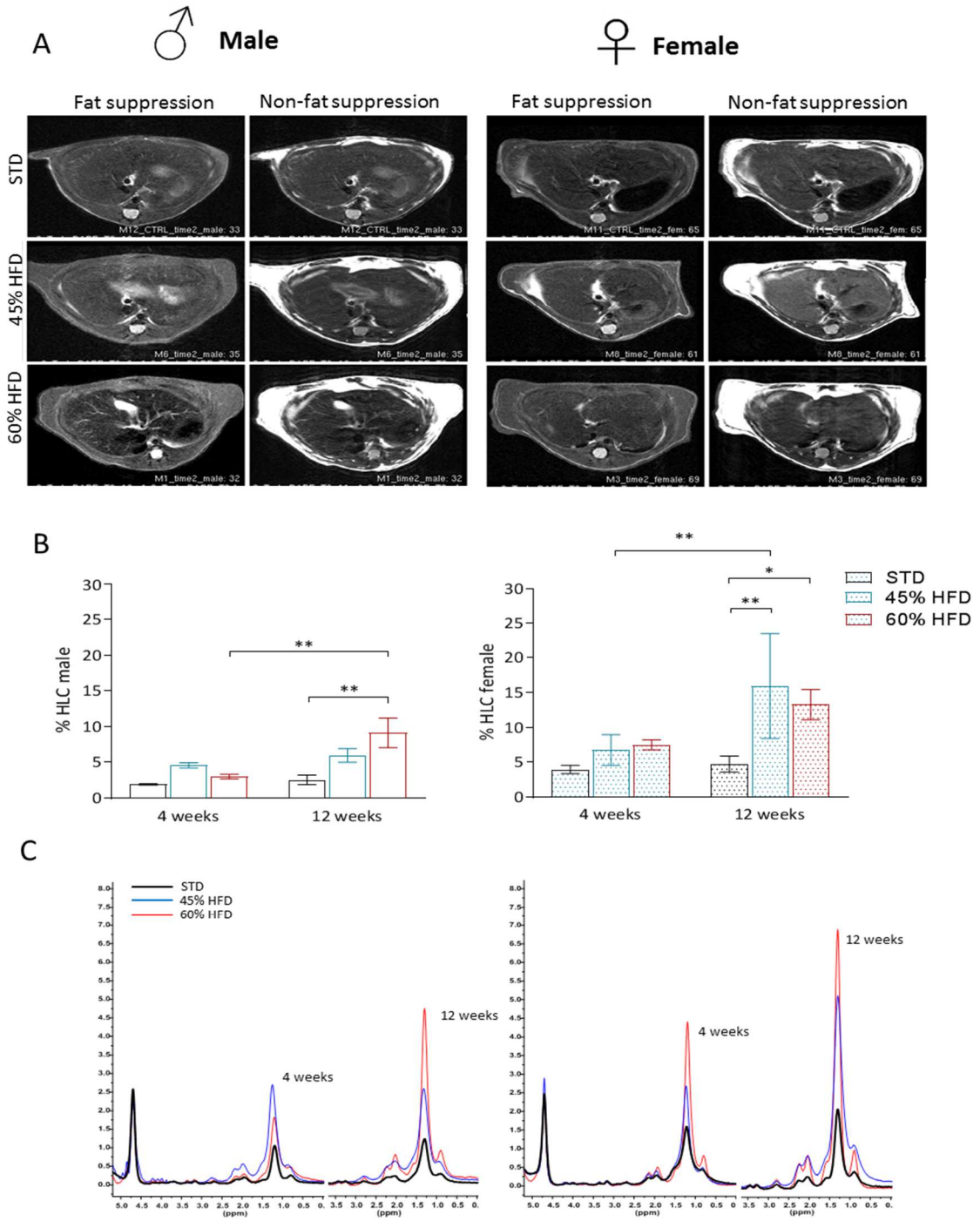

Figure 17 1H-NMR spectroscopy on liver region during HFD. A T2 MRI fat suppression (left) and non-fat suppression images (right) representation of male and female liver per group of study (STD, 45HFD and 60HFD) at 12 weeks from diet. B ^{1}H-NMR spectroscopy quantification of percentage of hepatic lipid content (%HLC) in male and female mice at 4 and 12 weeks of diet. C ^{1}H-NMR spectra of water and lipid peak obtained using spectroscopy analysis in male and female at 4 and 12 weeks of diet. Data are expressed as mean ± SD

Immunohistochemistry analysis on liver samples collected after sacrifice confirm lipid deposition into the liver parenchyma. Figure 18 showed H&E staining enhancing lipid deposition in HFD animals. Particularly evident in the 60HFD and 45HFD male mice (fig.18A) while female exhibit less lipid deposition, visible only on the 60HFD group (fig.18B). These results are in line with what observed on previous liver analysis on male mice while in female mice, even if % of HLC was high, lower lipid deposition was observed in the H&E staining.

Figure 18

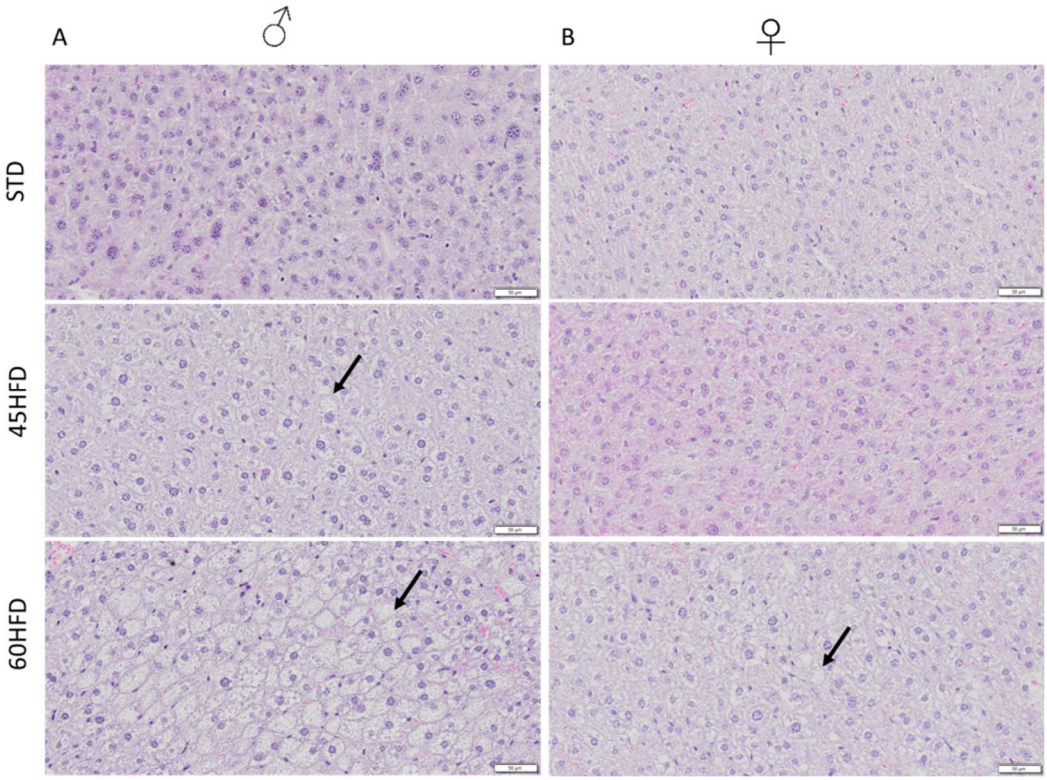

Figure 18 Hematoxylin and eosin (H&E) staining on HFD liver sample. A Male H&E staining in STD, 45HFD and 60HFD mice at 14 weeks of diet. B Female H&E staining in STD, 45HFD and 60HFD mice at 14 weeks of diet black arrow indicate lipid deposition inside the liver parenchyma, 15x magnification

Another parameter was measured in MRI to determine the increase in body circumference as a typical sign of metabolic dysfunction. MR T2 weighted sequence was applied to the liver region and using fat suppression and segmentation analysis, intra-abdominal fat accumulation was measured among HFD animals. Results in figure 19 revealed substantial fat accumulation in male HFDs mice compared to females. Anyhow, both animals showed significant increase in intra-abdominal fat

accumulation on late time point of analysis, but males showed higher visible visceral fat accumulation.

Altogether, data obtained from liver MRI evaluation confirm that male mice represent the major sex affected in the metabolic dysfunction and it is in relation to what seen in the characterization data sets of the HFD model.

Figure 19

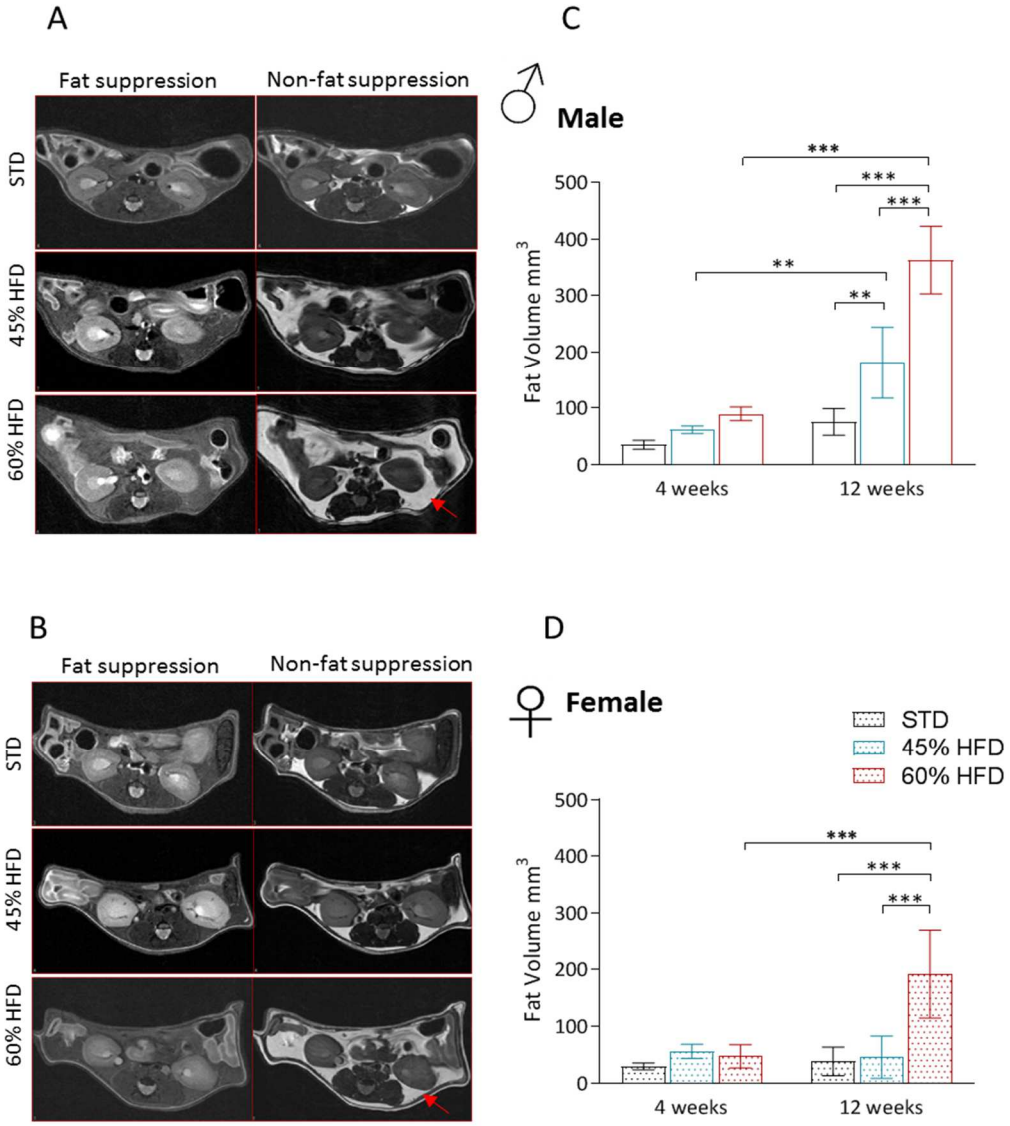

Figure 19 Intra-Abdominal fat accumulation and liver lipid droplets. A T2 MRI fat suppression (left) and non-fat suppression (right) representation of male intra-abdominal fat accumulation per group of diet (STD, 45HFD and 60HFD) at 12 weeks from diet. B T2 MRI fat suppression (left) and non-fat suppression (right) representation of female intra-abdominal fat accumulation per group of diet (STD, 45HFD and 60HFD) at 12 weeks from diet. C fat volume longitudinal quantification in male mice at 4 and 12 weeks of diet. D fat volume longitudinal quantification in female mice at 4 and 12 weeks of diet. Red arrows indicate visceral fat accumulation. Data are expressed as mean ± SD

4.3. HFD brain glucose metabolism

Brain glucose metabolism was investigated in the HFD model in order to describe brain responses to the metabolic syndrome and to analyse different brain region alteration in male and female mice. PET [^{18}F]-FDG brain imaging was performed longitudinally on a dedicated animal, replicated two times and results pool together to obtain an enough sample size for the analysis. As the glucose represents the major brain fuel, data were reported as ratio to total brain to investigate relative changes in brain region and in SUV to reveal if IR affected brain glucose consumption.

Early time point of analysis (7 and 12 weeks) did not reveal any significant difference among group and different brain regions compared to STD (fig. 20A/B) while after 35 weeks male HFDs mice revealed relative increment of [^{18}F]-FDG uptake occurring in the anterior part of the brain and a decrease was detected in cerebellar region (fig20C).

Figure 20

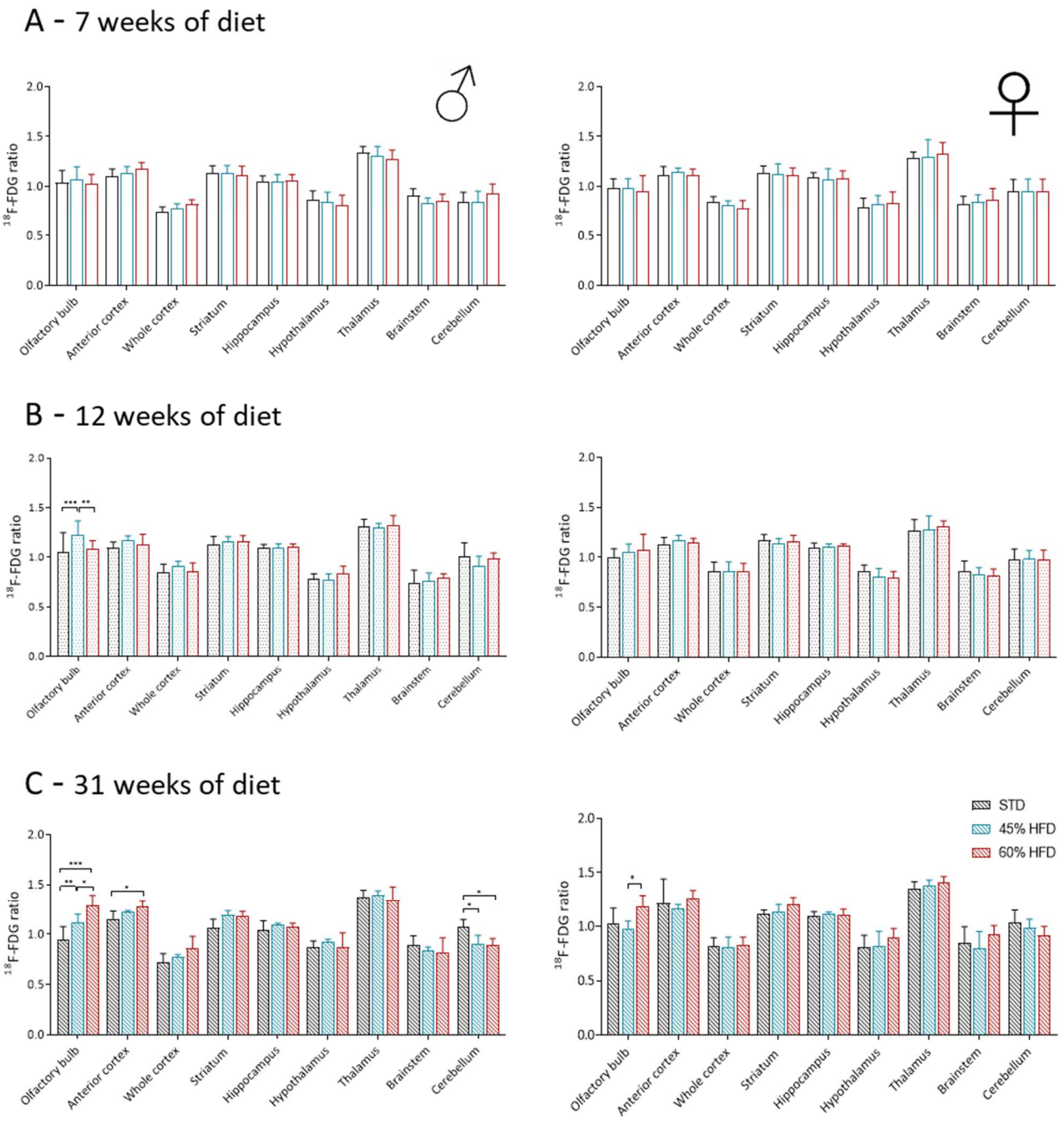

Figure 20 Brain glucose metabolism in HFD male and female mice. A Brain region [^{18}F]-FDG uptake in male (left) and female (right) mice at 7 weeks of diet regimen. B Brain region [^{18}F]-FDG uptake in male (left) and female (right) mice at 12 weeks of diet regimen. C Brain region [^{18}F]-FDG uptake in male (left) and female (right) mice at 31 weeks of diet regimen. Data are expressed as ratio to total brain uptake, mean ± SD

Specifically, olfactory bulb and anterior cortex showed significant relative increase in glucose uptake of 60HFD compared to STD mice at 31 weeks from diet regimen (fig. 21A/B). These relative changes were observed in female mice only for olfactory bulb region. Significant decrease was detected in the cerebellum of male HFDs mice while a trend was observed in females (fig. 21C). On the other hand, considering the whole groups of animals, SUV brain uptake of [^{18}F]-FDG was significantly reduced in 60HFD mice in comparison with STD mice only at weeks 7 (STD SUVmean: 2.30; 45HFD SUVmean: 1.88, 60HFD SUVmean: 1,69 *p=0.014). In male mice a trend of decrease was found at 31 weeks for the SUV total brain uptake (fig.21D).

Figure 21

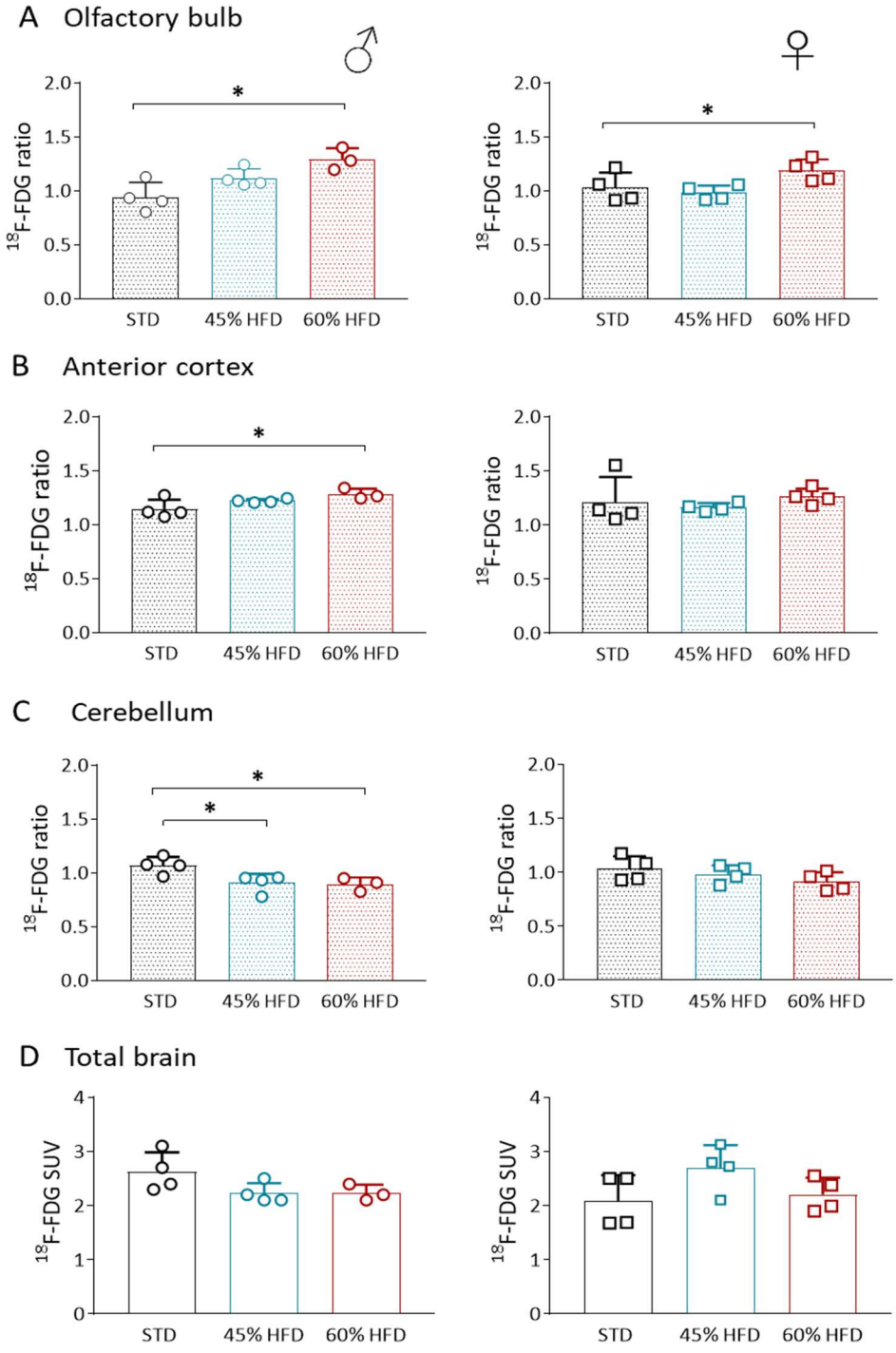

Figure 21 Brain glucose metabolism in HFD male and female mice at 35 weeks from diet. A [^{18}F]-FDG bran ratio tot total brain of olfactory bulb in male (left) and female (right) mice after 35 weeks of diet. B [^{18}F]-FDG bran ratio tot total brain of anterior cortex in male (left) and female (right) mice after 35 weeks of diet. C [^{18}F]-FDG bran ratio tot total brain of cerebellum in male (left) and female (right) mice after 35 weeks of diet. D [^{18}F]-FDG total brain SUV uptake in male (left) and female (right) mice at 35 weeks of diet. Data are expressed as mean ± SD

Group comparison indicated that with the exclusion of olfactory bulbs, in male brain, metabolism was more susceptible to HFD and that the effects observed were region specific.

We wondered whether different biochemical parameters measured peripherally could be correlated to the glucose relative increase/decrease in the brain. To this end, correlation analysis was performed between all ratios to total [^{18}F]-FDG brain region uptake to different factors including BMI, glycaemia and serum analysis of enzymes and proteins.

Heat map of Pearson's r coefficient reported in figure 22 revealed sex and regional differences in brain response to HFD. In male, brain regions were positively (red) or negatively (green) associated with BMI values and haemato-chemical parameters. In females this effect was scatter and not uniform. In male, positive correlation with strong ($r>7$ $p<0.01$) r positive values were significant between olfactory bulbs and cortex (including the anterior part) with BMI, total cholesterol and HDL, and whereas for the striatum Pearson's r value was significant only with total cholesterol. As for negative correlation, significant Pearson's r values were found between brainstem with and BMI and between cerebellum with and total cholesterol. In females, olfactory bulbs were significantly associated with ALT and striatum with AST. Finally, cerebellum that was negatively associated with ALT. Interestingly, no association were found in hypothalamus, hippocampus and thalamus, regions involved in regulation of food intake. Weak or no correlation were found for glucose and albumin. Data obtained from PET [^{18}F]-FDG and from correlation analysis indicated that in male but not in female mice HFD caused a redistribution of brain glucose uptake and that the modifications observed were associated with BMI and marker of systemic metabolic dysregulation. In females the effect was less evident and related to liver enzymes.

Figure 22

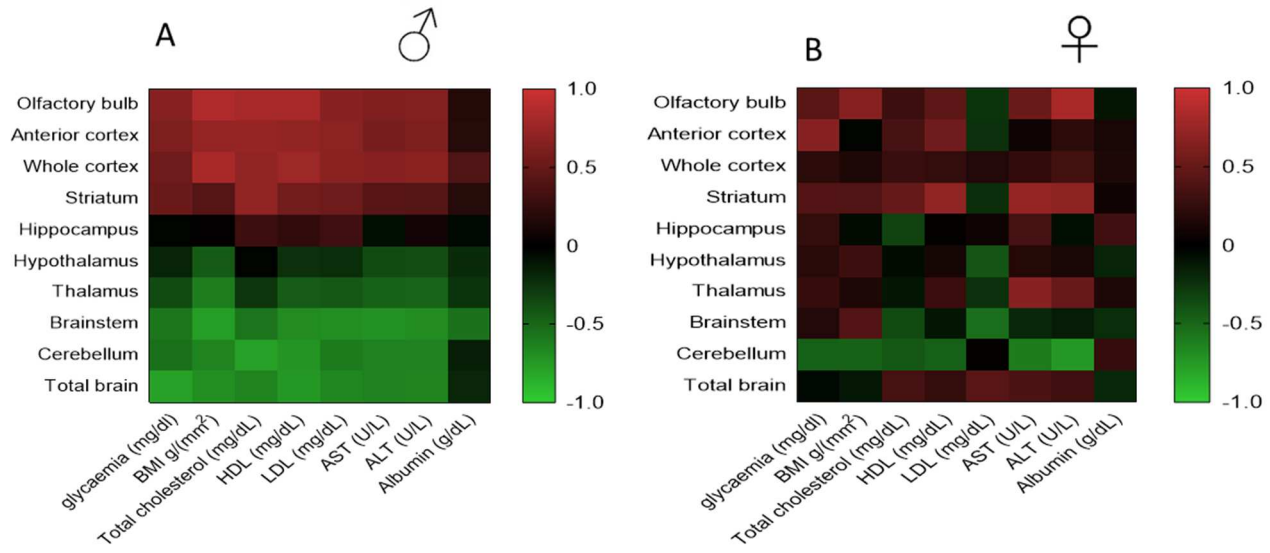

Figure 22 Heat map of glucose uptake correlation to peripheral biomarkers. A Male correlation matrix reporting Pearson's r at 35 weeks of diet of [^{18}F]-FDG regions uptake (ratio to total brain) to peripheral biomarkers. B A Female correlation matrix reporting Pearson's r at 35 weeks of diet of [^{18}F]-FDG regions uptake (ratio to total brain) to peripheral biomarkers. Red color indicates highly positive correlation (r=+0.7) while green negative correlation (r=-0.7)

4.4. Brain inflammation during HFD

Metabolic dysfunction was associated with low-grade inflammatory state due to the excessive free fatty acid deposition that is associated with increase in mitochondrial dysfunction, oxidative stress, proinflammatory cytokines and ROS species productions (Forrester et al., 2018). To this end, we wondered whether HFD could affect microglial activation which triggers upon homeostasis disturbance and neuroinflammatory state. TSPO radiotracer [^{18}F]-VC701 was used in in-vivo longitudinal PET imaging in all HFD male and female mice for the evaluation of activated microglia/macrophages.

Longitudinal analysis revealed significant increase in ratio to muscle [^{18}F]-VC701 tracer uptake all over the brain in 45 and 60HFD male mice after 31 weeks of diet compared to 7/12 weeks of diet (fig.23B/C left). Female mice showed the same significant increase in brain uptake only for the 60HFD group of animals at 31 weeks compared to the earlier time point of study (7 weeks) (fig.23C). This observation was statistically significant for all brain regions analysed.

Figure 23

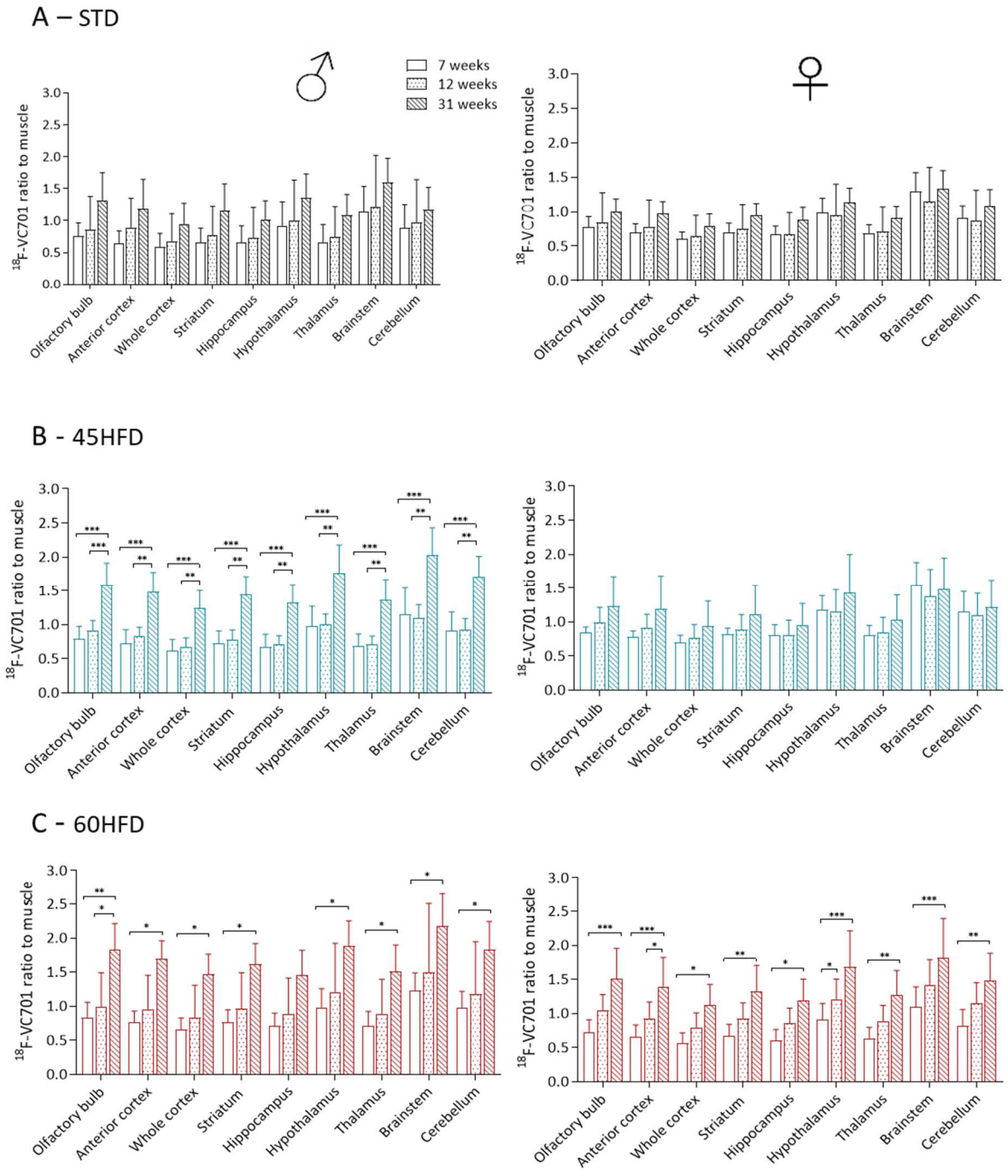

Figure 23 [^{18}F]-VC701 longitudinal brain uptake in HFD mice. A Brain region [^{18}F]-VC701 uptake in male (left) and female (right) mice at 7 weeks of diet regimen. B Brain region [^{18}F]-VC701 uptake in male (left) and female (right) mice at 12 weeks of diet regimen. C Brain region [^{18}F]-VC701 uptake in male (left) and female (right) mice at 35 weeks of diet regimen. Data are expressed as ratio to muscle uptake, mean ± SD

To better evaluate sex and diet effect on brain inflammation and microglial involvement, at the end of the experiment, Iba-1 marker for the activated microglial was measured post-mortem in the anterior cortex of male and female mice. Results showed a significant increase in Iba-1 level in 60HFD male mice and a trend toward an increase in 45HFD compared to STD, confirming [^{18}F]-VC701 PET results while female mice exhibit significant increase only for the 45HFD group when compared to STD, as shown in fig.24B.

These results suggest that a prolonged HFD exposure impacts a generalized microglial/macrophages activation, both in male and female mice.

Figure 24

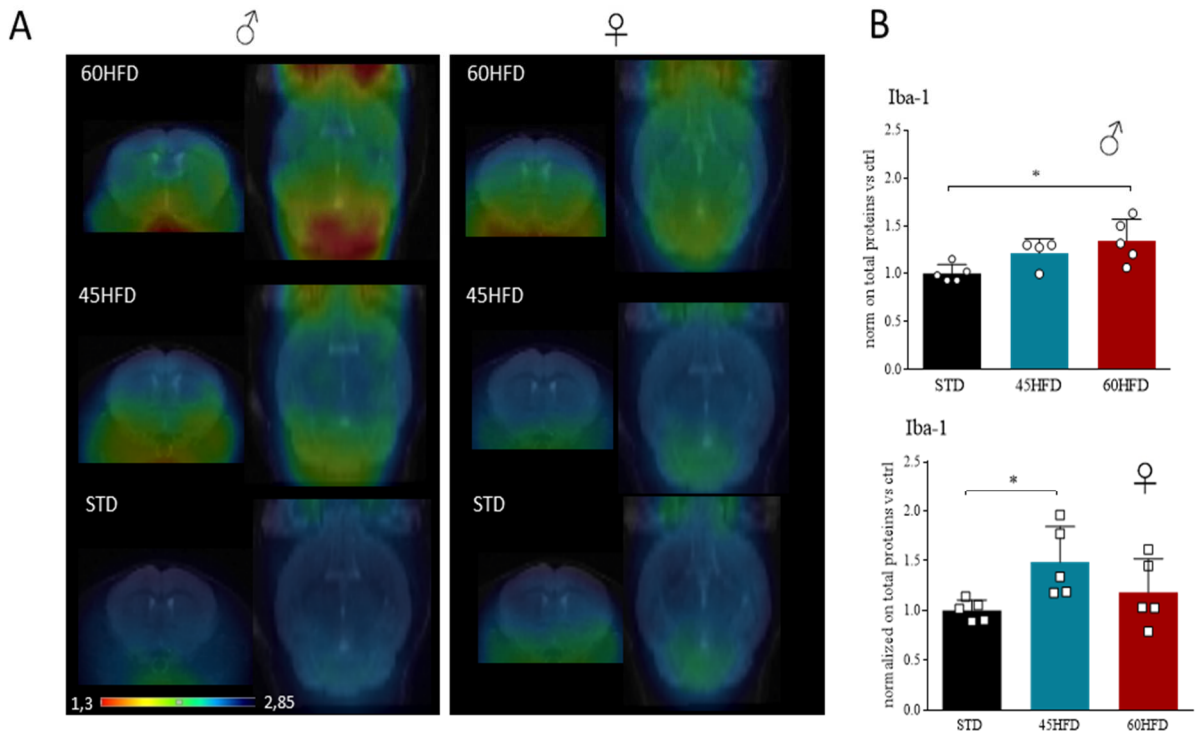

Figure 24 [^{18}F]-VC701 PET assessment of neuroinflammation in HFD brain. A [^{18}F]-VC701 PET brain uptakes images of male mice (left) and female mice (right), images are reported as ratio to muscle. B Iba-1 protein level quantification in anterior cortex of HFD male (above) and female (below) mice at 35 weeks from diet. Data are expressed as mean ± SEM

Furthermore, we investigated if [^{18}F]-VC701 tracer uptake increased could be related to the biochemical parameters derived from serum analysis and with BMI/glycaemia. To this end, as for glucose metabolism, we performed correlation study on neuroinflammatory radiotracer.

Notably, we obtained similar results as for the [^{18}F]-FDG tracer correlation analysis. Again, in male mice, [^{18}F]-VC701 normalized uptake value exhibited a highly positive correlation with BMI, total and LDL cholesterol, ALT and albumin in almost brain regions (fig.25A). Differentially to what observed with brain metabolism, no association was found with circulating HDL. Remarkably, female mice showed lower significant positive correlation between tracer and biochemical parameters despite a slight positive correlation occurring between all brain region tracer uptake and rising of glycaemia which was not so pronounced in male animals (fig.25B).

Figure 25

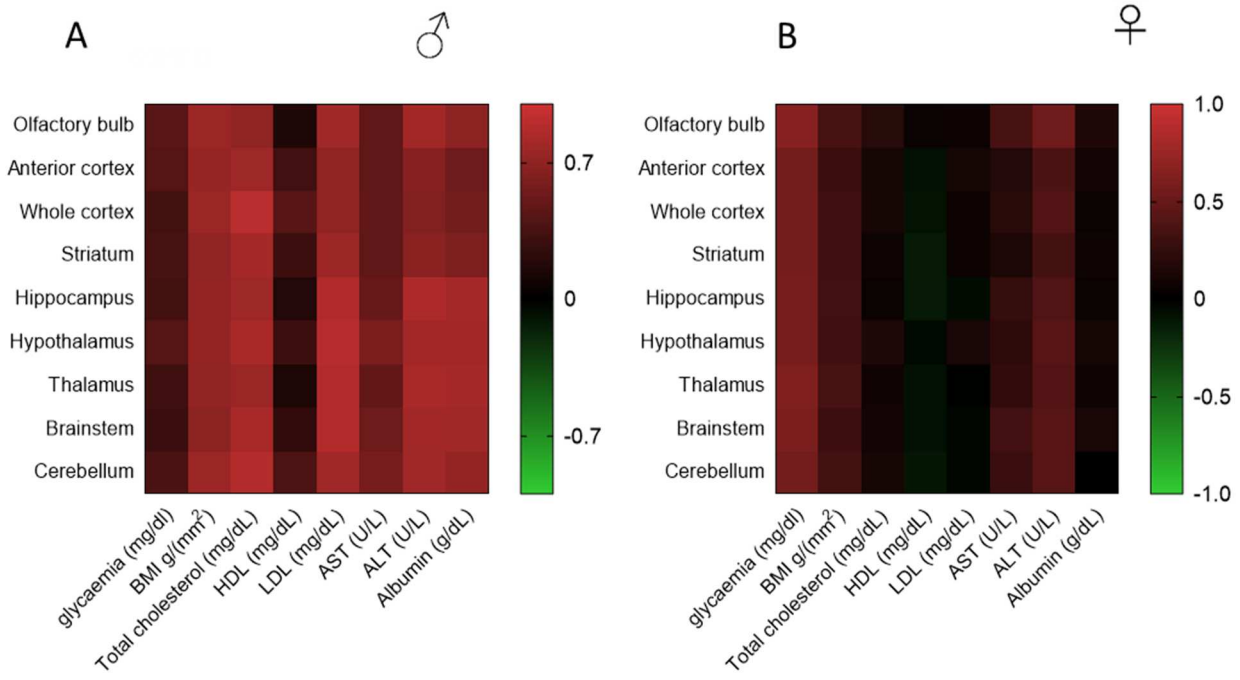

Figure 25 Heat map of TSPO tracer uptake correlation to peripheral biomarkers. A Male correlation matrix reporting Pearson's r at 35 weeks of diet of [^{18}F]-VC701 regions uptake (ratio to muscle) to peripheral biomarkers. B Female correlation matrix reporting Pearson's r at 35 weeks of diet of [^{18}F]-VC701 regions uptake (ratio to muscle) to peripheral biomarkers. Red colour indicate highly positive correlation (r=+0.7) while green negative correlation (r=-0.7)

4.5. Anterior cortex transcriptomic characterization under HFD regimen

Among all brain regions analysed in in vivo imaging study, anterior cortex showed an interesting reactivity to HFD regimen. Therefore, the impact of HFD on anterior brain cortex gene expression was studied. To this end, we performed transcriptomic analysis on bulk tissue to characterize male and female HFD anterior cortex, as the region implicated in many brain circuits also involving behaviour and cognition.

Interesting diet- and sex-related changes were found in gene expression transcriptome profile. By applying a setup of Fold Change=2 and p-value≤0.05, male mice revealed 1215 differentially expressed genes (DEGs) in the 60HFD vs STD comparison, in which 287 and 928 genes were up-regulated and downregulated respectively and 1332 DEGs for the 45HFD vs STD comparison, including 390 up-regulated and 942 downregulated genes (Figure 26A). A total of 2360 genes were detected in 60HFD female mice as DEGs whereas 1846 DEGs were selected in the 45HFD versus STD group (fig. 26B). Moreover, downregulation was again more prominent including 1532 genes for 60HFD and 1273 genes for the 45HFD group. Volcano plot reported in figure 28 A/B/C/D showed all significant genes that were found up or down regulated.

Figure 26

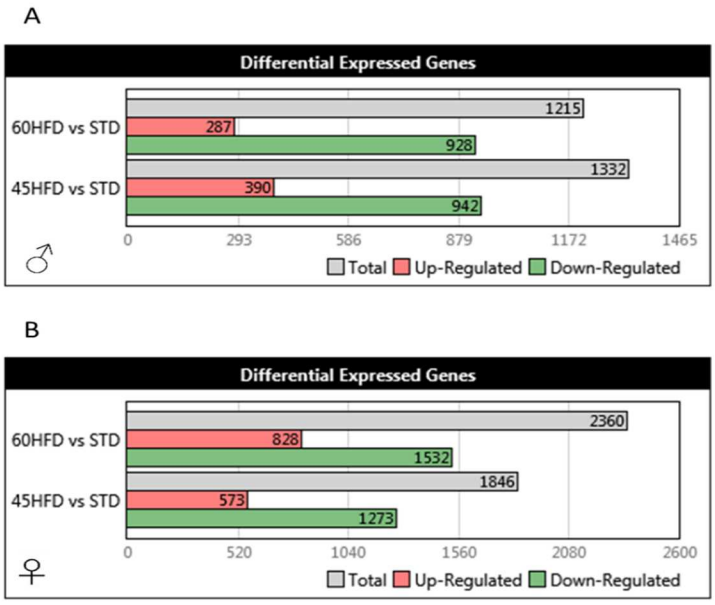

Figure 26 Differentially expressed genes (DEGs) in anterior cortex during HFD. A Male DEGs on half anterior cortex at 35 weeks from diet in 60HFD and 45HFD versus STD group. B Female DEGs on half-anterior cortex at 35 weeks from diet in 60HFD and 45HFD versus STD group

Venn diagram analysis of diet common genes in male mice revealed that 650 out of 1332 of the 45HFD genes were in common with the 1215 genes induced by 60HFD group, suggesting that HFD transcriptional changes seems to be already initiated in a 45HFD male brain mice (Figure 27E). Similar results were also observed in females. Venn diagram of Gene lists revealed that about 1368 out of 1846 45HFD genes were in common with the 2360 genes induced by 60HFD female mice (Figure 27F).

Gene Ontology (GO) analysis performed for the 1215 60HFD modulated genes in male mice showed a specific enrichment for genes belonging to the following functional annotation categories: *nervous system development; modulation of chemical synaptic transmission; modulation of excitatory postsynaptic potential; positive regulation of synaptic transmission* (Figure 28A). Kyoto Encyclopaedia of Genes and Genomes (KEEG) Pathways analysis found, for the same male 60HFD modulated genes, the following categories: *Synaptic Vesicle Cycle; Glutamatergic synapses; Thyroid Hormone Signalling pathways; cAMP signalling pathways* (Figure 28B). GO analysis for the modulated genes in 60HFD female brain anterior cortex, found enrichment for genes mainly belonging to *nervous system development; positive regulation of neuron projection development; anterograde trans-synaptic signalling; chemical synaptic transmission* (Figure 28C). KEEG Pathways analysis revealed for females the following categories: *Glutamatergic synapses; Protein processing in endoplasmic reticulum; Dopaminergic synapse* (Figure 28D).

Figure 27

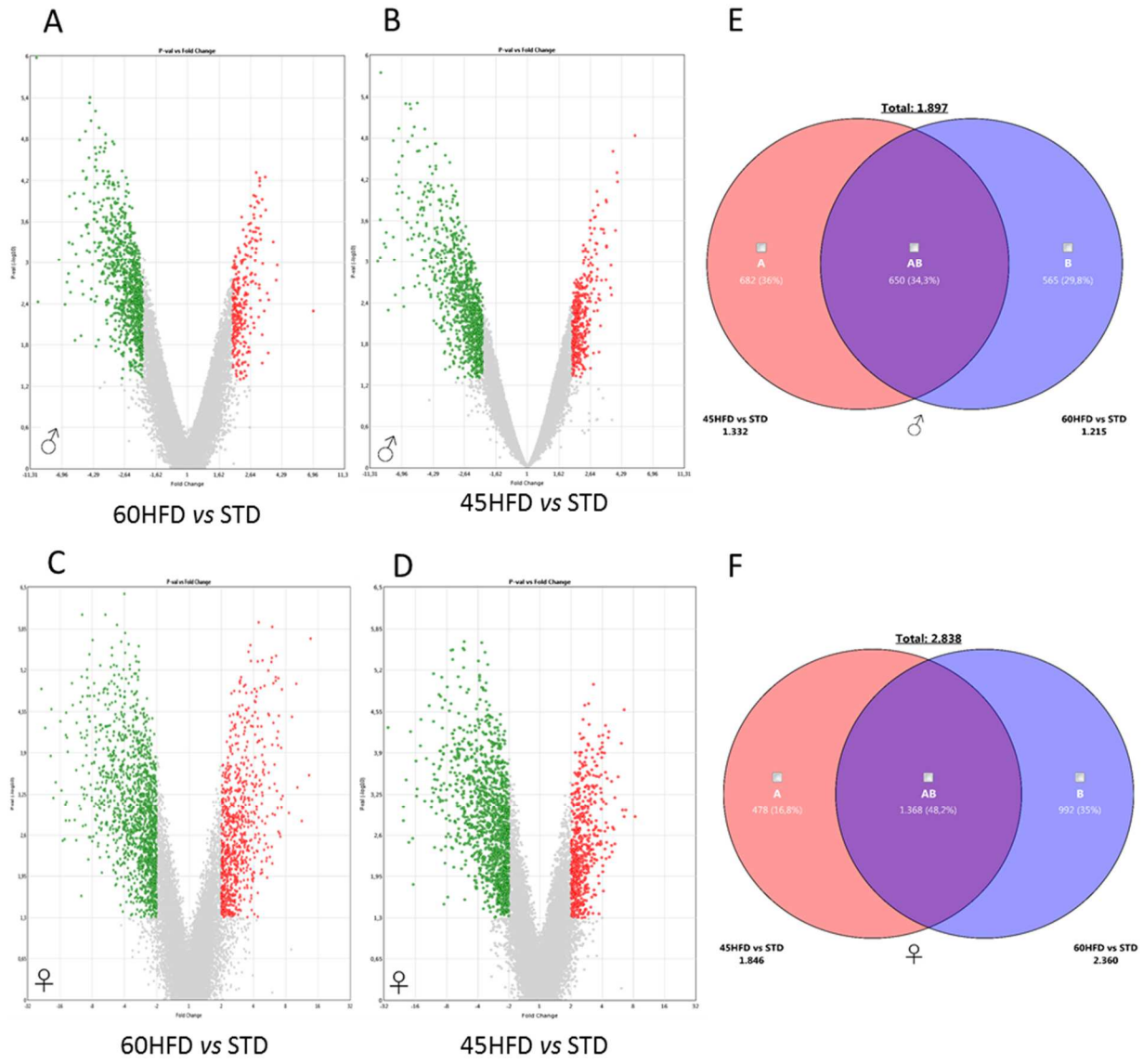

Figure 27 Volcano plot and Venn diagram of DEGs in male and female anterior cortex. A Volcano plot of 60HFD vs STD male mice. B Volcano plot of 45HFD vs STD male mice. C Volcano plot of 60HFD vs STD female mice. D Volcano plot of 45HFD vs STD female mice. Green spots indicate significantly downregulated genes while red spots indicate significantly upregulated genes. E Male Venn diagram of commonly shared genes between 60HFD and 45HFD. F Female Venn diagram of commonly shared genes between 60HFD and 45HFD

Figure 28

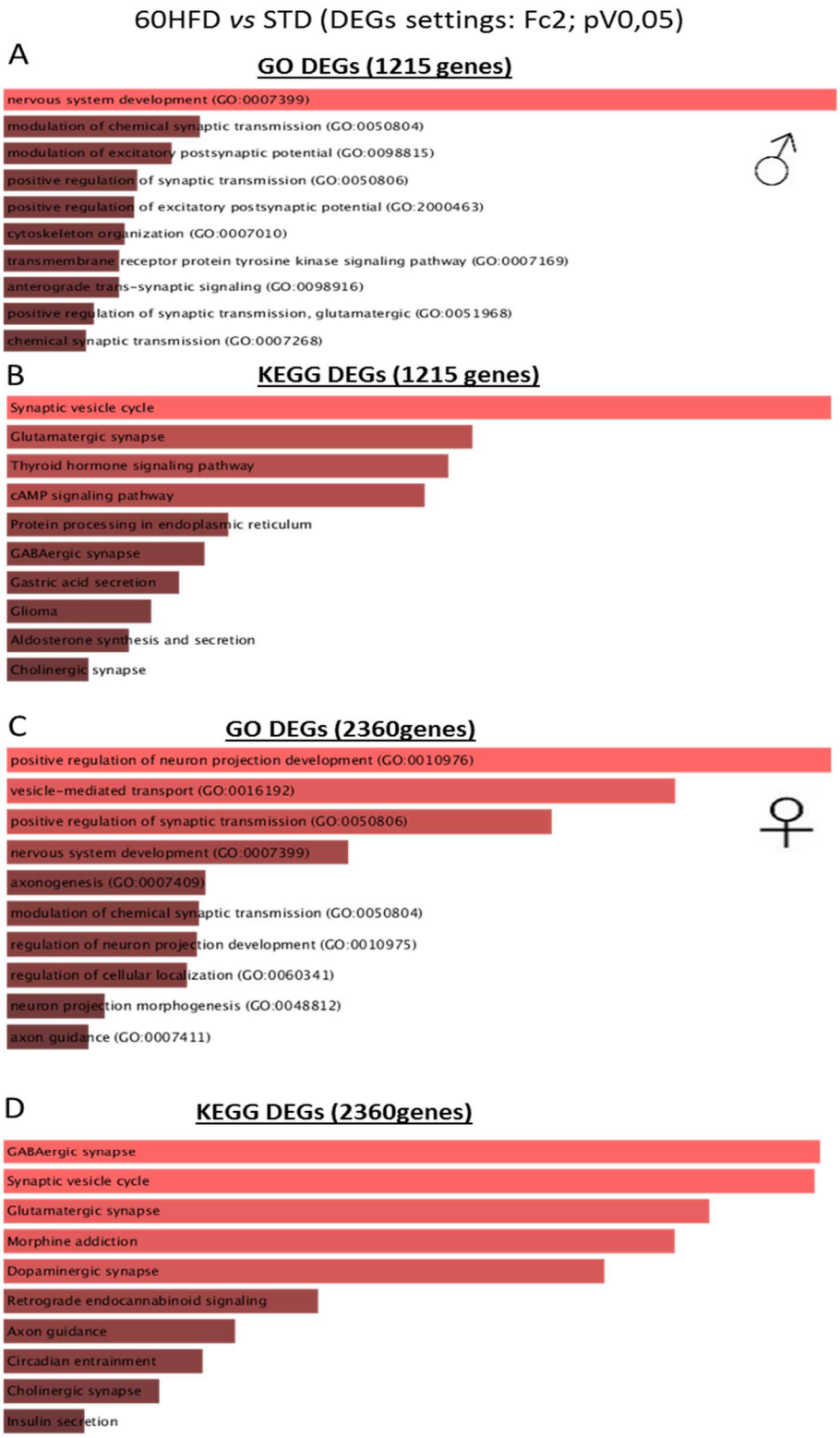

Figure 28 Gene Ontology (GO) and KEGG pathways analysis of specific genes enrichment. A GO analysis of 60HFD vs STD male mice. B KEGG analysis of 60HFD vs STD male mice. C GO analysis of 60HFD vs STD female mice. D KEGG analysis of 60HFD vs STD female mice. The length of each bar within the brighter red color represent the significance of specific gene-set

Finally, another GO analysis was performed to better define the specific genes modulated in the 60HFD condition that were upregulated or downregulated in both, male and female anterior cortex. First, we performed Venn diagram comparison of all genes modulated, in which 785 genes were commonly induced in male and female mice which annotation belongs to "*nervous system development*" whereas 1575 and 430 genes were specifically modulated in female and male respectively (Figure 29). Male mice GO data showed 287 upregulated genes with a specific enrichment for the "*positive regulation of muscle cell differentiation*" and specific enrichment was found for the 828-upregulated genes in 60HFD female mice, belonging to "*response to glucagon*", indicating possible female control of the glucagon/insulin metabolic processes.

Nervous system pathway includes Sema5A, CNTF and ACHE transcript associated with axonal guidance, neuronal development, cell signalling, differentiation and synaptic transmission (Lin et al., 2009; Blotnick and Anglister, 2016; Savolainen et al., 2018).

The female's exclusive pathway regarding response to glucagon include CREB1, ADC and GNG11 genes involved in glucagon effect, brain metabolism and cellular senescence (Jin et al., 2013; Hossain et al., 2006; de Mooij-van Malsen et al., 2009). Male's exclusive pathway include RBM4, BNIP2, NRG1 involved in neurite outgrowth, cell differentiation and regulation of splicing mechanism including these related to tau protein isoform, regulation of inflammatory factor (RBM4), cell apoptosis (BNIP2) and synaptic plasticity (NRG1) (Kar et al., 2006; Du et al., 2020; Huangfu et al., 2020; Levchenko et al., 2020; Mouton-Liger et al., 2020). The results obtained for the same analysis for the 60HFD groups were reported in the figure 30.

Figure 29

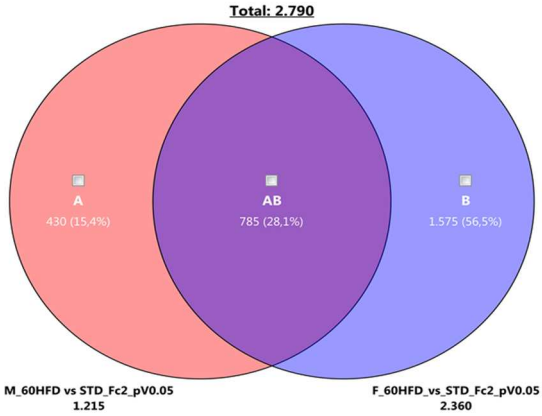

Figure 29 Venn diagram comparison of commonly induced genes in anterior cortex of male and female HFD mice

Figure 30

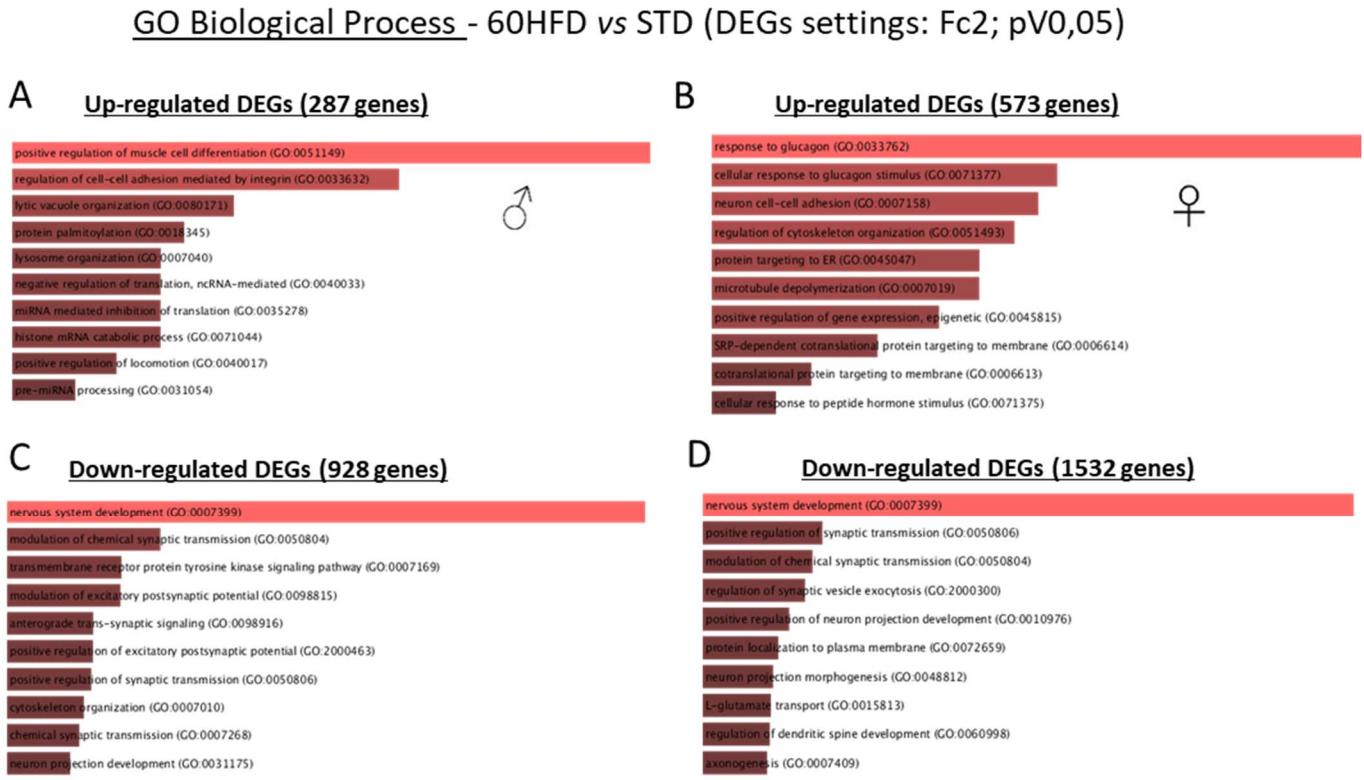

Figure 30 GO and KEGG analysis of specific up regulated or down regulated genes belonging exclusively to 60HFD male or female mice A GO analysis of upregulated DEGs in male 60HFD mice. B GO analysis of upregulated DEGs in female 60HFD mice. C GO analysis of down regulated DEGs in male 60HFD mice. D GO analysis of downregulated DEGs in female 60HFD mice. The length of each bar within the brighter red color represent the significance of specific gene-set

Taken together, these results showed an interesting de-regulation of gene expression in anterior cortex upon HFD regimen, with a prominent down regulation concerning the nervous system pathways. These biological processes found in the analysis appear to be similar in both male and female mice without any evident gender differences despite the response to glucagon, which was exclusively found for female mice. In conclusion, the pathways identified by gene expression analysis need further investigation to dissect the exact role in our model.

4.6. Anterior cortex post-mortem analysis

As for the transcriptome analysis, again, we wondered whether HFD could influence AKT signalling in the anterior cortex region as mechanism has been involved in the metabolism regulation, cell survivor, neurotrophic factor, growth and synaptic plasticity and has been linked to psychiatric disorder such as depression and anxiety like behaviour (Hers et al., 2011; Hauger et al., 2012).

In fact, we found a tendency toward an increase in both total AKT level and pAKT/AKT in the 60HFD male mice, without reaching significant value (fig. 31A). On the contrary, female 60HFD animals showed statistically significant increased level in both total AKT (χ^2=7.2; p=0.0178) and pAKT/AKT (χ^2=5.7; p=0.048) when compared to STD group, as reported in figure 31B.

Figure 31

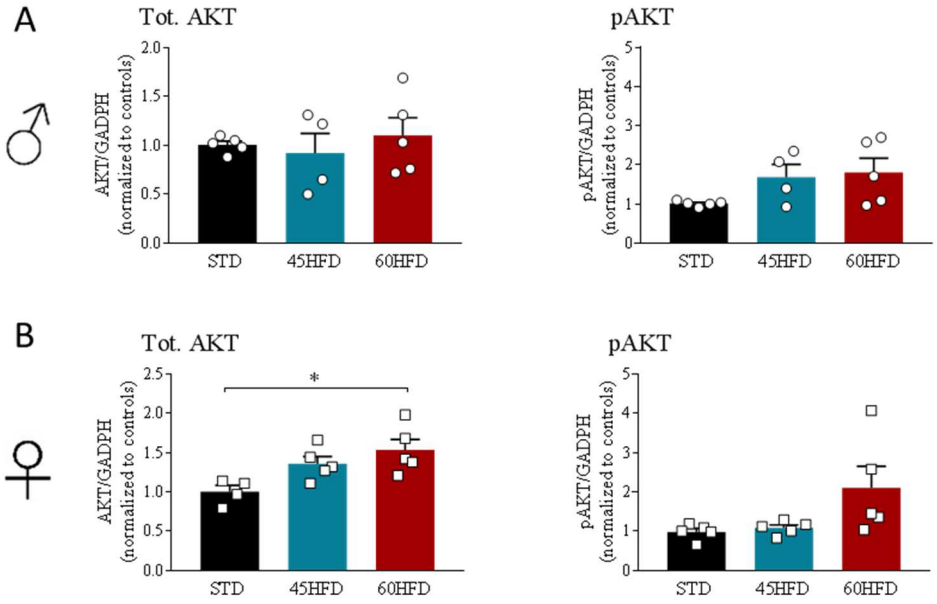

Figure 31 Western Blot analysis of the half-anterior cortex of HFD male and female mice. A Total AKT and pAKT protein level in the anterior cortex of male HFD mice. B Total AKT and pAKT protein level in the anterior cortex of female HFD mice. Data are normalized to the total GAPDH content and to control group and expressed as mean ± SEM

Finally, these data establish that a modulation of AKT activity occurs upon HFD regimen in which female mice are subjected.

4.7. Explorative analysis on brain metabolic connectivity during HFD

An explorative analysis was performed to address brain metabolic connectivity using pre-selected [^{18}F]-FDG roi-roi uptake for diet-related alterations in the brain. Analysis was performed in the two-time point (12 and 31 weeks of diet) in a population study (pooling male and female mice) and divided in three groups: STD (control group), 45HFD and 60HFD.

Different correlations among groups were found statistically significant and were reported in table 6 for the two time points of the study. Table 6 indicates all the correlations that were significant in at least one group of study, but the same correlations were reported also in groups that didn't reach significance in order to visualize the changes among groups or during time points of the same correlation. Pearson's r and relative p-value that indicated in bold black represent the significant correlation found in STD and HFDs groups.

Table 6 Brain [^{18}F]-FDG roi-roi correlation at 12 and 31 weeks from diet

p value on Pearson's R	12 weeks						31 weeks					
	STD		45HFD		60HFD		STD		45HFD		60HFD	
Roi-Roi correlation	r	p value	r	p value	r	p value	r	p value	r	p value	r	p value
olfactory bulb-anterior cortex	0,49	0,058	0,31	0,237	0,18	0,488	-0,002	0,996	**0,91**	**0,0013**	**0,87**	**0,01**
olfactory bulb-whole cortex	0,44	0,099	0,54	0,029	**0,69**	**0,003**	**0,91**	**0,001**	0,22	0,586	0,57	0,179
olfactory bulb-cerebellum	**-0,66**	**0,0006**	-0,56	0,021	**-0,64**	**0,007**	-0,79	0,019	-0,66	0,07	-0,86	0,012
anterior cortex-striatum	0,11	0,686	**0,66**	**0,004**	-0,02	0,917	0,2	0,633	0,51	0,187	0,42	0,34
anterior cortex-hippocampus	**-0,68**	**0,005**	-0,04	0,854	**-0,72**	**0,001**	0,2	0,633	-0,37	0,366	-0,01	0,969
anterior cortex-thalamus	-0,32	0,244	0,45	0,078	**-0,7**	**0,002**	-0,31	0,757	0,19	0,649	-0,12	0,502
whole cortex-hypothalamus	-0,13	0,631	-0,47	0,061	**-0,61**	**0,01**	-0,64	0,084	**-0,91**	**0,001**	**-0,88**	**0,008**
whole cortex-thalamus	**-0,84**	**≤0,0001**	**-0,69**	**0,002**	**-0,78**	**0,0003**	**-0,89**	**0,003**	-0,57	0,134	-0,68	0,088
whole cortex-brainstem	**-0,64**	**0,009**	**-0,63**	**0,008**	**-0,74**	**0,0009**	**-0,82**	**0,01**	**-0,92**	**0,0008**	**-0,9**	**0,005**
striatum-thalamus	-0,02	0,933	0,45	0,077	0,17	0,516	-0,4	0,32	**0,85**	**0,007**	0,73	0,057
striatum-hypothalamus	0,56	0,026	**0,76**	**0,0006**	0,46	0,072	0,19	0,639	0,62	0,095	0,71	0,07
striatum-cerebellum	-0,62	0,012	-0,52	0,037	**-0,63**	**0,006**	-0,6	0,113	-0,6	0,113	-0,55	0,194
hippocampus-thalamus	0,53	0,038	**0,62**	**0,01**	**0,76**	**0,0006**	0,03	0,938	0,38	0,344	0,37	0,409
thalamus-brainstem	0,41	0,125	0,21	0,43	0,42	0,181	**0,89**	**0,003**	0,34	0,407	0,78	0,037
hypothalamus-thalamus	-0,05	0,846	0,35	0,178	**0,68**	**0,003**	0,68	0,062	0,75	0,03	0,82	0,022
hypothalamus-brainstem	0,61	0,013	**0,62**	**0,009**	0,51	0,042	**0,85**	**0,007**	0,8	0,016	0,83	0,019
amygdala-cortex	0,39	0,146	-0,16	0,547	0,15	0,572	-0,15	0,705	**-0,93**	**0,0007**	**-0,86**	**0,01**
amygdala-striatum	0,59	0,018	**0,63**	**0,008**	0,6	0,012	0,61	0,106	0,56	0,147	0,63	0,122
amygdala-hypothalamus	**0,8**	**0,0003**	**0,86**	**≤0,0001**	0,44	0,08	0,72	0,04	**0,98**	**≤0,0001**	**0,96**	**0,0004**
amygdala-brainstem	0,23	0,394	0,49	0,051	0,054	0,842	0,39	0,326	**0,86**	**0,006**	**0,87**	**0,009**

Along with different changes, two correlations were found stable among the group and during time: cortico-thalamic and cortico-brainstem connectivity were found significantly negatively correlated in all experimental groups of study, in the two time-point of analysis. At 12 weeks of diet this

negative correlation was maintained in all groups of study with significant r value (see table 6). At a late time point, due to the reduced sample size available for the analysis, the control group significantly maintained both correlation while only cortex to brainstem correlation was significant in the HFD group. The cortico-thalamic correlation loses the significant p-value due to the small sample size but remains negatively correlated (45HFD r=-0,57; 60HFD r=-0,68).

Figure 32 shows all the significant correlation found between brain regions analysed in the STD and HFDs group in which heat map Pearson's r were reported indicating positive or negative value. After 12 weeks of diet 45HFD mice showed 8 significant correlations, 5 new correlations, 3 maintained and 3 loss correlations when compared to the STD group. A brain connectivity graphical representation was reported to better visualize direct connection between different brain regions. 60HFD, instead, indicates more significant correlation found indicating greater metabolic changes occurring in this type of diet. Totally, 11 correlation was found statistically significant from which 4 correlation maintained compared to STD, 6 new correlation and 1 loss.

In order to assess the diet-related alterations in metabolic correlations strength, z test was performed using z score (Pearson's r transformed to z score trough Fisher transformation). No significant difference was found when compared 45HFD or 60HFD to STD mice. Significant correlations strength was found only when comparing the two types of HFDs. Specifically, 60HFD showed less strength of correlation when compared to 45HFD for the amygdala-hypothalamus correlation (z test p-value: 0.019) while gain of strength negative in anterior cortex-hippocampus correlation (z test p-value: 0.014).

Figure 32

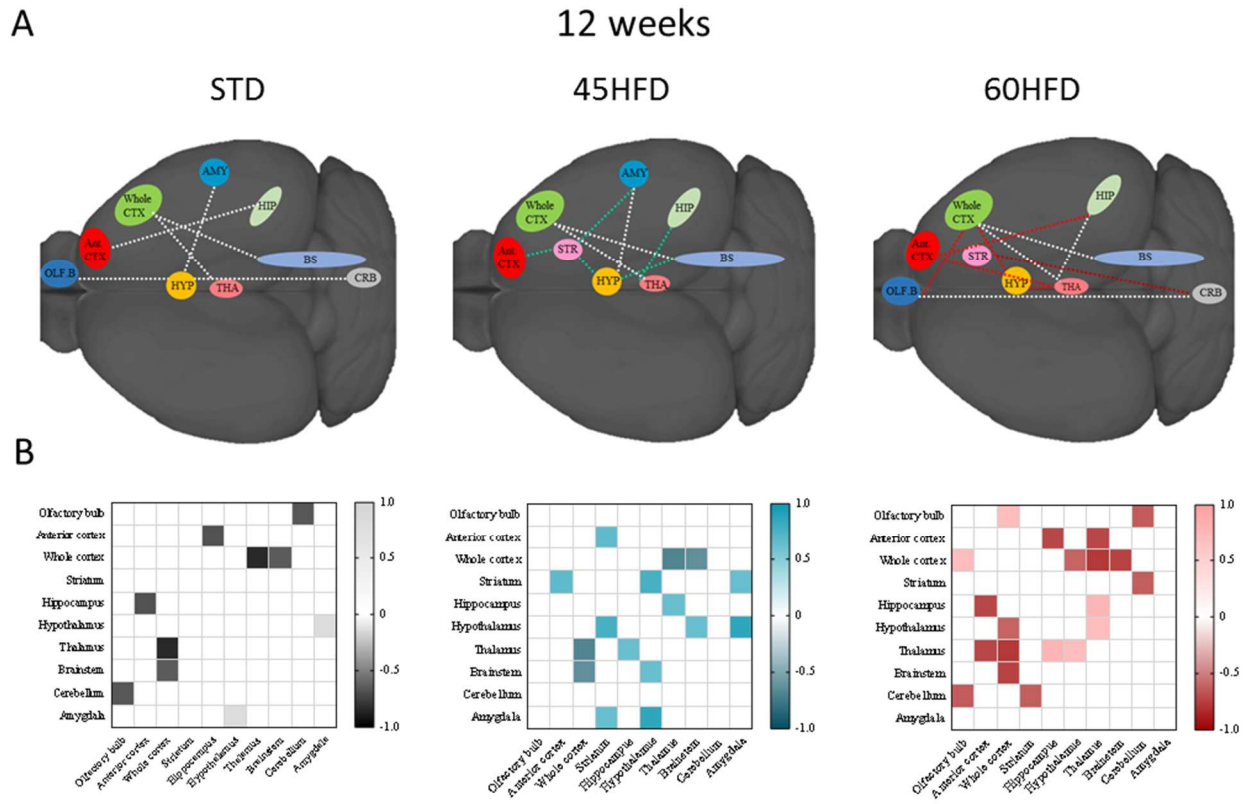

Figure 32 Correlation between different brain regions in HFD at 12 weeks of diet. A Schematic representation of significant correlation obtained from [^{18}F]-FDG roi-roi analysis in STD, 45HFD and 60HFD population (including both male and female mice) at 12 weeks from diet. White connection indicates correlation maintained as in STD group; Green connection indicates new correlation found in 45HFD mice while red connection indicates new correlation found in 60HFD mice. B Heat map reporting significant Pearson's r correlation coefficient found in STD, 45 and 60HFD animals

Chronic HFD diet exposure (up to 31 weeks of diet) showed similar results of correlations obtained at an early time point. Maintained correlations found in STD and HFDs that were not influenced by diet were also observed on late time point of analysis even if with smaller sample size available for the analysis. However, a lower number of correlations was found statistically significant as indicated in table 6. Among this, 45HFD mice showed three correlations indicate significant strength of correlation in the analysis performed comparing HFD to STD. Positive gain of correlation compared to STD for the olfactory bulb-anterior cortex correlation as confirmed also by z test for the connectivity strength (r=0.91, z test p-value: 0.009). Same trend was also observed for the 60HFD but not statistically significant (r=0.87). More powerful negative correlation occurred between amygdala and cortex (z test p-value:0.014) while gain of positive connection between amygdala and hypothalamic region (z test p-value: 0.018). Comparison between two HFD groups showed a non-

significant difference in the strength of connectivity. Figure 33 reported all correlations that were significant at 31 weeks of diet.

Figure 33

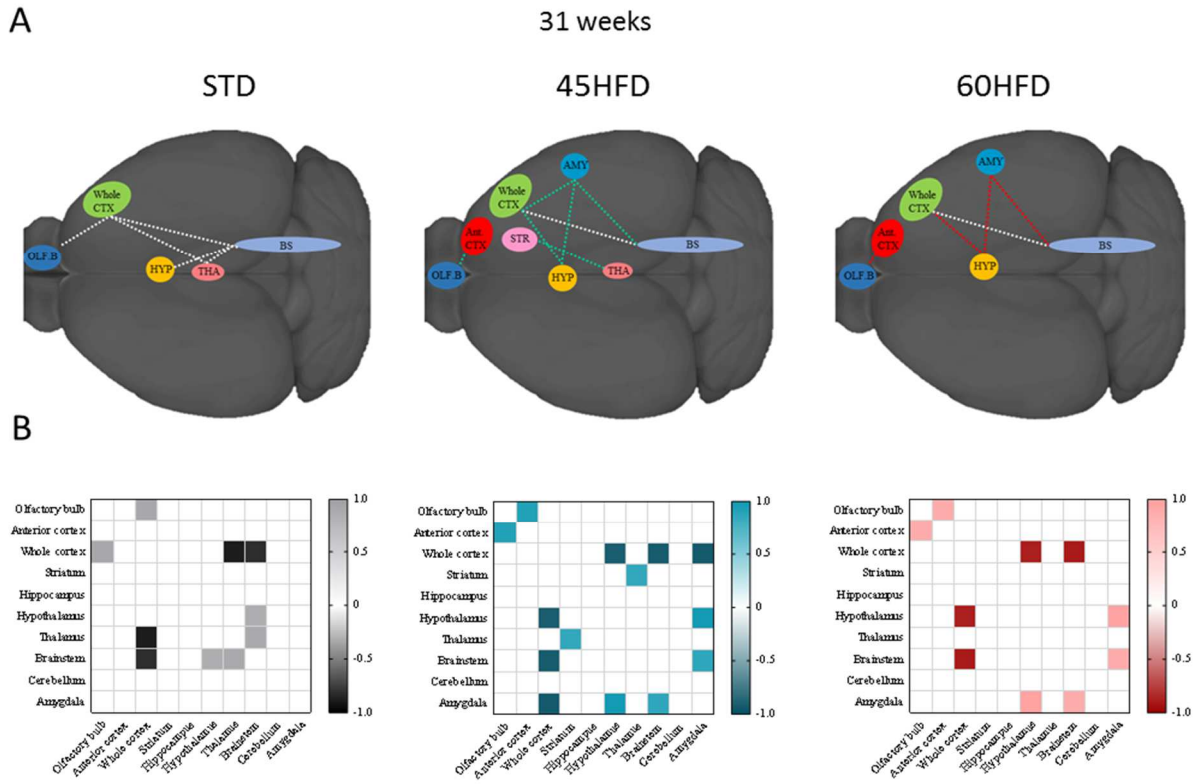

Figure 33 Correlation between different brain regions in HFD at 35 weeks of diet. A Schematic representation of significant correlation obtained from [^{18}F]-FDG roi-roi analysis in STD, 45HFD and 60HFD population (including both male and female mice) at 12 weeks from diet. White connection indicates correlation maintained as in STD group; Green connection indicates new correlation found in 45HFD mice while red connection indicates new correlation found in 60HFD mice. B Heat map reporting significant Pearson's r correlation coefficient found in STD, 45 and 60HFD animals

Summarizing, these explorative results indicate that chronic exposure to HFD could strengthen the correlation between different brain regions and induce changes in brain metabolism yet in earlier time points. These data are very preliminary due to the small sample size used and should be considered as a start point for further analysis.

5. DISCUSSION

5.1. Sex dimorphism in response to high fat diet induce metabolic syndrome

High fat diet is widely used to induce obesity in animal models and to study biological modifications associated with modern west style diets. Prolonged high caloric diet, particularly using fat rich in saturated fatty, triggers metabolic disorders, insulin resistance and T2D (Pedditzi et al., 2016). A limited knowledge of gender dependent physiological responses to MetS and obesity had been reached nowadays, as many publications in this field include only male as preferred sex. Our investigation aims to investigate sex differences during chronic exposure to HFD induce obesity. In specific, we used young male and female C57Bl/6 mice, a mouse model that favour diabetes and obesity development, to study the effect on prolonged exposure on two type of HFD high reached in lard (45% and 60%), in periphery and in central nervous system. Understanding sex dimorphism in metabolic disorders constitute an important component for the aetiology insight, both in human and in rodents, and in this latter one, taking in account also the strain (Wang et al., 2011). Nevertheless, most of the in vivo studies of MetS focused mainly on male mice as females reveal higher variability due to the estrogen cycle (Beery and Zucker, 2011). In our research, we include female mice with the purpose to describe not only the effect of HFD induced IR and MetS but also gender difference response. Despite a similar caloric intake, we observed a sex dependent differences in weight gain and metabolic response to HFD. Glucose tolerance, circulating glucose, cholesterol and BMI were higher in male mice, for both types of diet. These results are in agreement with studies published by others, reporting a higher vulnerability of body weight gain and metabolic alteration in comparison with pre-menopausal females (Hwang et al., 2010; Freire-Regatillo et al., 2020). From serum level analysis, we observed that both cholesterol components, HDL and LDL, increase after HFD consumption in male and female mice. An HFD induced increase of HDL levels is well-known in the mouse strain used in our study. However, the increase of HDL remains stable over time, whereas the increase of LDL was maximum for both sex at 35 weeks with a resulting increment of LDL/HDL ratios (Li et al., 2020).

5.2. Female are protected by HFD induced steatosis and abdominal fat accumulation

Obesity and MetS are described as a consequence of adipose tissue dysfunction and increase in waist circumference (Ghaben and Scherer, 2019). Using MRI, we found that both male and female mice fed with HFD exhibited increased in total hepatic lipid content in which females showed the highest response. Contrary to what was observed for % of hepatic lipid content at MRS, post-mortem IHC revealed higher and larger lipid droplets in male. As shown by Meda C, et al., under HFD in premenopausal female, liver reduce *denovo* lipogenesis and promote FA catabolism and by reducing lipid deposition, toxic accumulation of lipid droplet and circulating FA are lower (Meda et al., 2020). Similar effects were reported in the same study for cholesterol.

As for lipid droplet accumulation, in male intra-abdominal fat volume was definitely higher than in female, again confirming a sex dependent protection from HDF. This female result could be attributed to premenopausal lifetime in which female mice are studied and an effect associated with estrogen activity (Gambacciani et al., 1997; Clegg et al., 2007).

5.3. Brain metabolism and specific circuitry are modified in HFD induce metabolic syndrome

Using PET as an imaging tool and glucose analogue radiotracer [^{18}F]-FDG, it is possible to measure regional brain energy consumption related to glucose.

Results from brain PET [^{18}F]-FDG studies on obese or overweight subjects are heterogeneous and controversial. For example, whereas in the study of Volkow et al., BMI was negatively correlated with brain metabolism in prefrontal region, Wang et al., reported a positive correlation between brain FDG uptake and BMI (Wang et al., 2002; Volkow et al., 2009; Liu et al., 2017). Increased metabolism in posterior cingulum gyrus was also reported in sever obese woman in comparison with lean subjects' candidate that undergo to bariatric surgery (Marques et al., 2014; Rebelos et al., 2019; Nota et al., 2020). Sala et al. showed positive correlation between BMI and metabolic activity in aged female healthy volunteers (Sala et al., 2019). The heterogeneity of results and regional effect depends on the sampled population (BMI range, sex, age, presence of metabolic modifications and type of analysis: absolute quantification, SUV or relative FDG uptake). From group analysis, we found that in mice fed for 31 weeks with two regimens of HFD, the effect on FDG uptake depend on diet, time and sex. In particular, we failed to find any significant effects on global FDG uptake

measured as SUV if not at an early time after the beginning of HFD. No regional effect on SUV was present at regional level. When data were normalized for global uptake, we found after 31 weeks, a relative increase in the olfactory bulbs for male mice with both 45 and 60 HFD and only with the higher regimen in females. In fact, the olfactory bulb is connected with different brain regions including the olfactory cortex, hypothalamus, hippocampus, amygdala and cerebellum and participates in regulation of feeding behaviour. Recent findings demonstrated that this region participates to the regulation of peripheral metabolism and weight gain and this central role may explain both the increased metabolism as well as the positive association with peripheral markers observed in both females and male (Riera et al., 2017).

HFD affected also the anterior cortex and cerebellum producing a relative increment in the former and decrement in the latter. These data were confirmed by the correlation analysis showing that in male HFD, the redistribution of regional brain metabolism correlated all over the brain with BMI and peripheral metabolites except for hippocampus and hypothalamus whereas in females it was limited to selected brain regions and metabolite. In male the stronger associations were found for BMI and cholesterol and in females with ALT serum level.

All together, these finding indicated that male and female brain metabolism is differently affected by HFD and that the modification occurring reflect the sex driven response of periphery to a high fat dietetic regimen. This finding could be also associated with neural circuits involved in olfactory, sensory, reward and memory processing in which different cortical and subcortical regions are involved (Green et al., 2011; Blum et al., 2012).

5.4. Neuroinflammatory response are similar in HFD male and female mice

Low-grade neuroinflammation state in MetS has been also evaluated in our study using PET imaging [^{18}F]-VC701as radiopharmaceutical. [^{18}F]-VC701 is an agonist of TSPO receptor, whose levels increase on activated microglia/macrophages and astrocytes in response to neuronal or environmental injuries. This radiopharmaceutical has been developed in our laboratory and applied in different neuro-inflammatory conditions (Belloli et al., 2018; Murtaj et al., 2019).

Indeed, we showed that in both male and female HFD mice after longer exposure to HFD, neuroinflammation occurs, particularly for the 60HFD group but male start to show increased neuroinflammatory response earlier, starting from 12 weeks of HFD. Western blot data confirm

increased microglial activation in 60HFD male mice while female mice showed higher Iba-1 protein level in the 45HFD group.

To our knowledge, only one study explored brain inflammation using in vivo TSPO PET tool in HFD condition associated to AD and only in male mice, indicating increased TSPO uptake level associated to astrocyte and microglial activation in obese AD mice with transient response (Barron et al., 2016). Indeed, recent published article by Robinson and colleagues, investigate diet and metabolic status in AD mice under HFD condition including gender difference. Results showed that female HFD AD mice are more compromise than male HFD AD mice. Nevertheless, when compared control HFD male vs control HFD female, similar results were obtained as in our study, indicating male mice as more vulnerable sex, with more compromise glucose tolerance, major inflammatory reaction and greater liver dysfunction (Robison et al., 2020).

As for FDG, in male we found significant correlation between brain effect, BMI, peripheral metabolic markers associated with TSPO tracer. Indeed, in male brain region, we found a significant positive correlation between increase in TSPO tracer within the increase in glycaemia, BMI and serum level components, despite for HDL “the good cholesterol component”, which failed to significantly correlate as other biomarkers. On the contrary, female animals did not show any positive correlation despite a slight positive correlation with glycaemia.

Overall, our results indicate that HFD promotes brain inflammation and that in male this effect is associated with the peripheral response to the diet.

5.5. Anterior cortex revealed alteration in genome transcriptome and Akt activity upon HFD regimen

In order to better understand the molecular modification occurring in the anterior part of the cortex we performed a transcriptomic analysis on post-mortem specimens collected at 35 weeks after the beginning of the diet.

To our knowledge, a limited number of studies were focused on the effect of HFD of brain gene expression profile and none of them included the evaluation of sex effect. Results of one study focused on the hippocampus of female mice fed for 8 weeks with western diet showed an increase of transcript linked to blood brain barrier (BBB) integrity and cognition. Modifications of gene transcripts associated with cognition and neuroinflammation including triggering receptors expressed on myeloid cells 2 (TREM2), were reported in the cortex of AD mice fed with HFD for

three months. Finally, a study conducted in mice treated with 60% HFD in which miRNA expression in the prefrontal cortex was investigated, revealed that several miRNAs were differentially expressed upon HFD regimen. Pathways that were found mainly belong to Axon guidance Signalling, Insulin Growth-Factor 1 (IGF 1) Signalling and Nerve Growth-Factor (NGF) Signalling (Nam et al., 2017; Sonne et al., 2017; Labouesse et al., 2018; Nuthikattu et al., 2019; Valcarcel-Ares et al., 2019). As stated, our study represents the first one in which a bulk anterior cortex transcriptomic analysis was performed after a prolonged HFD exposure in male and female mice. First, both HFD regimens affect gene transcript in male and female anterior cortex. From Gene Ontology analysis, data showed a down regulation of *synaptic vesicle cycle pathway,* commonly to male and female. On the contrary, male showed a down regulation of transcript part of *nervous system development and synaptic vesicle cycle* whereas in female *positive regulation of neuron projection development, GABAergic synapses* were affected. Comparison analysis between male and female showed a common effect on reduced transcriptome profile of gene. In female up-regulated genes belonged to the "*response to glucagon*" ontogeny group, whereas in male, they were associated with "*positive regulation of muscle differentiation*". The first include gene transcript associate with glucagon effect, brain metabolism and cell functions (de Mooij-van Malsen et al., 2009; Jin et al., 2013; Wolf et al., 2014; Grieco et al., 2019) whereas the latter gene transcript involved in neurite outgrowth, cell differentiation and regulation of splicing mechanism including these related to tau protein isoform (Meda et al., 2000; Kar et al., 2006; Tarn et al., 2016) or synaptic plasticity (Mouton-Liger et al., 2020). This sex dependent signature might explain the different metabolic response observed in the anterior cortex of male mice in comparison with female HFD. On the other hand, the regional regulation of brain metabolism during IR represents an emerging issue for the potential impact on prevention and treatment development for AD. For this reason, the selected upregulation observed in female and male suggest a sex specific response and consequently vulnerability of brain to MetS and IR.

It has been established that glucagon, in particular GLP-1 is released from gut cells and can control glycaemia via increased insulin activity and glucagon secretion inhibition. Food intake and weight gain is also inhibited by GLP-1 (Drucker, 2018). Moreover, GLP-1 is linked to the vagal afferents that mediated satiety and it is known that obesity is characterized by the gut-brain axis dysfunction. In fact, study demonstrated that HFD could impair vagal signalling on GLP-1 activity with the result of

impaired satiety in obesity state (Al Helaili et al., 2020). Regarding what observed in our study, we could hypothesize that female mice seem to be involved in glucagon activity regulation perhaps involved in the regulation of food intake and satiety. Further studies needed to confirm and elucidate this peculiar aspect found in the study.

Finally, from anterior cortex tissue, we also analysed AKT protein level and its phosphorylation form as implicated in a variety of mechanisms associated with IR. It has been demonstrated that AKT regulates body size and adipogenesis, which damage mechanism leads to IR and diabetes. AKT is also expressed at neuronal level acting on synapses, cell survival and growth. Recent findings linked AKT to the astrocyte role in regulating glucose metabolism. In fact, AKT and pAKT regulate glycogen synthesis upon Adenosine Monophosphate-activated Protein Kinase (AMPK) orchestration via monitoring ATP/ADP ratio. Cholesterol sulphate altered this astrocyte mechanism leading to an increase in glycogen storage which acted on an increase in ATP production that might be neuroprotective. Moreover, our study revealed a significant increase in total AKT and pAKT in female mice in anterior cortex which could be related to the failed observation in glucose metabolism increase found in anterior cortex, as on contrary, seen in male mice. In fact, recent study reported that upregulation of AKT and downregulation of AMPK improve IR in the hypothalamus exerted by HFD. This aspect should be deeper analysed to understand potential protective role of AKT in astrocyte mediated glucose metabolism and specific sex different mechanism (Xu et al., 2018; Prah et al., 2019).

5.6. Explorative analysis on brain connectome revealed HFD modulation

Regulation of eating behaviour is a complex mechanism and involves different populations of neurons and the activity of selected neurotransmitters. The smell of food is processed by the olfactory bulb and its projection to the insula and prefrontal cortex. Specifically, OFC project to striatum inducing modification of neuronal activity in striato-hypothalamic and striato-pallidal circuits which are influenced by dopaminergic inputs and to the lateral hypothalamus (Cooper, 1986; Levin and Routh, 1996; Pak et al., 2018). Dopamine is implicated in the reward system including neurons from the VTA, which increases dopamine neurons activity after exposure to food into the ventral striatum (Norgren et al., 2006; Wise, 2006). However, chronic exposure to a food reward may promote adaptation of dopamine neurons activation with a consequence in

remodulation or alteration of brain circuits involved in food processing and reward systems (Schultz, 2010). PET imaging has been used to explore the effect of obesity on brain functional connectivity using PET and FDG as radioligand (Pak et al., 2018).

To test this hypothesis, we explore, although in a limited sample for type of analysis, the HFD induced modification in functional connectivity of the mouse brain. In particular, we performed a population study of functional correlations obtained from the [^{18}F]-FDG roi-roi analysis including pooled data of both sexes in the analysis. Preliminary results that we obtain, indicate two negative associations occurring in cortico-thalamic and cortico-brainstem connectivity present independently from time or diet. On the other hand, at 31 weeks post HFD, we found strong positive correlation in both HFDs group compared to STD within the olfactory bulb-anterior cortex region, which could be hypothesized to be related to the food smell processing enhancing its activity and confirming increased glucose uptake in the olfactory bulb observed in PET study, in male and female HFD mice. Moreover, at the same time point in the HFD group, amygdala was found to be negatively correlated with the cortex while positively with the hypothalamus, the brain region that regulates energy dependent feeding behaviour. Interestingly, recent study showed a brain circuit regulating feeding behaviour involving the insular cortex, the central nucleus of the amygdala and hypothalamic nuclear complex (Barbier et al., 2020). The increased connectivity present in HFD mice suggest and modified activity of these brain regions after a prolonged exposure to HFD.

Summarizing, preliminary results obtained from brain regions metabolic correlation with the limitation in sample size and lower [^{18}F]-PET imaging sensitivity and resolution, were able to provide a start point to further investigation on the effect of HFD on brain connectivity. From our exploratory analysis, several regions have been shown to be modulated by HFD. Interestingly, these regions are included in specific brain circuits involved in both energy and hedonic dependent feeding behaviour.

5.7. Limitation of the study and future directions

In our work we deeply characterize mouse model of obesity induced by two type of HFD mimicking modern western diet in which sex difference was deeply investigated. Nevertheless, study showed some limitations including lower sample size used for specific analysis such as brain metabolic connectivity and transcriptomic analysis of anterior cortex. For both, further studies are necessary to confirm the data obtained. For the transcriptomic study, genes that were modulated upon diet regimen should be verify using qRT-PCR, while for the brain connectivity, additional analysis should

be address in a well-design experiment with enough sample size to discover specific neural circuitry modulating feeding behaviour and gender response involved in cognitive function that could be related to obesity state. Those results should be considered as preliminary data and a start point for further investigation in which a deep comprehension of brain biology is needed.

Moreover, data obtained from female mice showed high variability, especially in the liver analysis of lipid content. In our study, female mice were not synchronized for the oestrous cycle or divided into different oestrous cycle phases that could modulate hepatic metabolism associated with different fertile periods of the female mice as reported in literature (Meda et al., 2020).

6. CONCLUSION

Summarizing, during my PhD work, I investigate sex difference response induced by systemic inflammation in young and aged mice and in a metabolic syndrome model induced by HFD chronic exposure applying multimodal imaging tools and molecular biology approach. From results obtained, sex difference and aging play a crucial role in regulation of several biological pathways including neuroinflammation, glucose metabolism and gene expression. Overall, this study aims to describe several biological questions regarding differences in sex response to metabolic syndrome.

The novelty of the research concerns the investigation in sex differences in response to HFD by applying in vivo non-invasive tool such as PET with difference radioligand and by using transcriptomic profile to study gene expression changes upon such regimen, as few published studies have been addressed to these topics. Our results could contribute to the knowledge of understanding complex syndrome in a sex specific manner.

Altogether, data obtained confirm that male mice are more vulnerable to develop IR and obesity, while female mice are somehow protected in a premenopausal period of life and this has an impact also on the brain.

For the first time to our knowledge, we reported transcriptome data from bulk tissue of male and female HFD mice, focusing on anterior cortex as brain region involved in plenty of mechanisms associated with several neural circuits and in cognition. We found pronounced down regulation of several genes involved in the nervous system development for both sexes and, interestingly, for female mice we found an upregulation of glucagon response which could be related to food intake regulation and exert some protective role that needs further elucidation.

In conclusion, future study should be directed on the sex dysmorphism in different pathology to better understand physiological aspect and to properly address sex-based therapy in human being.

7. ACKNOWLEDGEMENT

This work was supported by “AMANDA”: Abnormal metabolic states, cellular stressors and neurodegenerative processes”- Regione Lombardia, by the Italian Ministry of University and Research (MIUR) - Department of Excellence project PREMIA (PREcision MedIcine Approach: bringing biomarker research to clinic) and to Euro-BioImaging (www.eurobioimaging.eu) for providing access to imaging technologies and services via the MultiModal Molecular Imaging Italian Node (Italy).

The published work in Frontiers Aging Neuroscience was supported by the Project of the MIUR “Identification, validation and commercial development of new diagnostic and prognostic biomarkers for complex trait diseases (IVASCOMAR)” and by the European Union’s Seventh Framework Programme (FP7/2007-2013) under grant agreement in HEALTH-F2-2011-278850 (INMiND).

8. REFERENCES

Abizaid, A., Liu, Z.-W., Andrews, Z. B., Shanabrough, M., Borok, E., Elsworth, J. D., et al. (2006). Ghrelin modulates the activity and synaptic input organization of midbrain dopamine neurons while promoting appetite. *The Journal of Clinical Investigation* 116, 3229–3239. doi:10.1172/JCI29867.

Adler, E. S., Hollis, J. H., Clarke, I. J., Grattan, D. R., and Oldfield, B. J. (2012). Neurochemical characterization and sexual dimorphism of projections from the brain to abdominal and subcutaneous white adipose tissue in the rat. *J Neurosci* 32, 15913–15921. doi:10.1523/JNEUROSCI.2591-12.2012.

Agustí, A., García-Pardo, M. P., López-Almela, I., Campillo, I., Maes, M., Romaní-Pérez, M., et al. (2018). Interplay Between the Gut-Brain Axis, Obesity and Cognitive Function. *Frontiers in Neuroscience* 12, 155. doi:10.3389/fnins.2018.00155.

Al Helaili, A., Park, S. J., and Beyak, M. J. (2020). Chronic high fat diet impairs glucagon like peptide-1 sensitivity in vagal afferents. *Biochem Biophys Res Commun*. doi:10.1016/j.bbrc.2020.08.045.

Allison, D. B., Kaprio, J., Korkeila, M., Koskenvuo, M., Neale, M. C., and Hayakawa, K. (1996). The heritability of body mass index among an international sample of monozygotic twins reared apart. *Int J Obes Relat Metab Disord* 20, 501–506.

Amaro, E., and Barker, G. J. (2006). Study design in fMRI: basic principles. *Brain and Cognition* 60, 220–232. doi:10.1016/j.bandc.2005.11.009.

Argente-Arizón, P., Díaz, F., Ros, P., Barrios, V., Tena-Sempere, M., García-Segura, L. M., et al. (2018). The Hypothalamic Inflammatory/Gliosis Response to Neonatal Overnutrition Is Sex and Age Dependent. *Endocrinology* 159, 368–387. doi:10.1210/en.2017-00539.

Bachiller, S., Jiménez-Ferrer, I., Paulus, A., Yang, Y., Swanberg, M., Deierborg, T., et al. (2018). Microglia in Neurological Diseases: A Road Map to Brain-Disease Dependent-Inflammatory Response. *Frontiers in Cellular Neuroscience* 12, 488. doi:10.3389/fncel.2018.00488.

Bae, C. S., and Song, J. (2017). The Role of Glucagon-Like Peptide 1 (GLP1) in Type 3 Diabetes: GLP-1 Controls Insulin Resistance, Neuroinflammation and Neurogenesis in the Brain. *International Journal of Molecular Sciences* 18. doi:10.3390/ijms18112493.

Barberger-Gateau, P., Samieri, C., Féart, C., and Plourde, M. (2011). Dietary omega 3 polyunsaturated fatty acids and Alzheimer's disease: interaction with apolipoprotein E genotype. *Current Alzheimer Research* 8, 479–491. doi:10.2174/156720511796391926.

Barbier, M., Chometton, S., Pautrat, A., Miguet-Alfonsi, C., Datiche, F., Gascuel, J., et al. (2020). A basal ganglia-like cortical-amygdalar-hypothalamic network mediates feeding behavior. *Proc Natl Acad Sci U S A* 117, 15967–15976. doi:10.1073/pnas.2004914117.

Bassareo, V., and Di Chiara, G. (1999). Modulation of feeding-induced activation of mesolimbic dopamine transmission by appetitive stimuli and its relation to motivational state. *The European Journal of Neuroscience* 11, 4389–4397. doi:10.1046/j.1460-9568.1999.00843.x.

Beery, A. K., and Zucker, I. (2011). Sex bias in neuroscience and biomedical research. *Neurosci Biobehav Rev* 35, 565–572. doi:10.1016/j.neubiorev.2010.07.002.

Bell, C. G., Finer, S., Lindgren, C. M., Wilson, G. A., Rakyan, V. K., Teschendorff, A. E., et al. (2010). Integrated genetic and epigenetic analysis identifies haplotype-specific methylation in the FTO type 2 diabetes and obesity susceptibility locus. *PLoS One* 5, e14040. doi:10.1371/journal.pone.0014040.

Belloli, S., Zanotti, L., Murtaj, V., Mazzon, C., Di Grigoli, G., Monterisi, C., et al. (2018). 18F-VC701-PET and MRI in the in vivo neuroinflammation assessment of a mouse model of multiple sclerosis. *J Neuroinflammation* 15, 33. doi:10.1186/s12974-017-1044-x.

Bercik, P., Verdu, E. F., Foster, J. A., Macri, J., Potter, M., Huang, X., et al. (2010). Chronic gastrointestinal inflammation induces anxiety-like behavior and alters central nervous system biochemistry in mice. *Gastroenterology* 139, 2102-2112.e1. doi:10.1053/j.gastro.2010.06.063.

Berghöfer, B., Frommer, T., Haley, G., Fink, L., Bein, G., and Hackstein, H. (2006). TLR7 ligands induce higher IFN-alpha production in females. *J Immunol* 177, 2088–2096. doi:10.4049/jimmunol.177.4.2088.

Bhurosy, T., and Jeewon, R. (2014). Overweight and obesity epidemic in developing countries: a problem with diet, physical activity, or socioeconomic status? *TheScientificWorldJournal* 2014, 964236. doi:10.1155/2014/964236.

Blanquet, M., Legrand, A., Pélissier, A., and Mourgues, C. (2019). Socio-economics status and metabolic syndrome: A meta-analysis. *Diabetes & Metabolic Syndrome* 13, 1805–1812. doi:10.1016/j.dsx.2019.04.003.

Blotnick E, Anglister L. Exercise modulates synaptic acetylcholinesterase at neuromuscular junctions. Neuroscience. 2016 Apr 5;319:221-32. doi: 10.1016/j.neuroscience.2016.01.044. Epub 2016 Jan 25. PMID: 26820598.

Blum, K., Gardner, E., Oscar-Berman, M., and Gold, M. (2012). "Liking" and "wanting" linked to Reward Deficiency Syndrome (RDS): hypothesizing differential responsivity in brain reward circuitry. *Curr Pharm Des* 18, 113–118. doi:10.2174/138161212798919110.

Bochukova, E. G., Lawler, K., Croizier, S., Keogh, J. M., Patel, N., Strohbehn, G., et al. (2018). A Transcriptomic Signature of the Hypothalamic Response to Fasting and BDNF Deficiency in Prader-Willi Syndrome. *Cell Rep* 22, 3401–3408. doi:10.1016/j.celrep.2018.03.018.

Bonnefond, A., Raimondo, A., Stutzmann, F., Ghoussaini, M., Ramachandrappa, S., Bersten, D. C., et al. (2013). Loss-of-function mutations in SIM1 contribute to obesity and Prader-Willi-like features. *J Clin Invest* 123, 3037–3041. doi:10.1172/JCI68035.

Briançon-Marjollet, A., Pépin, J.-L., Weiss, J. W., Lévy, P., and Tamisier, R. (2014). Intermittent hypoxia upregulates serum VEGF. *Sleep Medicine* 15, 1425–1426. doi:10.1016/j.sleep.2014.07.006.

Barron, A. M., Tokunaga, M., Zhang, M.-R., Ji, B., Suhara, T., and Higuchi, M. (2016). Assessment of neuroinflammation in a mouse model of obesity and β-amyloidosis using PET. *Journal of Neuroinflammation* 13, 221. doi:10.1186/s12974-016-0700-x.

Brüning, J. C., Gautam, D., Burks, D. J., Gillette, J., Schubert, M., Orban, P. C., et al. (2000). Role of brain insulin receptor in control of body weight and reproduction. *Science (New York, N.Y.)* 289, 2122–2125. doi:10.1126/science.289.5487.2122.

Bryant, N. J., Govers, R., and James, D. E. (2002). Regulated transport of the glucose transporter GLUT4. *Nature Reviews. Molecular Cell Biology* 3, 267–277. doi:10.1038/nrm782.

Buckman, L. B., Hasty, A. H., Flaherty, D. K., Buckman, C. T., Thompson, M. M., Matlock, B. K., et al. (2014). Obesity induced by a high-fat diet is associated with increased immune cell entry into the central nervous system. *Brain, Behavior, and Immunity* 35, 33–42. doi:10.1016/j.bbi.2013.06.007.

Byrne, C. D., and Targher, G. (2015). NAFLD: A multisystem disease. *Journal of Hepatology* 62, S47–S64. doi:10.1016/j.jhep.2014.12.012.

Cahill, G. F. (2006). Fuel metabolism in starvation. *Annual Review of Nutrition* 26, 1–22. doi:10.1146/annurev.nutr.26.061505.111258.

Carnell, S., Gibson, C., Benson, L., Ochner, C. N., and Geliebter, A. (2012). Neuroimaging and obesity: current knowledge and future directions. *Obesity Reviews: An Official Journal of the International Association for the Study of Obesity* 13, 43–56. doi:10.1111/j.1467-789X.2011.00927.x.

Cavaliere C, Tramontano L, Fiorenza D, Alfano V, Aiello M, Salvatore M. Gliosis and Neurodegenerative Diseases: The Role of PET and MR Imaging. Front Cell Neurosci. 2020 Apr 2;14:75. doi: 10.3389/fncel.2020.00075. PMID: 32327973; PMCID: PMC7161920.

Challis, B. G., Coll, A. P., Yeo, G. S. H., Pinnock, S. B., Dickson, S. L., Thresher, R. R., et al. (2004). Mice lacking pro-opiomelanocortin are sensitive to high-fat feeding but respond normally to the acute anorectic effects of peptide-YY(3-36). *Proc Natl Acad Sci U S A* 101, 4695–4700. doi:10.1073/pnas.0306931101.

Cho, N. H., Shaw, J. E., Karuranga, S., Huang, Y., da Rocha Fernandes, J. D., Ohlrogge, A. W., et al. (2018). IDF Diabetes Atlas: Global estimates of diabetes prevalence for 2017 and projections for 2045. *Diabetes Research and Clinical Practice* 138, 271–281. doi:10.1016/j.diabres.2018.02.023.

Chobanian, A. V., Bakris, G. L., Black, H. R., Cushman, W. C., Green, L. A., Izzo, J. L., et al. (2003). Seventh report of the Joint National Committee on Prevention, Detection, Evaluation, and Treatment of High Blood Pressure. *Hypertension (Dallas, Tex.: 1979)* 42, 1206–1252. doi:10.1161/01.HYP.0000107251.49515.c2.

Chua, S. C., Chung, W. K., Wu-Peng, X. S., Zhang, Y., Liu, S. M., Tartaglia, L., et al. (1996). Phenotypes of mouse diabetes and rat fatty due to mutations in the OB (leptin) receptor. *Science* 271, 994–996. doi:10.1126/science.271.5251.994.

Cildir, G., Akıncılar, S. C., and Tergaonkar, V. (2013). Chronic adipose tissue inflammation: all immune cells on the stage. *Trends in Molecular Medicine* 19, 487–500. doi:10.1016/j.molmed.2013.05.001.

Cioffi, S., Martucciello, S., Fulcoli, F. G., Bilio, M., Ferrentino, R., Nusco, E., et al. (2014). Tbx1 regulates brain vascularization. *Hum Mol Genet* 23, 78–89. doi:10.1093/hmg/ddt400.

Clarke, R. E., Verdejo-Garcia, A., and Andrews, Z. B. (2018). The role of corticostriatal-hypothalamic neural circuits in feeding behaviour: implications for obesity. *Journal of Neurochemistry* 147, 715–729. doi:10.1111/jnc.14455.

Clegg, D. J., Brown, L. M., Zigman, J. M., Kemp, C. J., Strader, A. D., Benoit, S. C., et al. (2007). Estradiol-dependent decrease in the orexigenic potency of ghrelin in female rats. *Diabetes* 56, 1051–1058. doi:10.2337/db06-0015.

Clegg, D. J., Gotoh, K., Kemp, C., Wortman, M. D., Benoit, S. C., Brown, L. M., et al. (2011). Consumption of a high-fat diet induces central insulin resistance independent of adiposity. *Physiol Behav* 103, 10–16. doi:10.1016/j.physbeh.2011.01.010.

Cooper, S. J. (1986). Beta-carbolines characterized as benzodiazepine receptor agonists and inverse agonists produce bi-directional changes in palatable food consumption. *Brain Res Bull* 17, 627–637. doi:10.1016/0361-9230(86)90194-2.

Craft, S., Baker, L. D., Montine, T. J., Minoshima, S., Watson, G. S., Claxton, A., et al. (2012). Intranasal insulin therapy for Alzheimer disease and amnestic mild cognitive impairment: a pilot clinical trial. *Archives of Neurology* 69, 29–38. doi:10.1001/archneurol.2011.233.

De Felice, F. G. (2013). Alzheimer's disease and insulin resistance: translating basic science into clinical applications. *The Journal of Clinical Investigation* 123, 531–539. doi:10.1172/JCI64595.

de Mooij-van Malsen, A. J. G., van Lith, H. A., Oppelaar, H., Hendriks, J., de Wit, M., Kostrzewa, E., et al. (2009). Interspecies trait genetics reveals association of Adcy8 with mouse avoidance behavior and a human mood disorder. *Biol Psychiatry* 66, 1123–1130. doi:10.1016/j.biopsych.2009.06.016.

De Souza, C. T., Araujo, E. P., Bordin, S., Ashimine, R., Zollner, R. L., Boschero, A. C., et al. (2005). Consumption of a fat-rich diet activates a proinflammatory response and induces insulin resistance in the hypothalamus. *Endocrinology* 146, 4192–4199. doi:10.1210/en.2004-1520.

Deeds, M. C., Anderson, J. M., Armstrong, A. S., Gastineau, D. A., Hiddinga, H. J., Jahangir, A., et al. (2011). Single dose streptozotocin-induced diabetes: considerations for study design in islet transplantation models. *Lab Anim* 45, 131–140. doi:10.1258/la.2010.010090.

Della Torre, S., and Maggi, A. (2017). Sex Differences: A Resultant of an Evolutionary Pressure? *Cell Metab* 25, 499–505. doi:10.1016/j.cmet.2017.01.006.

Della Torre, S., Mitro, N., Meda, C., Lolli, F., Pedretti, S., Barcella, M., et al. (2018). Short-Term Fasting Reveals Amino Acid Metabolism as a Major Sex-Discriminating Factor in the Liver. *Cell Metab* 28, 256-267.e5. doi:10.1016/j.cmet.2018.05.021.

Delrue, M.-A., and Michaud, J. L. (2004). Fat chance: genetic syndromes with obesity. *Clinical Genetics* 66, 83–93. doi:10.1111/j.0009-9163.2004.00300.x.

Di Grigoli, G., Monterisi, C., Belloli, S., Masiello, V., Politi, L. S., Valenti, S., et al. (2015). Radiosynthesis and Preliminary Biological Evaluation of [18F]VC701, a Radioligand for Translocator Protein. *Mol Imaging* 14. doi:10.2310/7290.2015.00007.

Divoux, A., Tordjman, J., Lacasa, D., Veyrie, N., Hugol, D., Aissat, A., et al. (2010). Fibrosis in human adipose tissue: composition, distribution, and link with lipid metabolism and fat mass loss. *Diabetes* 59, 2817–2825. doi:10.2337/db10-0585.

Drucker, D. J. (2018). Mechanisms of Action and Therapeutic Application of Glucagon-like Peptide-1. *Cell Metab* 27, 740–756. doi:10.1016/j.cmet.2018.03.001.

Du L, Jiang Y, Sun Y. Astrocyte-derived exosomes carry microRNA-17-5p to protect neonatal rats from hypoxic-ischemic brain damage via inhibiting BNIP-2 expression. Neurotoxicology. 2020 Dec 10:S0161-813X(20)30213-8. doi: 10.1016/j.neuro.2020.12.006. Epub ahead of print. PMID: 33309839.

Eckel, R. H., Grundy, S. M., and Zimmet, P. Z. (2005). The metabolic syndrome. *Lancet (London, England)* 365, 1415–1428. doi:10.1016/S0140-6736(05)66378-7.

Enriori, P. J., Evans, A. E., Sinnayah, P., and Cowley, M. A. (2006). Leptin resistance and obesity. *Obesity (Silver Spring, Md.)* 14 Suppl 5, 254S-258S. doi:10.1038/oby.2006.319.

Færch, K., Torekov, S. S., Vistisen, D., Johansen, N. B., Witte, D. R., Jonsson, A., et al. (2015). GLP-1 Response to Oral Glucose Is Reduced in Prediabetes, Screen-Detected Type 2 Diabetes, and Obesity and Influenced by Sex: The ADDITION-PRO Study. *Diabetes* 64, 2513–2525. doi:10.2337/db14-1751.

Farooqi, I. S., Keogh, J. M., Yeo, G. S. H., Lank, E. J., Cheetham, T., and O'Rahilly, S. (2003). Clinical spectrum of obesity and mutations in the melanocortin 4 receptor gene. *N Engl J Med* 348, 1085–1095. doi:10.1056/NEJMoa022050.

Fesinmeyer, M. D., North, K. E., Ritchie, M. D., Lim, U., Franceschini, N., Wilkens, L. R., et al. (2013). Genetic risk factors for BMI and obesity in an ethnically diverse population: results from the population architecture using genomics and epidemiology (PAGE) study. *Obesity (Silver Spring)* 21, 835–846. doi:10.1002/oby.20268.

Forrester, S. J., Kikuchi, D. S., Hernandes, M. S., Xu, Q., and Griendling, K. K. (2018). Reactive Oxygen Species in Metabolic and Inflammatory Signaling. *Circ Res* 122, 877–902. doi:10.1161/CIRCRESAHA.117.311401.

Foster, J. A., Rinaman, L., and Cryan, J. F. (2017). Stress & the gut-brain axis: Regulation by the microbiome. *Neurobiology of Stress* 7, 124–136. doi:10.1016/j.ynstr.2017.03.001.

Frayling, T. M., Timpson, N. J., Weedon, M. N., Zeggini, E., Freathy, R. M., Lindgren, C. M., et al. (2007). A common variant in the FTO gene is associated with body mass index and predisposes to childhood and adult obesity. *Science* 316, 889–894. doi:10.1126/science.1141634.

Freire-Regatillo, A., Fernández-Gómez, M. J., Díaz, F., Barrios, V., Sánchez-Jabonero, I., Frago, L. M., et al. (2020). Sex differences in the peripubertal response to a short-term, high-fat diet intake. *J Neuroendocrinol* 32, e12756. doi:10.1111/jne.12756.

Gadian, D. G., and Radda, G. K. (1981). NMR studies of tissue metabolism. *Annual Review of Biochemistry* 50, 69–83. doi:10.1146/annurev.bi.50.070181.000441.

Gambacciani, M., Ciaponi, M., Cappagli, B., Piaggesi, L., De Simone, L., Orlandi, R., et al. (1997). Body weight, body fat distribution, and hormonal replacement therapy in early postmenopausal women. *J Clin Endocrinol Metab* 82, 414–417. doi:10.1210/jcem.82.2.3735.

Gardner, C. D., Trepanowski, J. F., Del Gobbo, L. C., Hauser, M. E., Rigdon, J., Ioannidis, J. P. A., et al. (2018). Effect of Low-Fat vs Low-Carbohydrate Diet on 12-Month Weight Loss in Overweight Adults and the Association With Genotype Pattern or Insulin Secretion: The DIETFITS Randomized Clinical Trial. *JAMA* 319, 667–679. doi:10.1001/jama.2018.0245.

Gautier, J. F., Chen, K., Salbe, A. D., Bandy, D., Pratley, R. E., Heiman, M., et al. (2000). Differential brain responses to satiation in obese and lean men. *Diabetes* 49, 838–846. doi:10.2337/diabetes.49.5.838.

Ghaben, A. L., and Scherer, P. E. (2019). Adipogenesis and metabolic health. *Nature Reviews. Molecular Cell Biology* 20, 242–258. doi:10.1038/s41580-018-0093-z.

Gluck, M. E., Viswanath, P., and Stinson, E. J. (2017). Obesity, Appetite, and the Prefrontal Cortex. *Current Obesity Reports* 6, 380–388. doi:10.1007/s13679-017-0289-0.

Goshu, E., Jin, H., Fasnacht, R., Sepenski, M., Michaud, J. L., and Fan, C.-M. (2002). Sim2 mutants have developmental defects not overlapping with those of Sim1 mutants. *Mol Cell Biol* 22, 4147–4157. doi:10.1128/mcb.22.12.4147-4157.2002.

Green, E., Jacobson, A., Haase, L., and Murphy, C. (2011). Reduced nucleus accumbens and caudate nucleus activation to a pleasant taste is associated with obesity in older adults. *Brain Res* 1386, 109–117. doi:10.1016/j.brainres.2011.02.071.

Greenberg, A. S., and Obin, M. S. (2006). Obesity and the role of adipose tissue in inflammation and metabolism. *The American Journal of Clinical Nutrition* 83, 461S-465S. doi:10.1093/ajcn/83.2.461S.

Grieco, M., Giorgi, A., Gentile, M. C., d'Erme, M., Morano, S., Maras, B., et al. (2019). Glucagon-Like Peptide-1: A Focus on Neurodegenerative Diseases. *Front Neurosci* 13, 1112. doi:10.3389/fnins.2019.01112.

Gürtler, A., Kunz, N., Gomolka, M., Hornhardt, S., Friedl, A. A., McDonald, K., et al. (2013). Stain-Free technology as a normalization tool in Western blot analysis. *Anal Biochem* 433, 105–111. doi:10.1016/j.ab.2012.10.010.

Guzzardi, M. A., Garelli, S., Agostini, A., Filidei, E., Fanelli, F., Giorgetti, A., et al. (2018). Food addiction distinguishes an overweight phenotype that can be reversed by low calorie diet. *European Eating Disorders Review: The Journal of the Eating Disorders Association* 26, 657–670. doi:10.1002/erv.2652.

Guzzardi, M. A., and Iozzo, P. (2019). Brain functional imaging in obese and diabetic patients. *Acta Diabetologica* 56, 135–144. doi:10.1007/s00592-018-1185-0.

Haggarty, P. (2013). Epigenetic consequences of a changing human diet. *Proc Nutr Soc* 72, 363–371. doi:10.1017/S0029665113003376.

Haltia, L. T., Rinne, J. O., Merisaari, H., Maguire, R. P., Savontaus, E., Helin, S., et al. (2007). Effects of intravenous glucose on dopaminergic function in the human brain in vivo. *Synapse (New York, N.Y.)* 61, 748–756. doi:10.1002/syn.20418.

Harding, I. H., Andrews, Z. B., Mata, F., Orlandea, S., Martínez-Zalacaín, I., Soriano-Mas, C., et al. (2018). Brain substrates of unhealthy versus healthy food choices: influence of homeostatic status and body mass index. *International Journal of Obesity (2005)* 42, 448–454. doi:10.1038/ijo.2017.237.

Hare, T. A., Camerer, C. F., and Rangel, A. (2009). Self-control in decision-making involves modulation of the vmPFC valuation system. *Science (New York, N.Y.)* 324, 646–648. doi:10.1126/science.1168450.

Hariri, N., and Thibault, L. (2010). High-fat diet-induced obesity in animal models. *Nutr Res Rev* 23, 270–299. doi:10.1017/S0954422410000168.

Hartimath, S. V., Khanapur, S., Boominathan, R., Jiang, L., Cheng, P., Yong, F. F., et al. (2019). Imaging adipose tissue browning using the TSPO-18kDa tracer [18F]FEPPA. *Molecular Metabolism* 25, 154–158. doi:10.1016/j.molmet.2019.05.003.

Hatting, M., Tavares, C. D. J., Sharabi, K., Rines, A. K., and Puigserver, P. (2018). Insulin regulation of gluconeogenesis. *Annals of the New York Academy of Sciences* 1411, 21–35. doi:10.1111/nyas.13435.

Hauger, R. L., Olivares-Reyes, J. A., Dautzenberg, F. M., Lohr, J. B., Braun, S., and Oakley, R. H. (2012). Molecular and cell signaling targets for PTSD pathophysiology and pharmacotherapy. *Neuropharmacology* 62, 705–714. doi:10.1016/j.neuropharm.2011.11.007.

Hers, I., Vincent, E. E., and Tavaré, J. M. (2011). Akt signalling in health and disease. *Cell Signal* 23, 1515–1527. doi:10.1016/j.cellsig.2011.05.004.

Hirvonen, J., Virtanen, K. A., Nummenmaa, L., Hannukainen, J. C., Honka, M.-J., Bucci, M., et al. (2011). Effects of insulin on brain glucose metabolism in impaired glucose tolerance. *Diabetes* 60, 443–447. doi:10.2337/db10-0940.

Hollmann, M., Hellrung, L., Pleger, B., Schlögl, H., Kabisch, S., Stumvoll, M., et al. (2012). Neural correlates of the volitional regulation of the desire for food. *International Journal of Obesity (2005)* 36, 648–655. doi:10.1038/ijo.2011.125.

Holloway, C. J., Cochlin, L. E., Emmanuel, Y., Murray, A., Codreanu, I., Edwards, L. M., et al. (2011). A high-fat diet impairs cardiac high-energy phosphate metabolism and cognitive function in healthy human subjects. *The American Journal of Clinical Nutrition* 93, 748–755. doi:10.3945/ajcn.110.002758.

Horwitz, B., Duara, R., and Rapoport, S. I. (1984). Intercorrelations of glucose metabolic rates between brain regions: application to healthy males in a state of reduced sensory input. *J Cereb Blood Flow Metab* 4, 484–499. doi:10.1038/jcbfm.1984.73.

Hotamisligil, G. S. (2010). Endoplasmic reticulum stress and the inflammatory basis of metabolic disease. *Cell* 140, 900–917. doi:10.1016/j.cell.2010.02.034.

Hu, S., Wang, L., Yang, D., Li, L., Togo, J., Wu, Y., et al. (2018). Dietary Fat, but Not Protein or Carbohydrate, Regulates Energy Intake and Causes Adiposity in Mice. *Cell Metabolism* 28, 415-431.e4. doi:10.1016/j.cmet.2018.06.010.

Huang, S., Rutkowsky, J. M., Snodgrass, R. G., Ono-Moore, K. D., Schneider, D. A., Newman, J. W., et al. (2012). Saturated fatty acids activate TLR-mediated proinflammatory signaling pathways. *Journal of Lipid Research* 53, 2002–2013. doi:10.1194/jlr.D029546.

Huangfu N, Zheng W, Xu Z, Wang S, Wang Y, Cheng J, Li Z, Cheng K, Zhang S, Chen X, Zhu J. RBM4 regulates M1 macrophages polarization through targeting STAT1-mediated glycolysis. Int Immunopharmacol. 2020 Jun;83:106432. doi: 10.1016/j.intimp.2020.106432. Epub 2020 Apr 2. PMID: 32248017.

Huszar, D., Lynch, C. A., Fairchild-Huntress, V., Dunmore, J. H., Fang, Q., Berkemeier, L. R., et al. (1997). Targeted disruption of the melanocortin-4 receptor results in obesity in mice. *Cell* 88, 131–141. doi:10.1016/s0092-8674(00)81865-6.

Hwang, L.-L., Wang, C.-H., Li, T.-L., Chang, S.-D., Lin, L.-C., Chen, C.-P., et al. (2010). Sex differences in high-fat diet-induced obesity, metabolic alterations and learning, and synaptic plasticity deficits in mice. *Obesity (Silver Spring)* 18, 463–469. doi:10.1038/oby.2009.273.

Ingelsson, E., and McCarthy, M. I. (2018). Human Genetics of Obesity and Type 2 Diabetes Mellitus: Past, Present, and Future. *Circ Genom Precis Med* 11, e002090. doi:10.1161/CIRCGEN.118.002090.

Iozzo, P., Guiducci, L., Guzzardi, M. A., and Pagotto, U. (2012). Brain PET imaging in obesity and food addiction: current evidence and hypothesis. *Obesity Facts* 5, 155–164. doi:10.1159/000338328.

Ipsen, D. H., Lykkesfeldt, J., and Tveden-Nyborg, P. (2018). Molecular mechanisms of hepatic lipid accumulation in non-alcoholic fatty liver disease. *Cellular and molecular life sciences: CMLS* 75, 3313–3327. doi:10.1007/s00018-018-2860-6.

Irizarry, R. A., Hobbs, B., Collin, F., Beazer-Barclay, Y. D., Antonellis, K. J., Scherf, U., et al. (2003). Exploration, normalization, and summaries of high density oligonucleotide array probe level data. *Biostatistics* 4, 249–264. doi:10.1093/biostatistics/4.2.249.

Isakson, P., Hammarstedt, A., Gustafson, B., and Smith, U. (2009). Impaired preadipocyte differentiation in human abdominal obesity: role of Wnt, tumor necrosis factor-alpha, and inflammation. *Diabetes* 58, 1550–1557. doi:10.2337/db08-1770.

Jena, P. K., Sheng, L., Di Lucente, J., Jin, L.-W., Maezawa, I., and Wan, Y.-J. Y. (2018). Dysregulated bile acid synthesis and dysbiosis are implicated in Western diet-induced systemic inflammation, microglial activation, and reduced neuroplasticity. *FASEB journal: official publication of the Federation of American Societies for Experimental Biology* 32, 2866–2877. doi:10.1096/fj.201700984RR.

Jin, N., Qian, W., Yin, X., Zhang, L., Iqbal, K., Grundke-Iqbal, I., et al. (2013). CREB regulates the expression of neuronal glucose transporter 3: a possible mechanism related to impaired brain glucose uptake in Alzheimer's disease. *Nucleic Acids Res* 41, 3240–3256. doi:10.1093/nar/gks1227.

Kachur, S., Lavie, C. J., de Schutter, A., Milani, R. V., and Ventura, H. O. (2017). Obesity and cardiovascular diseases. *Minerva Medica* 108, 212–228. doi:10.23736/S0026-4806.17.05022-4.

Kar A, Havlioglu N, Tarn WY, Wu JY. RBM4 interacts with an intronic element and stimulates tau exon 10 inclusion. J Biol Chem. 2006 Aug 25;281(34):24479-88. doi: 10.1074/jbc.M603971200. Epub 2006 Jun 15. PMID: 16777844; PMCID: PMC2072872.

Katzmarzyk, P. T., Pérusse, L., Rao, D. C., and Bouchard, C. (2000). Familial risk of overweight and obesity in the Canadian population using the WHO/NIH criteria. *Obes Res* 8, 194–197. doi:10.1038/oby.2000.21.

Kaur, Y., de Souza, R. J., Gibson, W. T., and Meyre, D. (2017). A systematic review of genetic syndromes with obesity. *Obes Rev* 18, 603–634. doi:10.1111/obr.12531.

Kautzky-Willer, A., Harreiter, J., and Pacini, G. (2016). Sex and Gender Differences in Risk, Pathophysiology and Complications of Type 2 Diabetes Mellitus. *Endocr Rev* 37, 278–316. doi:10.1210/er.2015-1137.

Keller, M., Hopp, L., Liu, X., Wohland, T., Rohde, K., Cancello, R., et al. (2017). Genome-wide DNA promoter methylation and transcriptome analysis in human adipose tissue unravels novel candidate genes for obesity. *Mol Metab* 6, 86–100. doi:10.1016/j.molmet.2016.11.003.

Kelly, D. M., and Jones, T. H. (2015). Testosterone and obesity. *Obes Rev* 16, 581–606. doi:10.1111/obr.12282.

Khan, T., Muise, E. S., Iyengar, P., Wang, Z. V., Chandalia, M., Abate, N., et al. (2009). Metabolic dysregulation and adipose tissue fibrosis: role of collagen VI. *Mol Cell Biol* 29, 1575–1591. doi:10.1128/MCB.01300-08.

Kilpeläinen, T. O., Zillikens, M. C., Stančákova, A., Finucane, F. M., Ried, J. S., Langenberg, C., et al. (2011). Genetic variation near IRS1 associates with reduced adiposity and an impaired metabolic profile. *Nat Genet* 43, 753–760. doi:10.1038/ng.866.

Kim, D. S., Choi, H.-I., Wang, Y., Luo, Y., Hoffer, B. J., and Greig, N. H. (2017). A New Treatment Strategy for Parkinson's Disease through the Gut-Brain Axis: The Glucagon-Like Peptide-1 Receptor Pathway. *Cell Transplantation* 26, 1560–1571. doi:10.1177/0963689717721234.

King, B. M. (2006). The rise, fall, and resurrection of the ventromedial hypothalamus in the regulation of feeding behavior and body weight. *Physiol Behav* 87, 221–244. doi:10.1016/j.physbeh.2005.10.007.

Klöting, N., and Blüher, M. (2014). Adipocyte dysfunction, inflammation and metabolic syndrome. *Reviews in Endocrine & Metabolic Disorders* 15, 277–287. doi:10.1007/s11154-014-9301-0.

Koeppen-Schomerus, G., Wardle, J., and Plomin, R. (2001). A genetic analysis of weight and overweight in 4-year-old twin pairs. *Int J Obes Relat Metab Disord* 25, 838–844. doi:10.1038/sj.ijo.0801589.

Kramer, P. R., Kramer, S. F., and Guan, G. (2004). 17 beta-estradiol regulates cytokine release through modulation of CD16 expression in monocytes and monocyte-derived macrophages. *Arthritis Rheum* 50, 1967–1975. doi:10.1002/art.20309.

Kratz, M., Coats, B. R., Hisert, K. B., Hagman, D., Mutskov, V., Peris, E., et al. (2014). Metabolic dysfunction drives a mechanistically distinct proinflammatory phenotype in adipose tissue macrophages. *Cell Metabolism* 20, 614–625. doi:10.1016/j.cmet.2014.08.010.

Labouesse, M. A., Polesel, M., Clementi, E., Müller, F., Markkanen, E., Mouttet, F., et al. (2018). MicroRNA Expression Profiling in the Prefrontal Cortex: Putative Mechanisms for the Cognitive Effects of Adolescent High Fat Feeding. *Sci Rep* 8, 8344. doi:10.1038/s41598-018-26631-x.

Lainez, N. M., Jonak, C. R., Nair, M. G., Ethell, I. M., Wilson, E. H., Carson, M. J., et al. (2018). Diet-Induced Obesity Elicits Macrophage Infiltration and Reduction in Spine Density in the Hypothalami of Male but Not Female Mice. *Front Immunol* 9, 1992. doi:10.3389/fimmu.2018.01992.

Lavie, C. J., Milani, R. V., and Ventura, H. O. (2008). Untangling the heavy cardiovascular burden of obesity. *Nature Clinical Practice. Cardiovascular Medicine* 5, 428–429. doi:10.1038/ncpcardio1257.

Le, D. S. N., Pannacciulli, N., Chen, K., Salbe, A. D., Del Parigi, A., Hill, J. O., et al. (2007). Less activation in the left dorsolateral prefrontal cortex in the reanalysis of the response to a meal in obese than in lean women and its association with successful weight loss. *The American Journal of Clinical Nutrition* 86, 573–579. doi:10.1093/ajcn/86.3.573.

Le, D. S. N. T., Pannacciulli, N., Chen, K., Del Parigi, A., Salbe, A. D., Reiman, E. M., et al. (2006). Less activation of the left dorsolateral prefrontal cortex in response to a meal: a feature of obesity. *The American Journal of Clinical Nutrition* 84, 725–731. doi:10.1093/ajcn/84.4.725.

Lee, J. Y., Sohn, K. H., Rhee, S. H., and Hwang, D. (2001). Saturated fatty acids, but not unsaturated fatty acids, induce the expression of cyclooxygenase-2 mediated through Toll-like receptor 4. *The Journal of Biological Chemistry* 276, 16683–16689. doi:10.1074/jbc.M011695200.

Lee, L., and Sanders, R. A. (2012). Metabolic Syndrome. *Pediatr Rev* 33, 459–468.

Lee, P. C., and Dixon, J. B. (2017). Food for Thought: Reward Mechanisms and Hedonic Overeating in Obesity. *Current Obesity Reports* 6, 353–361. doi:10.1007/s13679-017-0280-9.

Lenard, N. R., and Berthoud, H.-R. (2008). Central and peripheral regulation of food intake and physical activity: pathways and genes. *Obesity (Silver Spring, Md.)* 16 Suppl 3, S11-22. doi:10.1038/oby.2008.511.

Levchenko A, Vyalova NM, Nurgaliev T, Pozhidaev IV, Simutkin GG, Bokhan NA, Ivanova SA. *NRG1*, *PIP4K2A*, and *HTR2C* as Potential Candidate Biomarker Genes for Several Clinical Subphenotypes of Depression and Bipolar Disorder. Front Genet. 2020 Aug 25;11:936. doi: 10.3389/fgene.2020.00936. PMID: 33193575; PMCID: PMC7478333.

Levin, B. E., and Routh, V. H. (1996). Role of the brain in energy balance and obesity. *Am J Physiol* 271, R491-500. doi:10.1152/ajpregu.1996.271.3.R491.

Li, J., Wu, H., Liu, Y., and Yang, L. (2020). High fat diet induced obesity model using four strainsof mice: Kunming, C57BL/6, BALB/c and ICR. *Exp Anim* 69, 326–335. doi:10.1538/expanim.19-0148.

Liistro, T., Guiducci, L., Burchielli, S., Panetta, D., Belcari, N., Pardini, S., et al. (2010). Brain glucose overexposure and lack of acute metabolic flexibility in obesity and type 2 diabetes: a PET-[18F]FDG study in Zucker and ZDF rats. *Journal of Cerebral Blood Flow and Metabolism: Official Journal of the International Society of Cerebral Blood Flow and Metabolism* 30, 895–899. doi:10.1038/jcbfm.2010.27.

Lin L, Lesnick TG, Maraganore DM, Isacson O. Axon guidance and synaptic maintenance: preclinical markers for neurodegenerative disease and therapeutics. Trends Neurosci. 2009 Mar;32(3):142-9. doi: 10.1016/j.tins.2008.11.006. Epub 2009 Jan 21. PMID: 19162339; PMCID: PMC2954610.

Lindberg, M. K., Weihua, Z., Andersson, N., Movérare, S., Gao, H., Vidal, O., et al. (2002). Estrogen receptor specificity for the effects of estrogen in ovariectomized mice. *J Endocrinol* 174, 167–178. doi:10.1677/joe.0.1740167.

Lindqvist, A., Mohapel, P., Bouter, B., Frielingsdorf, H., Pizzo, D., Brundin, P., et al. (2006). High-fat diet impairs hippocampal neurogenesis in male rats. *European Journal of Neurology* 13, 1385–1388. doi:10.1111/j.1468-1331.2006.01500.x.

Litwin, S. E. (2008). Which measures of obesity best predict cardiovascular risk? *Journal of the American College of Cardiology* 52, 616–619. doi:10.1016/j.jacc.2008.05.017.

Liu, Z., Patil, I., Sancheti, H., Yin, F., and Cadenas, E. (2017). Effects of Lipoic Acid on High-Fat Diet-Induced Alteration of Synaptic Plasticity and Brain Glucose Metabolism: A PET/CT and 13C-NMR Study. *Sci Rep* 7, 5391. doi:10.1038/s41598-017-05217-z.

Lizcano, J. M., and Alessi, D. R. (2002). The insulin signalling pathway. *Current biology: CB* 12, R236-238. doi:10.1016/s0960-9822(02)00777-7.

Locke, A. E., Kahali, B., Berndt, S. I., Justice, A. E., Pers, T. H., Day, F. R., et al. (2015). Genetic studies of body mass index yield new insights for obesity biology. *Nature* 518, 197–206. doi:10.1038/nature14177.

Long, M. T., Pedley, A., Massaro, J. M., Hoffmann, U., Ma, J., Loomba, R., et al. (2018). A simple clinical model predicts incident hepatic steatosis in a community-based cohort: The Framingham Heart Study. *Liver Int* 38, 1495–1503. doi:10.1111/liv.13709.

Loomba-Albrecht, L. A., and Styne, D. M. (2009). Effect of puberty on body composition. *Curr Opin Endocrinol Diabetes Obes* 16, 10–15. doi:10.1097/med.0b013e328320d54c.

Lutz, T. A., and Woods, S. C. (2012). Overview of animal models of obesity. *Curr Protoc Pharmacol* Chapter 5, Unit5.61. doi:10.1002/0471141755.ph0561s58.

Ma, Y., Hof, P. R., Grant, S. C., Blackband, S. J., Bennett, R., Slatest, L., et al. (2005). A three-dimensional digital atlas database of the adult C57BL/6J mouse brain by magnetic resonance microscopy. *Neuroscience* 135, 1203–1215. doi:10.1016/j.neuroscience.2005.07.014.

Maggi, A., and Della Torre, S. (2018). Sex, metabolism and health. *Mol Metab* 15, 3–7. doi:10.1016/j.molmet.2018.02.012.

Mancini, M., Summers, P., Faita, F., Brunetto, M. R., Callea, F., De Nicola, A., et al. (2018). Digital liver biopsy: Bio-imaging of fatty liver for translational and clinical research. *World Journal of Hepatology* 10, 231–245. doi:10.4254/wjh.v10.i2.231.

Marques, E. L., Halpern, A., Corrêa Mancini, M., de Melo, M. E., Horie, N. C., Buchpiguel, C. A., et al. (2014). Changes in neuropsychological tests and brain metabolism after bariatric surgery. *J Clin Endocrinol Metab* 99, E2347-2352. doi:10.1210/jc.2014-2068.

Martin, B., Pearson, M., Brenneman, R., Golden, E., Keselman, A., Iyun, T., et al. (2008). Conserved and differential effects of dietary energy intake on the hippocampal transcriptomes of females and males. *PLoS One* 3, e2398. doi:10.1371/journal.pone.0002398.

McEwen, B. S., and Reagan, L. P. (2004). Glucose transporter expression in the central nervous system: relationship to synaptic function. *European Journal of Pharmacology* 490, 13–24. doi:10.1016/j.ejphar.2004.02.041.

McLean, F. H., Grant, C., Morris, A. C., Horgan, G. W., Polanski, A. J., Allan, K., et al. (2018). Rapid and reversible impairment of episodic memory by a high-fat diet in mice. *Scientific Reports* 8, 11976. doi:10.1038/s41598-018-30265-4.

McNay, E. C., Ong, C. T., McCrimmon, R. J., Cresswell, J., Bogan, J. S., and Sherwin, R. S. (2010). Hippocampal memory processes are modulated by insulin and high-fat-induced insulin resistance. *Neurobiology of Learning and Memory* 93, 546–553. doi:10.1016/j.nlm.2010.02.002.

McNay, E. C., and Pearson-Leary, J. (2020). GluT4: A central player in hippocampal memory and brain insulin resistance. *Experimental Neurology* 323, 113076. doi:10.1016/j.expneurol.2019.113076.

Meda, C., Barone, M., Mitro, N., Lolli, F., Pedretti, S., Caruso, D., et al. (2020). Hepatic ERα accounts for sex differences in the ability to cope with an excess of dietary lipids. *Mol Metab* 32, 97–108. doi:10.1016/j.molmet.2019.12.009.

Melo, H. M., Santos, L. E., and Ferreira, S. T. (2019). Diet-Derived Fatty Acids, Brain Inflammation, and Mental Health. *Frontiers in Neuroscience* 13, 265. doi:10.3389/fnins.2019.00265.

Messerli, F. H., Ventura, H. O., Reisin, E., Dreslinski, G. R., Dunn, F. G., MacPhee, A. A., et al. (1982). Borderline hypertension and obesity: two prehypertensive states with elevated cardiac output. *Circulation* 66, 55–60. doi:10.1161/01.cir.66.1.55.

Milanski, M., Degasperi, G., Coope, A., Morari, J., Denis, R., Cintra, D. E., et al. (2009). Saturated fatty acids produce an inflammatory response predominantly through the activation of TLR4 signaling in hypothalamus: implications for the pathogenesis of obesity. *The Journal of Neuroscience: The Official Journal of the Society for Neuroscience* 29, 359–370. doi:10.1523/JNEUROSCI.2760-08.2009.

Mittal, K., and Katare, D. P. (2016). Shared links between type 2 diabetes mellitus and Alzheimer's disease: A review. *Diabetes & Metabolic Syndrome* 10, S144-149. doi:10.1016/j.dsx.2016.01.021.

Mouton-Liger F, Dumurgier J, Cognat E, Hourregue C, Zetterberg H, Vanderstichele H, Vanmechelen E, Bouaziz-Amar E, Blennow K, Hugon J, Paquet C. CSF levels of the BACE1 substrate NRG1 correlate with cognition in Alzheimer's disease. Alzheimers Res Ther. 2020 Jul 20;12(1):88. doi: 10.1186/s13195-020-00655-w. PMID: 32690068; PMCID: PMC7372801.

Murtaj, V., Belloli, S., Di Grigoli, G., Pannese, M., Ballarini, E., Rodriguez-Menendez, V., et al. (2019). Age and Sex Influence the Neuro-inflammatory Response to a Peripheral Acute LPS Challenge. *Front Aging Neurosci* 11, 299. doi:10.3389/fnagi.2019.00299.

Myers, M. G., and Olson, D. P. (2012). Central nervous system control of metabolism. *Nature* 491, 357–363. doi:10.1038/nature11705.

Najam, S. S., Zglinicki, B., Vinnikov, I. A., and Konopka, W. (2019). MicroRNAs in the hypothalamic control of energy homeostasis. *Cell and Tissue Research* 375, 173–177. doi:10.1007/s00441-018-2876-0.

Nam, K. N., Mounier, A., Wolfe, C. M., Fitz, N. F., Carter, A. Y., Castranio, E. L., et al. (2017). Effect of high fat diet on phenotype, brain transcriptome and lipidome in Alzheimer's model mice. *Sci Rep* 7, 4307. doi:10.1038/s41598-017-04412-2.

Nemeroff, C. B., Lipton, M. A., and Kizer, J. S. (1978). Models of neuroendocrine regulation: use of monosodium glutamate as an investigational tool. *Dev Neurosci* 1, 102–109. doi:10.1159/000112561.

Newman, J. C., and Verdin, E. (2017). β-Hydroxybutyrate: A Signaling Metabolite. *Annual Review of Nutrition* 37, 51–76. doi:10.1146/annurev-nutr-071816-064916.

Nilsson, P. M., Tuomilehto, J., and Rydén, L. (2019). The metabolic syndrome - What is it and how should it be managed? *Eur J Prev Cardiol* 26, 33–46. doi:10.1177/2047487319886404.

Norgren, R., Hajnal, A., and Mungarndee, S. S. (2006). Gustatory reward and the nucleus accumbens. *Physiol Behav* 89, 531–535. doi:10.1016/j.physbeh.2006.05.024.

Nota, M. H. C., Vreeken, D., Wiesmann, M., Aarts, E. O., Hazebroek, E. J., and Kiliaan, A. J. (2020). Obesity affects brain structure and function- rescue by bariatric surgery? *Neuroscience and Biobehavioral Reviews* 108, 646–657. doi:10.1016/j.neubiorev.2019.11.025.

Nuthikattu, S., Milenkovic, D., Rutledge, J., and Villablanca, A. (2019). The Western Diet Regulates Hippocampal Microvascular Gene Expression: An Integrated Genomic Analyses in Female Mice. *Sci Rep* 9, 19058. doi:10.1038/s41598-019-55533-9.

Nuutila, P., Knuuti, M. J., Mäki, M., Laine, H., Ruotsalainen, U., Teräs, M., et al. (1995). Gender and insulin sensitivity in the heart and in skeletal muscles. Studies using positron emission tomography. *Diabetes* 44, 31–36. doi:10.2337/diab.44.1.31.

O'Brien, P. D., Hinder, L. M., Callaghan, B. C., and Feldman, E. L. (2017). Neurological consequences of obesity. *The Lancet. Neurology* 16, 465–477. doi:10.1016/S1474-4422(17)30084-4.

Okereke, O. I., Rosner, B. A., Kim, D. H., Kang, J. H., Cook, N. R., Manson, J. E., et al. (2012). Dietary fat types and 4-year cognitive change in community-dwelling older women. *Annals of Neurology* 72, 124–134. doi:10.1002/ana.23593.

O'Neil, A., Quirk, S. E., Housden, S., Brennan, S. L., Williams, L. J., Pasco, J. A., et al. (2014). Relationship between diet and mental health in children and adolescents: a systematic review. *American Journal of Public Health* 104, e31-42. doi:10.2105/AJPH.2014.302110.

O'Rahilly, S. (2009). Human genetics illuminates the paths to metabolic disease. *Nature* 462, 307–314. doi:10.1038/nature08532.

Ortega, R. M., Requejo, A. M., Andrés, P., López-Sobaler, A. M., Quintas, M. E., Redondo, M. R., et al. (1997). Dietary intake and cognitive function in a group of elderly people. *The American Journal of Clinical Nutrition* 66, 803–809. doi:10.1093/ajcn/66.4.803.

Ouchi, N., Parker, J. L., Lugus, J. J., and Walsh, K. (2011). Adipokines in inflammation and metabolic disease. *Nature Reviews. Immunology* 11, 85–97. doi:10.1038/nri2921.

Pak, K., Kim, S.-J., and Kim, I. J. (2018). Obesity and Brain Positron Emission Tomography. *Nucl Med Mol Imaging* 52, 16–23. doi:10.1007/s13139-017-0483-8.

Palmer, B. F., and Clegg, D. J. (2015). The sexual dimorphism of obesity. *Mol Cell Endocrinol* 402, 113–119. doi:10.1016/j.mce.2014.11.029.

Park, C. R. (2001). Cognitive effects of insulin in the central nervous system. *Neurosci Biobehav Rev* 25, 311–323. doi:10.1016/s0149-7634(01)00016-1.

Park, S. H., Jeon, W. K., Kim, S. H., Kim, H. J., Park, D. I., Cho, Y. K., et al. (2006). Prevalence and risk factors of non-alcoholic fatty liver disease among Korean adults. *J Gastroenterol Hepatol* 21, 138–143. doi:10.1111/j.1440-1746.2005.04086.x.

Patterson, C. M., Bouret, S. G., Park, S., Irani, B. G., Dunn-Meynell, A. A., and Levin, B. E. (2010). Large litter rearing enhances leptin sensitivity and protects selectively bred diet-induced obese rats from becoming obese. *Endocrinology* 151, 4270–4279. doi:10.1210/en.2010-0401.

Pedditzi, E., Peters, R., and Beckett, N. (2016). The risk of overweight/obesity in mid-life and late life for the development of dementia: a systematic review and meta-analysis of longitudinal studies. *Age Ageing* 45, 14–21. doi:10.1093/ageing/afv151.

Pérez, C., Fanizza, L. J., and Sclafani, A. (1999). Flavor preferences conditioned by intragastric nutrient infusions in rats fed chow or a cafeteria diet. *Appetite* 32, 155–170. doi:10.1006/appe.1998.0182.

Perry, R. J., Samuel, V. T., Petersen, K. F., and Shulman, G. I. (2014). The role of hepatic lipids in hepatic insulin resistance and type 2 diabetes. *Nature* 510, 84–91. doi:10.1038/nature13478.

Petrie, J. R., Guzik, T. J., and Touyz, R. M. (2018). Diabetes, Hypertension, and Cardiovascular Disease: Clinical Insights and Vascular Mechanisms. *The Canadian Journal of Cardiology* 34, 575–584. doi:10.1016/j.cjca.2017.12.005.

Pietiläinen, K. H., Kaprio, J., Rissanen, A., Winter, T., Rimpelä, A., Viken, R. J., et al. (1999). Distribution and heritability of BMI in Finnish adolescents aged 16y and 17y: a study of 4884 twins and 2509 singletons. *Int J Obes Relat Metab Disord* 23, 107–115. doi:10.1038/sj.ijo.0800767.

Pigeyre, M., Yazdi, F. T., Kaur, Y., and Meyre, D. (2016). Recent progress in genetics, epigenetics and metagenomics unveils the pathophysiology of human obesity. *Clin Sci (Lond)* 130, 943–986. doi:10.1042/CS20160136.

Pisitkun, P., Deane, J. A., Difilippantonio, M. J., Tarasenko, T., Satterthwaite, A. B., and Bolland, S. (2006). Autoreactive B cell responses to RNA-related antigens due to TLR7 gene duplication. *Science* 312, 1669–1672. doi:10.1126/science.1124978.

Pistillo, F., Fasoli, F., Moretti, M., McClure-Begley, T., Zoli, M., Marks, M. J., et al. (2016). Chronic nicotine and withdrawal affect glutamatergic but not nicotinic receptor expression in the mesocorticolimbic pathway in a region-specific manner. *Pharmacol Res* 103, 167–176. doi:10.1016/j.phrs.2015.11.016.

Portune, K. J., Beaumont, M., Davila, A.-M., Tomé, D., Blachier, F., and Sanz, Y. (2016). Gut microbiota role in dietary protein metabolism and health-related outcomes: The two sides of the coin. *Trends in Food Science and Technology* 57, 213–232. doi:10.1016/j.tifs.2016.08.011.

Prah, J., Winters, A., Chaudhari, K., Hersh, J., Liu, R., and Yang, S.-H. (2019). Cholesterol sulfate alters astrocyte metabolism and provides protection against oxidative stress. *Brain Res* 1723, 146378. doi:10.1016/j.brainres.2019.146378.

Pritchard, L. E., Turnbull, A. V., and White, A. (2002). Pro-opiomelanocortin processing in the hypothalamus: impact on melanocortin signalling and obesity. *J Endocrinol* 172, 411–421. doi:10.1677/joe.0.1720411.

Rahman, M. H., Bhusal, A., Lee, W.-H., Lee, I.-K., and Suk, K. (2018). Hypothalamic inflammation and malfunctioning glia in the pathophysiology of obesity and diabetes: Translational significance. *Biochemical Pharmacology* 153, 123–133. doi:10.1016/j.bcp.2018.01.024.

Raichle, M. E. (2001). Cognitive neuroscience. Bold insights. *Nature* 412, 128–130. doi:10.1038/35084300.

Ran, C., Albrecht, D. S., Bredella, M. A., Yang, J., Yang, J., Liang, S. H., et al. (2018). PET Imaging of Human Brown Adipose Tissue with the TSPO Tracer [11C]PBR28. *Mol Imaging Biol* 20, 188–193. doi:10.1007/s11307-017-1129-z.

Rebelos, E., Immonen, H., Bucci, M., Hannukainen, J. C., Nummenmaa, L., Honka, M.-J., et al. (2019). Brain glucose uptake is associated with endogenous glucose production in obese patients before and after bariatric surgery and predicts metabolic outcome at follow-up. *Diabetes Obes Metab* 21, 218–226. doi:10.1111/dom.13501.

Reger, M. A., Watson, G. S., Green, P. S., Wilkinson, C. W., Baker, L. D., Cholerton, B., et al. (2008). Intranasal insulin improves cognition and modulates beta-amyloid in early AD. *Neurology* 70, 440–448. doi:10.1212/01.WNL.0000265401.62434.36.

Riera, C. E., Tsaousidou, E., Halloran, J., Follett, P., Hahn, O., Pereira, M. M. A., et al. (2017). The Sense of Smell Impacts Metabolic Health and Obesity. *Cell Metab* 26, 198-211.e5. doi:10.1016/j.cmet.2017.06.015.

Robblee, M. M., Kim, C. C., Porter Abate, J., Valdearcos, M., Sandlund, K. L. M., Shenoy, M. K., et al. (2016). Saturated Fatty Acids Engage an IRE1α-Dependent Pathway to Activate the NLRP3 Inflammasome in Myeloid Cells. *Cell Reports* 14, 2611–2623. doi:10.1016/j.celrep.2016.02.053.

Robison LS, Gannon OJ, Thomas MA, Salinero AE, Abi-Ghanem C, Poitelon Y, Belin S, Zuloaga KL. Role of sex and high-fat diet in metabolic and hypothalamic disturbances in the 3xTg-AD mouse model of Alzheimer's disease. J Neuroinflammation. 2020 Sep 29;17(1):285. doi: 10.1186/s12974-020-01956-5. PMID: 32993686; PMCID: PMC7526387.

Rogol, A. D. (2010). Sex steroids, growth hormone, leptin and the pubertal growth spurt. *Endocr Dev* 17, 77–85. doi:10.1159/000262530.

Roh, E., and Kim, M. S. (2016). Brain Regulation of Energy Metabolism. *Endocrinology and Metabolism (Seoul, Korea)* 31, 519–524. doi:10.3803/EnM.2016.31.4.519.

Rolls, E. T. (2004). The functions of the orbitofrontal cortex. *Brain and Cognition* 55, 11–29. doi:10.1016/S0278-2626(03)00277-X.

Rosqvist, F., Iggman, D., Kullberg, J., Cedernaes, J., Johansson, H.-E., Larsson, A., et al. (2014). Overfeeding polyunsaturated and saturated fat causes distinct effects on liver and visceral fat accumulation in humans. *Diabetes* 63, 2356–2368. doi:10.2337/db13-1622.

Rothemund, Y., Preuschhof, C., Bohner, G., Bauknecht, H.-C., Klingebiel, R., Flor, H., et al. (2007). Differential activation of the dorsal striatum by high-calorie visual food stimuli in obese individuals. *NeuroImage* 37, 410–421. doi:10.1016/j.neuroimage.2007.05.008.

Rudebeck, P. H., and Murray, E. A. (2014). The orbitofrontal oracle: cortical mechanisms for the prediction and evaluation of specific behavioral outcomes. *Neuron* 84, 1143–1156. doi:10.1016/j.neuron.2014.10.049.

Ryan, S., Arnaud, C., Fitzpatrick, S. F., Gaucher, J., Tamisier, R., and Pépin, J.-L. (2019). Adipose tissue as a key player in obstructive sleep apnoea. *European Respiratory Review: An Official Journal of the European Respiratory Society* 28. doi:10.1183/16000617.0006-2019.

Sala, A., Malpetti, M., Ferrulli, A., Gianolli, L., Luzi, L., Perani, D., et al. (2019). High body mass index, brain metabolism and connectivity: an unfavorable effect in elderly females. *Aging (Albany NY)* 11, 8573–8586. doi:10.18632/aging.102347.

Salamone, J. D., Cousins, M. S., and Snyder, B. J. (1997). Behavioral functions of nucleus accumbens dopamine: empirical and conceptual problems with the anhedonia hypothesis. *Neuroscience and Biobehavioral Reviews* 21, 341–359. doi:10.1016/s0149-7634(96)00017-6.

Saltiel, A. R., and Kahn, C. R. (2001). Insulin signalling and the regulation of glucose and lipid metabolism. *Nature* 414, 799–806. doi:10.1038/414799a.

Savolainen M, Emerich D, Kordower JH. Disease Modification Through Trophic Factor Delivery. Methods Mol Biol. 2018;1780:525-547. doi: 10.1007/978-1-4939-7825-0_24. PMID: 29856034.

Schulman, I. H., and Zhou, M.-S. (2009). Vascular insulin resistance: a potential link between cardiovascular and metabolic diseases. *Current Hypertension Reports* 11, 48–55. doi:10.1007/s11906-009-0010-0.

Schultz, W. (2010). Subjective neuronal coding of reward: temporal value discounting and risk. *Eur J Neurosci* 31, 2124–2135. doi:10.1111/j.1460-9568.2010.07282.x.

Schwartz, M. W., Woods, S. C., Porte, D., Seeley, R. J., and Baskin, D. G. (2000). Central nervous system control of food intake. *Nature* 404, 661–671. doi:10.1038/35007534.

Sherling, D. H., Perumareddi, P., and Hennekens, C. H. (2017). Metabolic Syndrome. *Journal of Cardiovascular Pharmacology and Therapeutics* 22, 365–367. doi:10.1177/1074248416686187.

Shi, J., Wittke-Thompson, J. K., Badner, J. A., Hattori, E., Potash, J. B., Willour, V. L., et al. (2008). Clock genes may influence bipolar disorder susceptibility and dysfunctional circadian rhythm. *Am J Med Genet B Neuropsychiatr Genet* 147B, 1047–1055. doi:10.1002/ajmg.b.30714.

Soares, A. F., Duarte, J. M. N., and Gruetter, R. (2018). Increased hepatic fatty acid polyunsaturation precedes ectopic lipid deposition in the liver in adaptation to high-fat diets in mice. *MAGMA* 31, 341–354. doi:10.1007/s10334-017-0654-8.

Sonne, S. B., Yadav, R., Yin, G., Dalgaard, M. D., Myrmel, L. S., Gupta, R., et al. (2017). Obesity is associated with depot-specific alterations in adipocyte DNA methylation and gene expression. *Adipocyte* 6, 124–133. doi:10.1080/21623945.2017.1320002.

Sripetchwandee, J., Chattipakorn, N., and Chattipakorn, S. C. (2018). Links Between Obesity-Induced Brain Insulin Resistance, Brain Mitochondrial Dysfunction, and Dementia. *Frontiers in Endocrinology* 9, 496. doi:10.3389/fendo.2018.00496.

Stockhorst, U., de Fries, D., Steingrueber, H.-J., and Scherbaum, W. A. (2004). Insulin and the CNS: effects on food intake, memory, and endocrine parameters and the role of intranasal insulin administration in humans. *Physiol Behav* 83, 47–54. doi:10.1016/j.physbeh.2004.07.022.

Stranahan, A. M., Norman, E. D., Lee, K., Cutler, R. G., Telljohann, R. S., Egan, J. M., et al. (2008). Diet-induced insulin resistance impairs hippocampal synaptic plasticity and cognition in middle-aged rats. *Hippocampus* 18, 1085–1088. doi:10.1002/hipo.20470.

Szalay, C., Aradi, M., Schwarcz, A., Orsi, G., Perlaki, G., Németh, L., et al. (2012). Gustatory perception alterations in obesity: an fMRI study. *Brain Research* 1473, 131–140. doi:10.1016/j.brainres.2012.07.051.

Takeuchi, O., and Akira, S. (2010). Pattern recognition receptors and inflammation. *Cell* 140, 805–820. doi:10.1016/j.cell.2010.01.022.

Tan, B. L., and Norhaizan, M. E. (2019). Effect of High-Fat Diets on Oxidative Stress, Cellular Inflammatory Response and Cognitive Function. *Nutrients* 11. doi:10.3390/nu11112579.

Thaler, J. P., Yi, C.-X., Schur, E. A., Guyenet, S. J., Hwang, B. H., Dietrich, M. O., et al. (2012). Obesity is associated with hypothalamic injury in rodents and humans. *The Journal of Clinical Investigation* 122, 153–162. doi:10.1172/JCI59660.

Torres, S. J., and Nowson, C. A. (2007). Relationship between stress, eating behavior, and obesity. *Nutrition (Burbank, Los Angeles County, Calif.)* 23, 887–894. doi:10.1016/j.nut.2007.08.008.

Tsigos, C., and Chrousos, G. P. (2002). Hypothalamic-pituitary-adrenal axis, neuroendocrine factors and stress. *Journal of Psychosomatic Research* 53, 865–871. doi:10.1016/s0022-3999(02)00429-4.

Tsochatzis, E. A., Manolakopoulos, S., Papatheodoridis, G. V., and Archimandritis, A. J. (2009). Insulin resistance and metabolic syndrome in chronic liver diseases: old entities with new implications. *Scandinavian Journal of Gastroenterology* 44, 6–14. doi:10.1080/00365520802273058.

Tura, A., Pacini, G., Moro, E., Vrbíková, J., Bendlová, B., and Kautzky-Willer, A. (2018). Sex- and age-related differences of metabolic parameters in impaired glucose metabolism and type 2 diabetes compared to normal glucose tolerance. *Diabetes Res Clin Pract* 146, 67–75. doi:10.1016/j.diabres.2018.09.019.

Valcarcel-Ares, M. N., Tucsek, Z., Kiss, T., Giles, C. B., Tarantini, S., Yabluchanskiy, A., et al. (2019). Obesity in Aging Exacerbates Neuroinflammation, Dysregulating Synaptic Function-Related Genes and Altering Eicosanoid Synthesis in the Mouse Hippocampus: Potential Role in Impaired Synaptic Plasticity and Cognitive Decline. *J Gerontol A Biol Sci Med Sci* 74, 290–298. doi:10.1093/gerona/gly127.

van Dam, R. M., and Seidell, J. C. (2007). Carbohydrate intake and obesity. *European Journal of Clinical Nutrition* 61 Suppl 1, S75-99. doi:10.1038/sj.ejcn.1602939.

Van Herck, M. A., Vonghia, L., and Francque, S. M. (2017). Animal Models of Nonalcoholic Fatty Liver Disease-A Starter's Guide. *Nutrients* 9. doi:10.3390/nu9101072.

Vegiopoulos, A., Rohm, M., and Herzig, S. (2017). Adipose tissue: between the extremes. *The EMBO journal* 36, 1999–2017. doi:10.15252/embj.201696206.

Vilar-Gomez, E., Calzadilla-Bertot, L., Wai-Sun Wong, V., Castellanos, M., Aller-de la Fuente, R., Metwally, M., et al. (2018). Fibrosis Severity as a Determinant of Cause-Specific Mortality in Patients With Advanced Nonalcoholic

Fatty Liver Disease: A Multi-National Cohort Study. *Gastroenterology* 155, 443-457.e17. doi:10.1053/j.gastro.2018.04.034.

Vinuesa, A., Bentivegna, M., Calfa, G., Filipello, F., Pomilio, C., Bonaventura, M. M., et al. (2019). Early Exposure to a High-Fat Diet Impacts on Hippocampal Plasticity: Implication of Microglia-Derived Exosome-like Extracellular Vesicles. *Molecular Neurobiology* 56, 5075–5094. doi:10.1007/s12035-018-1435-8.

Volkow, N. D., Fowler, J. S., and Wang, G.-J. (2003). The addicted human brain: insights from imaging studies. *The Journal of Clinical Investigation* 111, 1444–1451. doi:10.1172/JCI18533.

Volkow, N. D., and O'Brien, C. P. (2007). Issues for DSM-V: should obesity be included as a brain disorder? *Am J Psychiatry* 164, 708–710. doi:10.1176/ajp.2007.164.5.708.

Volkow, N. D., Wang, G.-J., and Baler, R. D. (2011). Reward, dopamine and the control of food intake: implications for obesity. *Trends in Cognitive Sciences* 15, 37–46. doi:10.1016/j.tics.2010.11.001.

Volkow, N. D., Wang, G.-J., Fowler, J. S., and Telang, F. (2008). Overlapping neuronal circuits in addiction and obesity: evidence of systems pathology. *Philosophical Transactions of the Royal Society of London. Series B, Biological Sciences* 363, 3191–3200. doi:10.1098/rstb.2008.0107.

Volkow, N. D., Wang, G.-J., Telang, F., Fowler, J. S., Goldstein, R. Z., Alia-Klein, N., et al. (2009). Inverse association between BMI and prefrontal metabolic activity in healthy adults. *Obesity (Silver Spring)* 17, 60–65. doi:10.1038/oby.2008.469.

Wang, D. D., Li, Y., Chiuve, S. E., Stampfer, M. J., Manson, J. E., Rimm, E. B., et al. (2016). Association of Specific Dietary Fats With Total and Cause-Specific Mortality. *JAMA internal medicine* 176, 1134–1145. doi:10.1001/jamainternmed.2016.2417.

Wang, G.-J., Volkow, N. D., Felder, C., Fowler, J. S., Levy, A. V., Pappas, N. R., et al. (2002). Enhanced resting activity of the oral somatosensory cortex in obese subjects. *Neuroreport* 13, 1151–1155. doi:10.1097/00001756-200207020-00016.

Wang, G.-J., Volkow, N. D., Telang, F., Jayne, M., Ma, J., Rao, M., et al. (2004). Exposure to appetitive food stimuli markedly activates the human brain. *NeuroImage* 21, 1790–1797. doi:10.1016/j.neuroimage.2003.11.026.

Wang, G.-J., Volkow, N. D., Telang, F., Jayne, M., Ma, Y., Pradhan, K., et al. (2009a). Evidence of gender differences in the ability to inhibit brain activation elicited by food stimulation. *Proceedings of the National Academy of Sciences of the United States of America* 106, 1249–1254. doi:10.1073/pnas.0807423106.

Wang, G.-J., Volkow, N. D., Thanos, P. K., and Fowler, J. S. (2009b). Imaging of brain dopamine pathways: implications for understanding obesity. *Journal of Addiction Medicine* 3, 8–18. doi:10.1097/ADM.0b013e31819a86f7.

Wang, X., Magkos, F., and Mittendorfer, B. (2011). Sex differences in lipid and lipoprotein metabolism: it's not just about sex hormones. *J Clin Endocrinol Metab* 96, 885–893. doi:10.1210/jc.2010-2061.

Weinstein, G., Zelber-Sagi, S., Preis, S. R., Beiser, A. S., DeCarli, C., Speliotes, E. K., et al. (2018). Association of Nonalcoholic Fatty Liver Disease With Lower Brain Volume in Healthy Middle-aged Adults in the Framingham Study. *JAMA neurology* 75, 97–104. doi:10.1001/jamaneurol.2017.3229.

White, N. M. (1996). Addictive drugs as reinforcers: multiple partial actions on memory systems. *Addiction (Abingdon, England)* 91, 921–949; discussion 951-965.

Whitmer, R. A., Gustafson, D. R., Barrett-Connor, E., Haan, M. N., Gunderson, E. P., and Yaffe, K. (2008). Central obesity and increased risk of dementia more than three decades later. *Neurology* 71, 1057–1064. doi:10.1212/01.wnl.0000306313.89165.ef.

Wise, R. A. (2006). Role of brain dopamine in food reward and reinforcement. *Philos Trans R Soc Lond B Biol Sci* 361, 1149–1158. doi:10.1098/rstb.2006.1854.

Wolf, E. J., Rasmusson, A. M., Mitchell, K. S., Logue, M. W., Baldwin, C. T., and Miller, M. W. (2014). A genome-wide association study of clinical symptoms of dissociation in a trauma-exposed sample. *Depress Anxiety* 31, 352–360. doi:10.1002/da.22260.

Wu, Ct., and Morris, J. R. (2001). Genes, genetics, and epigenetics: a correspondence. *Science* 293, 1103–1105. doi:10.1126/science.293.5532.1103.

Xu, N., Meng, H., Liu, T.-Y., Feng, Y.-L., Qi, Y., Zhang, D.-H., et al. (2018). Sterol O-acyltransferase 1 deficiency improves defective insulin signaling in the brains of mice fed a high-fat diet. *Biochem Biophys Res Commun* 499, 105–111. doi:10.1016/j.bbrc.2018.02.122.

Xu, Y., Nedungadi, T. P., Zhu, L., Sobhani, N., Irani, B. G., Davis, K. E., et al. (2011). Distinct hypothalamic neurons mediate estrogenic effects on energy homeostasis and reproduction. *Cell Metab* 14, 453–465. doi:10.1016/j.cmet.2011.08.009.

Yang, H., Graham, L. C., Reagan, A. M., Grabowska, W. A., Schott, W. H., and Howell, G. R. (2019). Transcriptome profiling of brain myeloid cells revealed activation of Itgal, Trem1, and Spp1 in western diet-induced obesity. *J Neuroinflammation* 16, 169. doi:10.1186/s12974-019-1527-z.

Yang, J. D., Abdelmalek, M. F., Guy, C. D., Gill, R. M., Lavine, J. E., Yates, K., et al. (2017). Patient Sex, Reproductive Status, and Synthetic Hormone Use Associate With Histologic Severity of Nonalcoholic Steatohepatitis. *Clin Gastroenterol Hepatol* 15, 127-131.e2. doi:10.1016/j.cgh.2016.07.034.

Youngson, N. A., and Morris, M. J. (2013). What obesity research tells us about epigenetic mechanisms. *Philos Trans R Soc Lond B Biol Sci* 368, 20110337. doi:10.1098/rstb.2011.0337.

Zhang, Y., Liu, J., Yao, J., Ji, G., Qian, L., Wang, J., et al. (2014). Obesity: pathophysiology and intervention. *Nutrients* 6, 5153–5183. doi:10.3390/nu6115153.

Zierath, J. R., Ryder, J. W., Doebber, T., Woods, J., Wu, M., Ventre, J., et al. (1998). Role of skeletal muscle in thiazolidinedione insulin sensitizer (PPARgamma agonist) action. *Endocrinology* 139, 5034–5041. doi:10.1210/endo.139.12.6364.

9. Annex 1– PhD publication

During the first two years of my PhD project, I worked also on the effect of sex and aging on brain inflammation, characterizing an animal model of the disease.

I conducted experiments regarding inflammation during aging using WT C57Bl/6J mice. 17 months old mice as aged animals and 2 months old as adult animals, both male and female, were injected intraperitoneally with 0.63 mg/kg of Lipopolysaccharide (LPS) to induce systemic inflammation and sacrificed 6h later. Mice brain was divided, and half hemisphere was used for brain tissue sampling study with [^{18}F]-VC701 TSPO radiotracer to determine a brain inflammation level, and half tissue used to evaluate microglial phenotype. Brain regions of interest that I analysed include cortex, striatum, hippocampus and cerebellum. Aged male and female mice showed a significant tracer uptake increased in the cortical region compared to adult one. Regarding RT-PCR study, I analysed different microglial markers (TSPO; TREM-2, IL-1β; IL-6; TNF-α; TREML2) to evaluate microglial phenotype. I observed different behaviour from different gene expression analysis in male and females and during aging indicating important influences of these two variables. We showed that LPS induced a pro-inflammatory reaction in the brain of male and female mice as indicated by the up-regulation of IL-1b, TNF-a and IL-6 gene expression. However, in agreement with [^{18}F]-VC701 studies, the effect of LPS on pro-inflammatory cytokine transcript levels was significantly increased in aged compared to adult females, as well as in aged females compared to aged males. Immunocytochemistry was also performed on a separate animal group to confirm microglial and astrocyte activation upon neuroinflammatory response. Increased Iba-1 expression was present particularly in the cerebral cortex of LPS-treated aged animals, whereas GFAP immunoreactivity was higher in aged females in all the cerebral areas analysed. These results were published in 2019 as original article in Frontiers Aging Neuroscience as reported below (Murtaj et al., 2019).

Age and Sex Influence the Neuro-inflammatory Response to a Peripheral Acute LPS Challenge

Valentina Murtaj[1,2], Sara Belloli[2,3], Giuseppe Di Grigoli[2,3], Maria Pannese[4], Elisa Ballarini[5,6], Virginia Rodriguez-Menendez[5,6,] Paola Marmiroli[5,6], Andrea Cappelli[7], Valeria Masiello[2], Cristina Monterisi[6], Giuseppe Bellelli[8], Paola Panina-Bordignon[4,9]*† and Rosa Maria Moresco[2,6]*†

[1] PhD Program in Neuroscience, School of Medicine and Surgery, University of Milano-Bicocca, Monza, Italy

[2] PET and Nuclear Medicine Unit, San Raffaele Scientific Institute, Milan, Italy

[3] Institute of Molecular Bioimaging and Physiology of National Reasearch Council, Segrate, Italy

[4] Neuroimmunology Unit, Division of Neuroscience, IRCCS San Raffaele Scientific Institute, Milan, Italy

[5] Milan Center for Neuroscience, School of Medicine and Surgery, University of Milano-Bicocca, Monza, Italy

[6] Department of Medicine and Surgery, Tecnomed Foundation, University of Milano-Bicocca, Monza, Italy

[7] Department of Biotechnology, Chemistry and Pharmacy, University of Siena, Siena, Italy

[8] Acute Geriatric Unit, School of Medicine and Surgery, San Gerardo Hospital, University of Milano-Bicocca, Monza, Italy

[9] School of Medicine and Surgery, San Raffaele Vita-Salute University, Milan, Italy

Abstract

Aging is associated with an exaggerated response to peripheral inflammatory challenges together with behavioural and cognitive deficits. Studies considering both age and sex remain limited, despite sex dimorphism of astrocytes and microglial cells is largely recognized. To fill this knowledge gap, we investigated the effect of a single intraperitoneal lipopolysaccharide (LPS) administration in adult and aged mice. We assessed the expression of different inflammatory mediators, and the microglial response through binding of [18F]-VC701 tracer to translocator protein (TSPO) receptors in the male and female brain. Aged female brain showed a higher pro-inflammatory response to LPS compared to adult female and to aged male, as revealed by ex vivo binding to TSPO receptors and pro-inflammatory mediator transcript levels. The highest astroglial reaction was observed in the brain of aged females. Differently to the other groups of animals, in aged males LPS challenge did not affect transcription of triggering receptor expressed on myeloid cells 2 (TREM2). In conclusion, our study shows that in the mouse's brain the neuro-inflammatory response to an acute peripheral insult is sex- and age-dependent. Moreover, our results might set the basis for further studies aimed at identifying sex-related targets involved in the modulation of the aberrant neuro-inflammatory

response that characterizes aging. This knowledge could be relevant for the treatment of conditions such as delirium and dementia.

Introduction

The activation of the peripheral immune system is reflected by a pro-inflammatory milieu in the central nervous system (CNS; Norden and Godbout, 2013). The mechanisms of neuroinflammation are the subject of an intense pre-clinical research effort. However, most studies focus only on male animals, as preferred sex. A recent systematic review showed that only 3 out of 51 publications included both male and female mice or rats, and only a few of them focused on aged animals (Hoogland et al., 2015). This issue is relevant since ample evidence support sex-related differences in age-dependent neurodegenerative disorders (Bouman et al., 2005; Marriott and Huet-Hudson, 2006; Azad et al., 2007; Ycaza Herrera and Mather, 2015; Vom Steeg et al., 2016). Precise regulation of the immune responses maintains brain tissue homeostasis, while a chronic inflammatory state may influence the loss of neuronal function and plasticity (Besedovsky and Rey, 2008). In the presence of immune senescence, systemic inflammation represents a major precipitating factor for cognitive disorders (Perry, 2004; Costantini et al., 2018).

A neuro-inflammatory response induced by peripheral challenge with lipopolysaccharide (LPS) has been recently demonstrated in the brain of adult healthy volunteers using Positron Emission Tomography (PET) and a radio ligand for in vivo imaging of brain inflammation (Sandiego et al., 2015). However, most evidence on molecular and pathological CNS effects induced by peripheral inflammatory challenges, particularly during aging, derive from pre-clinical studies on rodents (Cunningham and Maclullich, 2013). As shown in the literature, aging is associated with an exaggerated response to peripheral inflammatory challenges together with behavioral and cognitive deficits (Hoogland et al., 2015; Schreuder et al., 2017). Indeed, in neurodegenerative disorders as well as in normal aging, microglia cells lose their supportive role in neuroplasticity and undertake a primed over-reactive phenotype promoting cognitive decline and synaptic dysfunction (Godbout and Johnson, 2006; Maclullich et al., 2008; Teeling and Perry, 2009). A recent gene expression profiling of microglia showed that aging is associated with over-expression of immune-related genes with an intermediate signature between acute and primed microglial genes (Holtman et al., 2015).

The association between genes regulating monocytes or microglial response with neurodegenerative disorders also supports the major role that neuroinflammation exerts in cognitive dysfunction. An example of this is the Triggering Receptor Expressed on Myeloid (TREM), a key component of innate and adaptive immunity, which is expressed by a variety of innate cells of the myeloid lineage including neutrophils, monocytes, osteoclasts, macrophages, dendritic cells and microglia. In particular, TREM2 has been shown to bind to poly-anionic ligands such as bacterial LPS and phospholipids (Wang et al., 2015). Upon ligand binding, TREM2 signals intracellularly through the adaptor protein DAP12, eventually regulating different cellular functions like phagocytosis, cytokine production, proliferation and survival (Thankam et al., 2016). Genetic studies have identified TREM2 variants that are associated with an increased risk of Alzheimer's disease (AD; Zheng et al., 2018). Another protein of potential interest is the TREM cells Like 2 (TREML2 also named TLT2). TREML2 is upregulated on B cells, neutrophils and macrophages during inflammation, and recent data suggest a potential modulatory role in pro-inflammatory responses (Thomas et al., 2016). Indeed, a missense variant of TREML2 (rs3747742) has been associated with a reduced susceptibility to develop AD (Benitez et al., 2014; Bhattacharjee et al., 2014; Zhao and Lukiw, 2015). Females have a higher prevalence of AD compared to males; thus sex is included among the risk factors for dementia (McCarthy et al., 2012). Using in vivo imaging, Mosconi et al. (2017) demonstrated the presence of AD endo-phenotypes in the brain of asymptomatic peri-menopausal or menopausal women when compared to age-matched men.

Sex dimorphism of astrocytes and microglial cells is largely recognized and has been recently demonstrated by Villa et al. (2018). Adult female microglial cells carry a neuroprotective phenotype even when transplanted into male brain (Amateau and McCarthy, 2002; Hanamsagar et al., 2017; Villa et al., 2018). Interestingly, this protective phenotype seems to be in contrast with what has been observed in aged subjects, as suggested by a whole genome profile showing that old female brains exhibit higher transcription of genes of the complement system when compared to old males. The different neuro-inflammatory signatures may explain the sex-specific susceptibility to cognitive disorders (Mangold et al., 2017).

Translocator protein (TSPO) has been shown to be a reliable biomarker of microglia activation in a large number of studies of neuro-inflammation by pre-clinical imaging (Liu et al., 2014). During brain injury or inflammatory insults, TSPO is overexpressed in activated microglia cells. For this reason,

TSPO ligands for PET imaging have been extensively used for the in vivo monitoring of microglia activation/macrophage infiltration in different neuropsychiatric conditions as well as in neurodegenerative and neuro-inflammatory animal models (Liu et al., 2014).

Currently, not only is there a lack of studies on the inflammatory responses in males and females but also studies considering both sex and age remain limited. For this reason, the main goal of this study was to test whether sex and age influence the early brain response to an acute peripheral inflammatory challenge. This experimental setting could reproduce the delirium syndrome, a transient and serious neurocognitive disorder characterized by an acute onset and fluctuating course (Inouye et al., 2014) To this aim, we investigated the effect of a single intraperitoneal LPS administration in male and female, adult and aged mice.

Materials and Methods

Animals and LPS Challenge

Adult (2 months) and aged (17–18 months) non-breeding male and female C57Bl/6J mice were purchased from Charles River. Animals were maintained and handled in compliance with our institutional guidelines for the care and use of experimental animals (IACUC) and the national law for animals used in research (Prot. N. SK552/2012 D.lsg. 116/1992 and N. 722/2016-PR D.lsg. 26/2016). Mice were housed in the San Raffaele Hospital animal facility, maintained in 12/12 h light/dark cycle with access ad libitum to food and water. Following 1 week of acclimation, one group of 2 months old mice (adult) were processed according to the experimental tasks described below, whereas another group of mice was maintained until reaching the age of 17–18 months (aged) and were further processed. A total number of 76 mice were included in the study. For each experimental task, adult and aged mice of both sexes were randomly assigned to LPS or vehicle (saline) treatment as reported in Table 1 and in the diagram below (Figure 1). Animals were intraperitoneally injected with 0.63 mg/kg of LPS (Lipopolysaccharides of Escherichia coli, serotype 055:B5; Sigma-Aldrich) freshly dissolved in sterile saline prior to injection, or vehicle (2 mg/5 ml saline), and neuro-inflammatory responses were evaluated 6 h later (Biesmans et al., 2013).

Table 1. Age, body weight, sample size and treatment dosage of each experimental group.

Experimental group	Age	Body weight (g)	[^{18}F]-VC701 binding (*n*)	RT-PCR (*n*)	IHC (*n*)	Dosage (LPS/vehicle)
Adult males + LPS	2 months	26.9 ± 2.7	8	5/8	3	0.63 mg/kg
Adult males vehicle	2 months	26.1 ± 1.6	8	5/8	3	50 µl saline
Adult females + LPS	2 months	18.3 ± 3.6	8	4/8	3	0.63 mg/kg
Adult females vehicle	2 months	19.6 ± 1.1	8	5/8	3	30 µl saline
Aged males + LPS	17/18 months	35.5 ± 2.5	8	5/8	3	0.63 mg/kg
Aged male vehicle	17/18 months	36.4 ± 3.3	8	5/8	3	50 µl saline
Aged females + LPS	17/18 months	31.1 ± 4.2	8	5/8	3	0.63 mg/kg
Aged females vehicle	17/18 months	34.2 ± 6.6	8	5/8	3	50 µl saline

FIGURE 1

Figure 1. Schematic diagram of the experimental design and readouts.

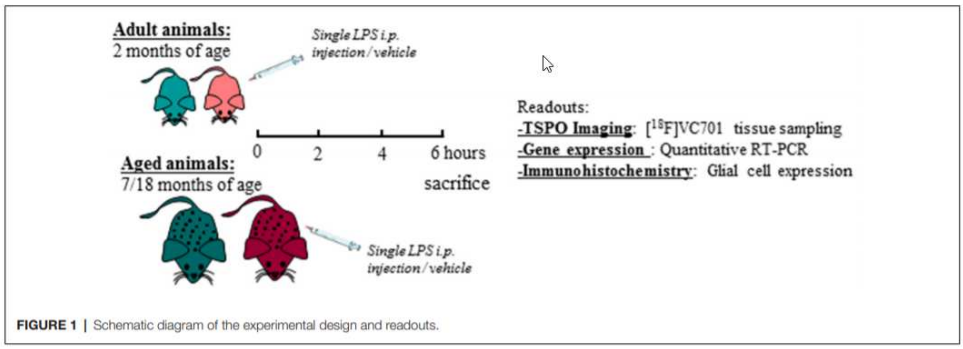

FIGURE 1 | Schematic diagram of the experimental design and readouts.

Ex vivo Binding of [18F]-VC701 to TSPO Protein

There were eight mice per group and treatment was dedicated to ex vivo imaging studies. Microglia activation was evaluated using the [18F]-labeled VC701, a TSPO radio ligand developed in our facility (Di Grigoli et al., 2015; Belloli et al., 2018). This radiopharmaceutical binds to 18 kDa TSPO. In this study, we used the novel TSPO tracer [18F]-VC701 that allows to obtain adequate signal to noise ratios for the measurements of TSPO binding in mouse brain (Belloli et al., 2018). Binding of [18F]-VC701 was evaluated ex vivo at 6 h after the intraperitoneal administration of LPS or saline. Animals were injected with 4.55 ± 1.85 MBq (specific activity: 3.17 ± 1.4 Ci/µMole) of [18F]-VC701 through the tail vein and sacrificed under light anesthesia 120 min later. Blood samples were collected and counted in a gamma counter (LKB Compugamma CS1282, Wallac). Brains were rapidly removed and divided into two hemispheres. Cortex, hippocampus and cerebellum were collected and placed in pre-weighed tubes. Radioactivity concentration was counted while the tissue used for RT-PCR was stored at −80°C for transcript measurement. After counting, tissue and blood radioactivity concentration were corrected for the half-life of [18F] (108.9 min) and expressed as percentage of

the injected dose per gram of tissue (%I.D./g). To avoid a potential confounding effect due to differences in blood circulating levels, binding data were also normalized to blood uptake value.

RNA Extraction and RT-qPCR Analysis

RT-PCR analysis was performed on five out of the eight animals/group that was used for the [18F]-VC701 experiments. One mouse in the adult female LPS-treated group was excluded due to insufficient mRNA availability. The brain areas (cortex, striatum, hippocampus and cerebellum) were dissected, homogenized in the supplied homogenization buffer and stored at −80°C. Total RNA was extracted with the Promega Maxwell® 16 LEV simplyRNA kit using the Maxwell® 16 Instrument (Promega). cDNA synthesis was performed using 250 ng of total RNA with the ThermoScript RT-PCR System (Invitrogen) and Random Primers (Promega) in a final volume of 20 µl according to the manufacturer's instructions. The cDNA from each sample was used to perform RT-qPCR using LightCycler 480 SYBR Green I Master Mix (Roche) on the LightCycler 480 Instrument (Roche). β-actin was used as housekeeping gene for sample normalization. All analyses were performed in triplicate. The 2−ΔΔCT method was used to calculate the relative changes in gene expression in LPS-treated relative to vehicle-treated mice. The two-way ANOVA following by Tukey post hoc test was used to evaluate statistical significance between LPS-treated groups while parametric unpaired Student's t-test were used to compare LPS-treated to control group. Genes and relative primer sets used are listed in Table 2.

Table 2. Genes and relative primer list used in gene expression analysis.

TABLE 2 | Genes and relative primer list used in gene expression analysis.

Name	Primer sequence (5′-3′)
β-actin F	5′-gactcctatgtgggtgacgagg-3′
β-actin R	5′ catggctggggtgttgaaggtc-3′
Trem2 F	5′-gcacctccaggaatcaagag-3′
Trem2 R	5′-gggtccagtgaggatctgaa-3′
Trem2L F	5′-tggtggtggtgttgacatttcttcc-3′
Trem2L R	5′atccagggtttagcatagttgctgc-3′
Tspo F	5′-tcagcggctaccaacct-3′
Tspo R	5′-caggattcaggcatggtgat-3′
Il-1β F	5′-gcccatcctctgtgactcat-3′
Il-1β R	5′-aggccacaggtattttgtcg-3′
Tnf-α F	5′-cctgtagcccacgtcgtag-3′
Tnf-α R	5′-gggagtagacaaggtacaaccc-3′
Il4 F	5′-tcaacccccagctagttgtc-3′
Il4 R	5′-tgttcttcgttgctgtgagg-3′
Arg1 F	5′-ttgggtggatgctcacactg-3′
Arg1 R	5′-gtacacgatgtctttggcaga-3′
IL-6 F	5′-agttgccttcttgggactga-3′
IL-6 R	5′-tccacgatttcccagagaac-3′

Immunohistochemistry (IHC)

Immunohistochemistry (IHC) and histopathologic analysis were performed in distinct adult and aged female mice (n = 3 per group and treatment). Mice were sacrificed 6 h after LPS or vehicle challenge and perfused with PBS followed by 4% paraformaldehyde (PFA). Brains were removed, post-fixed in PFA 4% for 24 h, cryo-protected overnight in 20% sucrose and 10 µm sections were cut on a cryostat for histological analysis in bright-field microscopy, slices were stained using standard protocols for hematoxylin and eosin (using Mayer's Hematoxylin, BioOptica #05-06002/L and Eosin, BioOptica #05-10002/L).

For IHC, slices were immuno-stained with polyclonal rabbit anti-Iba-1 antibody (Wako, #019-19741) and polyclonal rabbit anti-GFAP antibody (Novus Biologicals, #NB300-141). Any endogenous peroxidase activity was quenched by incubating the slices with 0.3% H2O2 in methanol for 10 min at RT. Both antibodies were used at a dilution of 1:1,000, incubated for 1 h at RT with EXPOSE rabbit specific HRP/DAB detection IHC kit (Abcam, #ab80437). DAB chromogen was than applied to each section for 5 min at RT and counterstained with Mayer's hematoxylin, dehydrated and mounted with Eukitt (BioOptica, #09-00100). Positive and negative controls were run simultaneously. Slides were acquired with Aperio AT2 digital scanner at a magnification of 40× (Leica Biosystems). Region of interest (ROI) were drowned manually on half hemisphere for cortex, on the entire hippocampus, and on a selected region of the cerebellum. Percentage of positive cells were calculated using Aperio eSlide Manager (Leica Biosystems). From the data obtained (weak, medium and strong positive intensity), weak positive was not included in the analysis as considered as background.

Statistical Analysis

Statistical evaluation of [18F]-VC701 tracer uptake was carried out using two-way ANOVA for Multiple Comparisons with a Tukey post hoc correction with gender, aging and treatment as covariates. Data representing radio ligand uptake in each LPS-treated and vehicle group were analyzed through parametric unpaired Student's t-test. For gene expression studies, data were normalized to housekeeping gene followed by a fold change evaluation comparing data to internal control group. Data derived from comparison of LPS-treated groups were statistically analyzed using two-way ANOVA for Multiple Comparisons with a Tukey post hoc correction, while for those reported on Supplementary Figures, data were statistically evaluated using parametric unpaired

Student's t-test. Immunohistochemical analyses were performed using two-way ANOVA for Multiple Comparison with Tukey post hoc correction.

Analyses were performed using the Prism V6.0 software (GraphPad Prism, San Diego, CA, USA). Statistical significance was accepted when *p < 0.05, **p < 0.01, and ***p < 0.001.

Results

Peripheral Exposure to LPS Influences Sex- and Age-Dependent Microglia Activation

TSPO expression in different brain areas of adult and aged untreated and LPS-treated male and female mice was evaluated by ex vivo binding of [18F]-VC701 to TSPO, 6 h after LPS/vehicle injection. LPS treatment induced a statistically significant increase ($p < 0.05$) of tracer's uptake in the cortex and cerebellum of aged males, and in cortex and hippocampus of aged females (Supplementary Figure S1). Higher uptake of [18F]-VC701 was observed in the cortex of aged vs. adult LPS-treated females (Figure 2). This age-dependent effect was not observed in males. The percentage of tracer's uptake in the cortex and hippocampal areas was significantly higher in LPS-treated aged females compared to age-matched vehicle (cortex 51.6%, $p \leq 0.017$; hippocampus 86.4% $p \leq 0.010$; cerebellum ns, 36.1%, data not shown). Tissue to blood ratio of tracer's uptake in LPS-treated females, expressed as % of injected dose per gram of tissue (%I.D./g), is shown in Table 3.

FIGURE 2

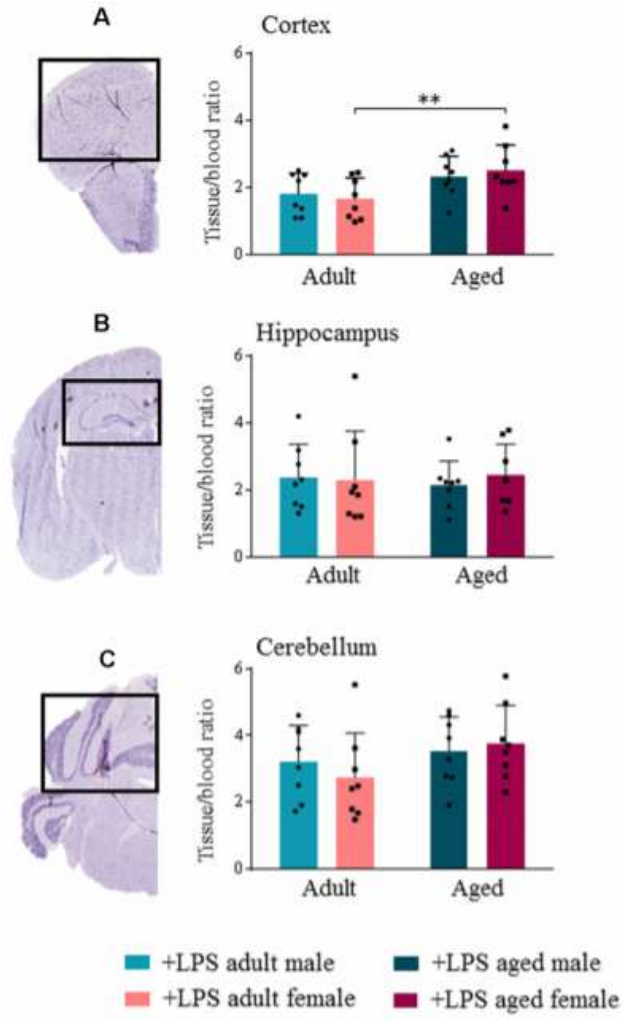

Figure 2. Translocator protein (TSPO) tracer uptake reveal microglial activation increased in aged female lipopolysaccharide (LPS)-treated animals. [18F]-VC701 brain tracer uptake in cortex (A); hippocampus (B) and cerebellum (C) on LPS-treated adult and aged male and female mice. Data were analyzed using two-way ANOVA analysis with Tukey post hoc and are expressed as percentage (%) of injected dose per gram of tissue to blood ratio, mean ± SD, eight mice per group; Mouse brain-stained slices (cortex, hippocampus and cerebellum) derived from immunohistochemistry (IHC) studies. *p < 0.05; **p < 0.01; ***p < 0.001.

Table 3. Tissue to blood [18F]-VC701 uptake ratio.

Brain Region	Tissue/blood ratio (%I.D./g; mean ± SD)	
	LPS-treated adult females	LPS-treated aged females
Cortex	1.6 ± 0.6	2.52 ± 0.7
Hippocampus	2.31 ± 1.4	2.46 ± 0.9
Cerebellum	2.75 ± 1.3	3.75 ± 1.1

Female Brain Shows a Higher Pro-inflammatory Response to LPS During Aging

In order to confirm that the higher [18F]-VC701 uptake was associated with a pro-inflammatory response of microglia, we measured the levels of IL-1β, TNF-α, IL-6, IL-4 and Arg-1 transcripts in LPS-treated and untreated mice. In all brain regions, peripheral LPS injection induced neuroinflammation irrespective of sex and age, as shown by significantly increased transcript levels of IL-1β, IL-6 and TNF-α (Supplementary Figures S2A–C, S3A–C). Arg-1 and IL-4 transcripts were negligibly expressed in both LPS-treated and untreated mice (data not shown).

In agreement with [18F]-VC701 uptake results, in female but not in male brain, age affected levels of the pro-inflammatory cytokines IL-1β, TNF-α and IL-6 in response to the LPS challenge. Aged females compared to adult females showed increased levels of IL-1β and IL-6 in all areas, which was statistically significant in the cortex for IL-1β, and in both cortex and cerebellum for IL-6 (Figures 3A,C). No age-dependent effects on IL-1β, TNF-α and IL-6 transcript levels were detected in males. Increased IL-1β transcript levels in the cortex and IL-6 in the cerebellum were detected in aged females compared to aged males (Figures 3A,C). TNF-α transcript levels were increased in the cortex and hippocampus of aged compared to adult females, although the differences were not statistically significant (Figure 3B).

FIGURE 3

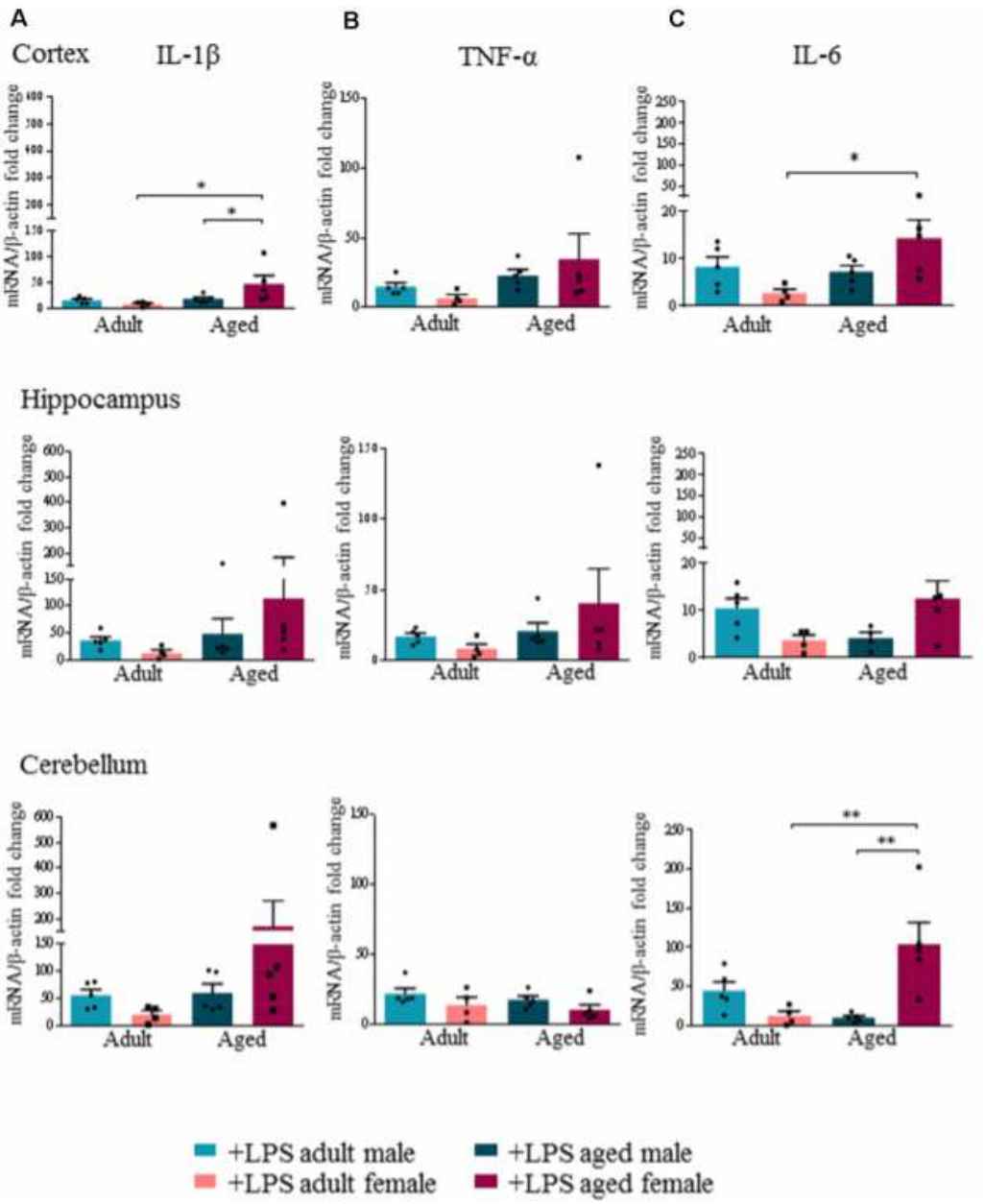

Figure 3. Increased expression levels of pro-inflammatory cytokines in aged LPS treated mice. Gene expression analysis of IL-1β (A), TNF-α (B) and IL-6 (C) by RT-qPCR in cortex, hippocampus and cerebellum of all LPS-treated animals. All the values were normalized to mouse β-actin and expressed as fold change referred to internal control group. Bars represent the average of triplicate measurements and error bars represent ± SEM, five animals per group. Statistical analysis was performed using two-way ANOVA following by Tukey post hoc test of the relative mRNA expression of LPS-treated mice previously normalized to internal control group. *$p < 0.05$; **$p < 0.01$; ***$p < 0.001$.

Sex and Age Effect on Transcript Levels of Markers of Microglia Activation

Interestingly, we found an age- and sex-dependent effect on the expression of the neuro-inflammatory markers TREM2 and TREML2 after LPS administration. Our results showed that peripheral LPS injection induced a significant decrease of TREM2 transcript levels in all brain regions of adult males and females (Supplementary Figure S2D). Yet in aged males, LPS injection did not decrease TREM2 transcript levels, which were instead significantly decreased in all brain regions of aged females (Supplementary Figure S3D). When we specifically compared TREM2 transcript levels among LPS-treated mice, we found that they were significantly higher in aged males compared to aged females ($p < 0.0002$), while no differences were detected in adult mice of both sexes (Figure 4A).

FIGURE 4

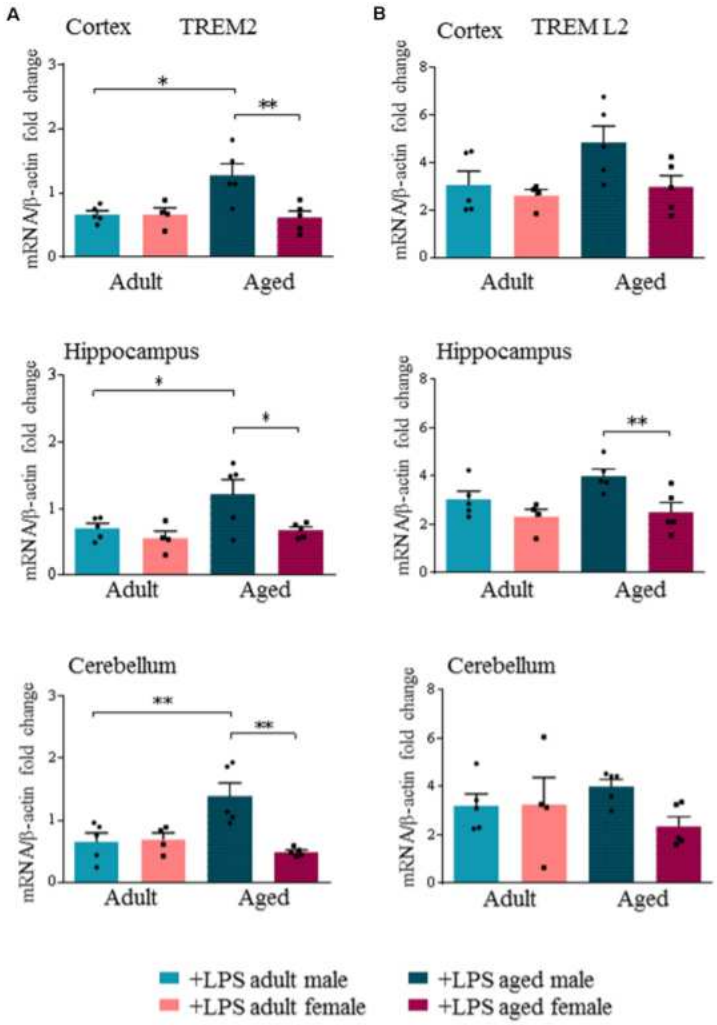

Figure 4. Triggering receptor expressed on myeloid cells like 2 (TREM2) is differentially expressed in aged LPS treated mice. Gene expression analysis of TREM2 (A), TREML2 (B), two immunomodulatory markers by RT-qPCR in cortex, hippocampus and cerebellum of all LPS-treated animals. All the values were normalized to mouse β-actin and expressed as fold change referred to internal control group. Bars represent the average of triplicate measurements and error bars represent ± SEM, five animals per group. Statistical analysis was performed using two-way ANOVA following by Tukey post hoc test of the relative mRNA expression of LPS-treated mice previously normalized to internal control group. *$p < 0.05$; **$p < 0.01$; ***$p < 0.001$.

TREML2 transcript levels were significantly increased in the hippocampus of aged males compared to aged females ($p < 0.01$), and in the cortex, although not reaching statistical significance (Figure 4B, Supplementary Figures S2E, S3E).

Microglia Activation and Astrogliosis in Aged Female Animals

As major differences in the neuro-inflammatory response to LPS were observed in females, we further evaluated glia activation in females by IHC. In all LPS-treated females, H&E staining showed no sign of neuronal loss or morphological changes in the three brain areas examined (cortex, cerebellum and hippocampus, data not shown). In LPS-treated aged females an increased percentage of Iba-1 positive cells were detected when compared to LPS-treated adult females, and vehicle-treated adult and aged females, which is indicative of a higher inflammatory status (Figure 5A, cortex). Microglia activation was suggested by cell morphology in the cerebral and cerebellar cortex of LPS-treated aged vs. LPS-treated adult females and vehicle-treated females (Figures 5A–C, cortex and cerebellum). In the hippocampus both LPS and vehicle-treated aged females showed a higher degree of Iba-1 immunoreactivity in comparison with adult females reaching statistical significance in vehicle-treated aged vs. vehicle-treated adult mice (Figure 5C, hippocampus).

FIGURE 5

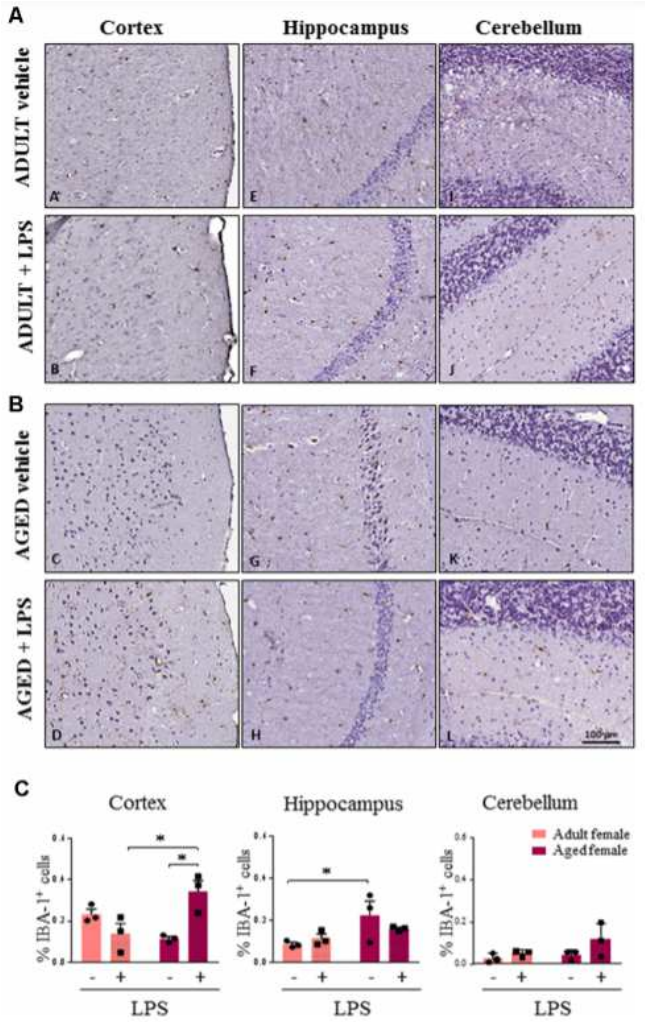

Figure 5. Increased IBA1 immunoreactivity and changes in glia morphology in brain areas of LPS-treated aged vs. LPS-treated adult females. (A) Immunostaining of Iba-1+ cells in cerebral cortex, hippocampus and cerebellum from one representative vehicle and one representative LPS-treated adult female mouse. (B) Immunostaining of Iba-1+ cells in cerebral cortex, hippocampus and cerebellum from one representative vehicle and one representative LPS-treated aged female mouse. (C) Quantification of the percentage of Iba-1+ cells in cortex, hippocampus and cerebellum of all female groups used in the study. Data are expressed as mean ± SEM of selected region of interest (ROI) performed on three animals per group, scale bar = 100 µm. *p < 0.05; **p < 0.01; ***p < 0.001.

Astroglial cells showed an increase in GFAP immunoreactivity in aged compared to adult females (Figures 6A,B). This observation was consistent in the cortex, cerebellum and hippocampus of aged females where astrocytes also showed hyperplasia of cytoplasm and of cellular processes resembling an activated phenotype. Quantification analysis showed a significant higher percentage of GFAP positive cells in cortex and hippocampus of aged compared to adult females. A similar trend

was observed also in the cerebellar region (Figure 6C). Furthermore, in the sections where olfactory bulb was present, a general increase in immunoreactivity for both Iba-1 and GFAP was observed, again more evident in LPS-treated aged females for Iba-1 and in vehicle and LPS-treated aged females for GFAP (data not shown).

FIGURE 6

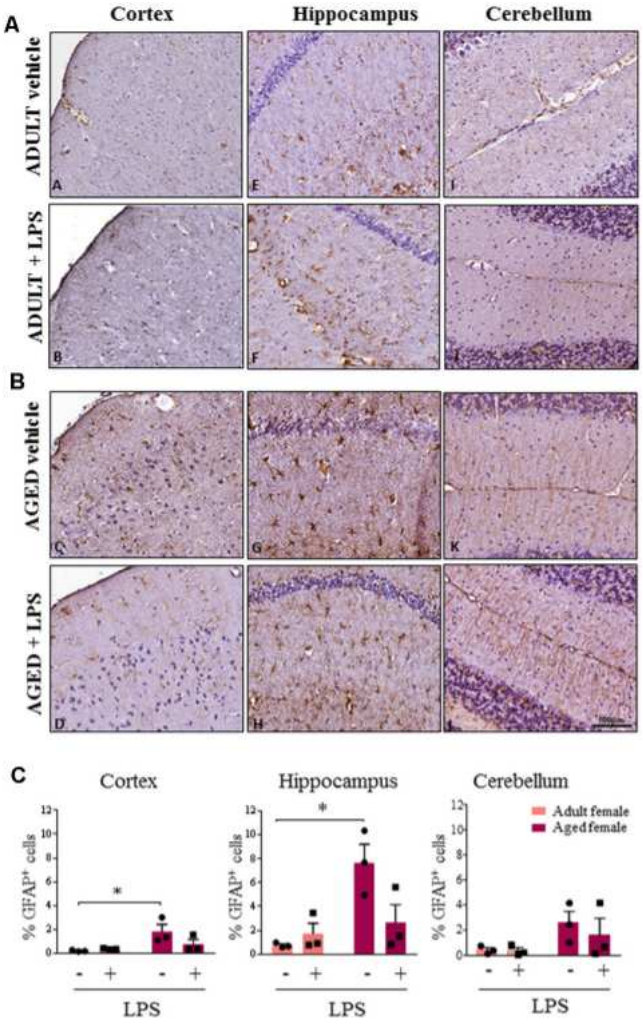

Figure 6. Increased astrocytosis and changes in glia morphology in brain areas of LPS-treated and vehicle-treated aged females. (A) Immunostaining of GFAP+ cell in cerebral cortex, hippocampus and cerebellum from one representative vehicle and one representative LPS-treated adult female mouse. (B) Immunostaining of GFAP+ astrocyte cells in cerebral cortex, hippocampus and cerebellum from one representative vehicle and one representative LPS-treated aged female mouse. (C) Quantification of percentage of GFAP+ cells in cortex, hippocampus and cerebellum of all female groups used in the study. Data are expressed as mean ± SEM of selected ROI performed on three animals per group, scale bar = 100 µm. *p < 0.05; ** p < 0.01; ***p < 0.001.

Discussion

In this study, we demonstrate for the first time that both age and sex influence an early neuro-inflammatory response after an acute mild peripheral LPS challenge in mice. In comparison to control conditions, LPS-treated aged male and female mice showed an increase [18F]-VC701 binding indicative of higher expression of TSPO. A prominent effect was observed in LPS-treated aged compared to adult females. [18F]-VC701 is a structural analog of PK11195, which targets 18 kDa TSPO (Di Grigoli et al., 2015). TSPO's main role is to transport cholesterol across the outer mitochondrial membrane. While TSPO is negligibly expressed in the normal brain parenchyma, its expression increases upon microglia activation and macrophage infiltration (Betlazar et al., 2018). Thus, TSPO up-regulation has been mainly associated with a pro-inflammatory status of microglia (Bonsack et al., 2016). PET-TSPO has been successfully applied to image the neuro-inflammatory reaction to LPS administration in the brain of human subjects, showing an increased binding of the TSPO radiotracer [11C]-PBR28 in all brain regions (Sandiego et al., 2015). Co-localization of TSPO with CD206-positive alternatively activated microglia has also been reported (Liu et al., 2015). Our results, although obtained from analysis of whole tissue are in agreement with transcriptomic data of purified microglia (Villa et al., 2018). Villa et al. (2018) demonstrated that microglia cells were sexually differentiated in the adult brain, as male mice carried a phenotype more poised to inflammatory reactions than female microglia. Moreover, in females, microglia displayed neuroprotective features in an acute pre-clinical model of ischemic insult (Villa et al., 2018). Gene sexual dimorphism has also been reported in humans by Berchtold et al. (2008). This study shows that males display a greater number of gene expression changes (mainly downregulation) during the transition to the sixth and seventh decade of life while females show more prominent gene expression changes later in life, during the eighth and ninth decade of life. Moreover, increased immune activation was greater in the female brain, as shown by a higher percentage of up-regulated genes involved in the immune response and inflammation (34% in males and 50% in females; Berchtold et al., 2008).

To better understand the nature of the microglia response, we evaluated the effect of the peripheral LPS challenge on transcription of a few inflammatory mediators: IL-1β, TNF-α, IL-6, Arg1 and IL-4. We showed that LPS induced a pro-inflammatory reaction in the brain of male and female mice as indicated by the up-regulation of IL-1β, TNF-α and IL-6 gene expression. However, in agreement

with [18F]-VC701 studies, the effect of LPS on pro-inflammatory cytokine transcript levels was significantly increased in aged compared to adult females, as well as in aged females compared to aged males.

As a major age effect was observed in females, we further analyzed microglia and astrocyte status by IHC in all brain regions of adult and aged females. In agreement with TSPO expression and pro-inflammatory cytokine transcript levels, we found an increased expression of microglia and astrocyte markers in LPS-treated and vehicle-treated aged compared to adult females, with some regional differences. Increased Iba-1 expression was present particularly in the cerebral cortex of LPS-treated aged animals, whereas GFAP immunoreactivity was higher in aged females in all the cerebral areas examined, regardless of LPS administration. Finally, the higher Iba-1 and GFAP signals detected in aged females was associated with a different cellular morphology. Altogether, our results highlight the acute onset of a higher neuro-inflammatory response in aged females. A similar response was also reported in female 3xTg-AD mice, where neuroinflammation was associated with progressive cognitive decline that increased as a function of age (Belfiore et al., 2019).

Microglia, as the primary source of pro-inflammatory cytokines, are pivotal mediators of neuroinflammation (Colonna and Butovsky, 2017). The amplitude and duration of the context-dependent activation of microglia are regulated by many pattern-recognition receptors, and immune receptors that deliver either activating or inhibitory signals. TREM2 and TREML2 are two microglia/monocyte regulators with potential and opposite roles in neurodegenerative disorders such as AD (Zsido et al., 2017). We show that acute peripheral administration of LPS induced an opposite modulation of TREM2 and TREML2 transcripts. In all groups analyzed, except aged male mice, we showed that LPS reduced TREM2 while increasing TREML2 transcript levels. TREM2 regulates critical functions of microglia including inhibition of pro-inflammatory responses and stimulation of phagocytosis of apoptotic neurons (Piccio et al., 2008). TREM2-transduced myeloid precursors mediate nervous tissue debris clearance and facilitate recovery in an animal model of multiple sclerosis (Takahashi et al., 2005, 2007). Moreover, TREM2 binds poly-anionic ligands including LPS (Wang et al., 2015). Previous findings showed that LPS stimulation suppressed TREM2 levels in microglia, at the same time inducing pro-inflammatory cytokines secretion (Zheng et al., 2016). Peripheral LPS challenge (at a similar dose to that used in our study) induced up-regulation of TREML2 and down-regulation of TREM2 levels in microglia, and increase of pro-inflammatory

cytokines (Zheng et al., 2016; Zhang et al., 2017). In particular, reduction of TREM2 was associated with a decreased microglia proliferation, an effect that was absent when TREML2 was knocked down.

During aging, microglia undergo cellular senescence losing regenerative and trophic functions (Mecca et al., 2018). According to Colonna and Wang (2016) TREM2 protects the aged brain from insults. Indeed, carrying a loss of function mutations in the TREM2 gene represents an important risk factor for dementia (Gao et al., 2017). In vitro experiments demonstrated that, silencing of TREM2 exacerbated LPS-induced pro-inflammatory response in BV2 microglia (Zhong et al., 2015), In contrast, overexpression of TREM2 lowered the pro-inflammatory response, thus supporting the hypothesis that TREM2 expression modulates the acute and transient pro-inflammatory responses induced by LPS (Zhong et al., 2015). Thus, the higher TREM2 expression observed in aged male mice might represent a strategy to counterbalance the pro-inflammatory milieu of aging, partially sustained by activation of signaling pathways mediated by TREML2, which likely activates apoptosis and modulates microglial functions (de Freitas et al., 2012; Zheng et al., 2016).

In aged female brains, we observed up-regulation of reactive GFAP-positive astroglia in all the regions examined independently from LPS administration. Although GFAP expression is limited to only a fraction of astrocytes with a substantial regional heterogeneity, its expression has been associated with reactive astrogliosis (Verkhratsky and Nedergaard, 2018). During aging, high levels of GFAP expression were identified as “mild to moderate astrogliosis” while the presence of cellular hypertrophy in addition to GFAP increase appears to be associated to “severe diffuse astrogliosis” (Cohen and Torres, 2019). Matias et al. (2019) reported that the astrocyte response to brain aging showed intra-regional heterogeneity (Matias et al., 2019): astrocytes in the hippocampal region presented an age-dependent hypertrophy, similar to the astrocyte morphology detected in our study, which may contribute to synapse loss and neuroinflammation.

Interestingly, increased levels of neuro-inflammatory markers, including GFAP, are present in the brain of AD patients. Recently Barroeta-Espar et al. (2019) demonstrated reduced levels of GFAP and a different pattern of cytokines expression in subjects resilient to AD pathology. This selected population of aged subjects harbour plaque and tangle loads that in some cases are equivalent to those found in AD, although in absence of the typical patterns of neuronal/synaptic loss seen in the pathology. These findings suggest that down-regulation of neuroinflammation is one of the

differential traits of human brain resilience to AD pathology, a mechanism that might be less efficient in female brain. Implications of our findings may impact the development of clinical phenotypes such as delirium and dementia. Delirium is one of the most common neuropsychiatric conditions among older people, which is known to develop as an acute consequence of peripheral infection or inflammation originating outside the brain (Cerejeira et al., 2010; Franceschi and Campisi, 2014; Bu et al., 2015; Morandi et al., 2018). The higher the level of frailty, the higher the likelihood of developing delirium in reaction to an inflammatory stimulus (Bellelli et al., 2017; Persico et al., 2018). Neuroinflammation has also been recognized as a pathophysiological mechanism of dementia, especially AD, again with frailty as a modulating factor of the disease clinical expression (Tao et al., 2018; Wallace et al., 2019).

Future studies should explore chronic neuroinflammation and morphological-functional changes in glial cell upon repetitive systemic insult or an acute severe neural event. As the cortex represents in our study the most important region influenced by sex and age, we will further explore gene modulation of specific pathways trough transcriptomic analysis of cortical glia in adult and aged female and male mice. Furthermore, specific behavioural phenotypes such as attention and active inhibitory processes associated with cognitive frailty will be investigated.

Finally, it would be appropriate to ascertain if age- and sex-specific patterns of neuroinflammation could be identifiable in humans too, and to clarify the mechanisms involved in such differences.

Conclusion

In conclusion, the results of this study show that the neuro-inflammatory response of a mouse's brain to an acute peripheral LPS challenge is sex- and age-dependent and is likely to involve multiple cellular and molecular regulators of neuronal functions. Our results might set the basis for further studies aimed at characterizing sex-related targets involved in the modulation of the neuro-inflammatory response in aging. This knowledge could be relevant for the treatment of conditions such as delirium and dementia.

Data Availability Statement

The raw data supporting the conclusions of this manuscript will be made available by the authors, without undue reservation, to any qualified researcher.

Ethics Statement

The animal study was approved by our Institutional Guidelines for the Care and Use of Experimental Animals (IACUC) and the National Law for animals used in research (Prot. N. SK552/2012 D.lsg. 116/1992 and N. 722/2016-PR D.lsg. 26/2016).

Author Contributions

VMu: data generation, collection, analysis and interpretation, and manuscript drafting. SB and GG: data generation and collection. MP: support in qRT-PCR data generation and analysis. EB, VR-M, and PM: support in IHC data analysis and interpretation. AC, VMa, and CM: production and validation of the tracer [18F]-VC701. GB: critical review of the manuscript. PP-B and RM: study conception and design, manuscript preparation. All the authors approved the final version of the manuscript.

Funding

This work was supported by grants from: The Italian Ministry of Education, University and Research (Ministero dell'Istruzione, dell'Universitá e della Ricerca; MIUR) Project "Identification, validation and commercial development of new diagnostic and prognostic biomarkers for complex trait diseases (IVASCOMAR, Prot. CTN01 00177 165430)".

Conflict of Interest

The authors declare that the research was conducted in the absence of any commercial or financial relationships that could be construed as a potential conflict of interest.

Acknowledgments

We thank Pasquale Simonelli for technical support with animal preparation and ex vivo binding experiments.

Supplementary Material

The Supplementary Material for this article can be found online at: https://www.frontiersin.org/articles/10.3389/fnagi.2019.00299/full#supplementary-material.

References

1. Amateau, S. K., and McCarthy, M. M. (2002). Sexual differentiation of astrocyte morphology in the developing rat preoptic area. J. Neuroendocrinol. 14, 904–910. doi: 10.1046/j.1365-2826.2002.00858.x PubMed Abstract | CrossRef Full Text | Google Scholar
2. Azad, N. A., Al Bugami, M., and Loy-English, I. (2007). Gender differences in dementia risk factors. Gend. Med. 4, 120–129. doi: 10.1016/s1550-8579(07)80026-x PubMed Abstract | CrossRef Full Text | Google Scholar
3. Barroeta-Espar, I., Weinstock, L. D., Perez-Nievas, B. G., Meltzer, A. C., Chong, M. S. T., Amaral, A. C., et al. (2019). Distinct cytokine profiles in human brains resilient to Alzheimer's pathology. Neurobiol. Dis. 121, 327–337. doi: 10.1016/j.nbd.2018.10.009 PubMed Abstract | CrossRef Full Text | Google Scholar
4. Belfiore, R., Rodin, A., Ferreira, E., Velazquez, R., Branca, C., Caccamo, A., et al. (2019). Temporal and regional progression of Alzheimer's disease-like pathology in 3xTg-AD mice. Aging Cell 18:e12873. doi: 10.1111/acel.12873 PubMed Abstract | CrossRef Full Text | Google Scholar
5. Bellelli, G., Moresco, R., Panina-Bordignon, P., Arosio, B., Gelfi, C., Morandi, A., et al. (2017). Is delirium the cognitive harbinger of frailty in older adults? A review about the existing evidence. Front. Med. 4:188. doi: 10.3389/fmed.2017.00188 PubMed Abstract | CrossRef Full Text | Google Scholar
6. Belloli, S., Zanotti, L., Murtaj, V., Mazzon, C., Di Grigoli, G., Monterisi, C., et al. (2018). 18F-VC701-PET and MRI in the in vivo neuroinflammation assessment of a mouse model of multiple sclerosis. J. Neuroinflammation 15:33. doi: 10.1186/s12974-017-1044-x PubMed Abstract | CrossRef Full Text | Google Scholar
7. Benitez, B. A., Jin, S. C., Guerreiro, R., Graham, R., Lord, J., Harold, D., et al. (2014). Missense variant in TREML2 protects against Alzheimer's disease. Neurobiol. Aging 35, 1510.e1519–1526.e1519. doi: 10.1016/j.neurobiolaging.2013.12.010 PubMed Abstract | CrossRef Full Text | Google Scholar
8. Berchtold, N. C., Cribbs, D. H., Coleman, P. D., Rogers, J., Head, E., Kim, R., et al. (2008). Gene expression changes in the course of normal brain aging are sexually dimorphic. Proc. Natl. Acad. Sci. U S A 105, 15605–15610. doi: 10.1073/pnas.0806883105 PubMed Abstract | CrossRef Full Text | Google Scholar
9. Besedovsky, H. O., and Rey, A. (2008). "Brain cytokines as integrators of the immune-neuroendocrine network," in Handbook of Neurochemistry and Molecular Neurobiology, eds A. Lajtha, A. Galoyan and H. O. Besedovsky (Boston, MA: Springer), 3–17. Google Scholar
10. Betlazar, C., Harrison-Brown, M., Middleton, R. J., Banati, R., and Liu, G. J. (2018). Cellular sources and regional variations in the expression of the neuroinflammatory marker translocator protein (TSPO) in the normal brain. Int. J. Mol. Sci. 19:E2707. doi: 10.3390/ijms19092707 PubMed Abstract | CrossRef Full Text | Google Scholar
11. Bhattacharjee, S., Zhao, Y., and Lukiw, W. J. (2014). Deficits in the miRNA-34a-regulated endogenous TREM2 phagocytosis sensor-receptor in Alzheimer's disease (AD); an update. Front. Aging Neurosci. 6:116. doi: 10.3389/fnagi.2014.00116 PubMed Abstract | CrossRef Full Text | Google Scholar
12. Biesmans, S., Meert, T. F., Bouwknecht, J. A., Acton, P. D., Davoodi, N., De Haes, P., et al. (2013). Systemic immune activation leads to neuroinflammation and sickness behavior in mice. Mediators Inflamm. 2013:271359. doi: 10.1155/2013/271359 PubMed Abstract | CrossRef Full Text | Google Scholar

13. Bonsack, F. T., Alleyne, C. H. Jr., and Sukumari-Ramesh, S. (2016). Augmented expression of TSPO after intracerebral hemorrhage: a role in inflammation? J. Neuroinflammation 13:151. doi: 10.1186/s12974-016-0619-2 PubMed Abstract | CrossRef Full Text | Google Scholar
14. Bouman, A., Heineman, M. J., and Faas, M. M. (2005). Sex hormones and the immune response in humans. Hum. Reprod. Update 11, 411–423. doi: 10.1093/humupd/dmi008 PubMed Abstract | CrossRef Full Text | Google Scholar
15. Bu, X. L., Yao, X. Q., Jiao, S. S., Zeng, F., Liu, Y. H., Xiang, Y., et al. (2015). A study on the association between infectious burden and Alzheimer's disease. Eur. J. Neurol. 22, 1519–1525. doi: 10.1111/ene.12477 PubMed Abstract | CrossRef Full Text | Google Scholar
16. Cerejeira, J., Firmino, H., Vaz-Serra, A., and Mukaetova-Ladinska, E. B. (2010). The neuroinflammatory hypothesis of delirium. Acta Neuropathol. 119, 737–754. doi: 10.1007/s00401-010-0674-1 PubMed Abstract | CrossRef Full Text | Google Scholar
17. Cohen, J., and Torres, C. (2019). Astrocyte senescence: evidence and significance. Aging Cell 18:e12937. doi: 10.1111/acel.12937 PubMed Abstract | CrossRef Full Text | Google Scholar
18. Colonna, M., and Butovsky, O. (2017). Microglia function in the central nervous system during health and neurodegeneration. Annu. Rev. Immunol. 35, 441–468. doi: 10.1146/annurev-immunol-051116-052358 PubMed Abstract | CrossRef Full Text | Google Scholar
19. Colonna, M., and Wang, Y. (2016). TREM2 variants: new keys to decipher Alzheimer disease pathogenesis. Nat. Rev. Neurosci. 17, 201–207. doi: 10.1038/nrn.2016.7 PubMed Abstract | CrossRef Full Text | Google Scholar
20. Costantini, E., D'Angelo, C., and Reale, M. (2018). The role of immunosenescence in neurodegenerative diseases. Mediators Inflamm. 2018:6039171. doi: 10.1155/2018/6039171 PubMed Abstract | CrossRef Full Text | Google Scholar
21. Cunningham, C., and Maclullich, A. M. (2013). At the extreme end of the psychoneuroimmunological spectrum: delirium as a maladaptive sickness behaviour response. Brain Behav. Immun. 28, 1–13. doi: 10.1016/j.bbi.2012.07.012 PubMed Abstract | CrossRef Full Text | Google Scholar
22. de Freitas, A., Banerjee, S., Xie, N., Cui, H. C., Davis, K. I., Friggeri, A., et al. (2012). Identification of TLT2 as an engulfment receptor for apoptotic cells. J. Immunol. 188, 6381–6388. doi: 10.4049/jimmunol.1200020 PubMed Abstract | CrossRef Full Text | Google Scholar
23. Di Grigoli, G., Monterisi, C., Belloli, S., Masiello, V., Politi, L. S., Valenti, S., et al. (2015). Radiosynthesis and preliminary biological evaluation of [18F]VC701, a radioligand for translocator protein. Mol. Imaging 14:6. doi: 10.2310/7290.2015.00007 PubMed Abstract | CrossRef Full Text | Google Scholar
24. Franceschi, C., and Campisi, J. (2014). Chronic inflammation (inflammaging) and its potential contribution to age-associated diseases. J. Gerontol. A Biol. Sci. Med. Sci. 69, S4–S9. doi: 10.1093/gerona/glu057 PubMed Abstract | CrossRef Full Text | Google Scholar

25. Gao, L., Jiang, T., Yao, X. Y., Yu, L., Yang, X. L., and Li, Y. S. (2017). TREM2 and the progression of Alzheimer's disease. Curr. Neurovasc. Res. 14, 177–183. doi: 10.2174/1567202614666170404165201 PubMed Abstract | CrossRef Full Text | Google Scholar
26. Godbout, J. P., and Johnson, R. W. (2006). Age and neuroinflammation: a lifetime of psychoneuroimmune consequences. Neurol. Clin. 24, 521–538. doi: 10.1016/j.ncl.2006.03.010 PubMed Abstract | CrossRef Full Text | Google Scholar
27. Hanamsagar, R., Alter, M. D., Block, C. S., Sullivan, H., Bolton, J. L., and Bilbo, S. D. (2017). Generation of a microglial developmental index in mice and in humans reveals a sex difference in maturation and immune reactivity. Glia 65, 1504–1520. doi: 10.1002/glia.23176 PubMed Abstract | CrossRef Full Text | Google Scholar
28. Holtman, I. R., Raj, D. D., Miller, J. A., Schaafsma, W., Yin, Z., Brouwer, N., et al. (2015). Induction of a common microglia gene expression signature by aging and neurodegenerative conditions: a co-expression meta-analysis. Acta Neuropathol. Commun. 3:31. doi: 10.1186/s40478-015-0203-5 PubMed Abstract | CrossRef Full Text | Google Scholar
29. Hoogland, I. C., Houbolt, C., van Westerloo, D. J., van Gool, W. A., and van de Beek, D. (2015). Systemic inflammation and microglial activation: systematic review of animal experiments. J. Neuroinflammation 12:114. doi: 10.1186/s12974-015-0332-6 PubMed Abstract | CrossRef Full Text | Google Scholar
30. Inouye, S. K., Westendorp, R. G., and Saczynski, J. S. (2014). Delirium in elderly people. Lancet 383, 911–922. doi: 10.1016/S0140-6736(13)60688-1 PubMed Abstract | CrossRef Full Text | Google Scholar
31. Liu, B., Le, K. X., Park, M. A., Wang, S., Belanger, A. P., Dubey, S., et al. (2015). In vivo detection of age- and disease-related increases in neuroinflammation by 18F-GE180 TSPO MicroPET imaging in wild-type and Alzheimer's transgenic mice. J. Neurosci. 35, 15716–15730. doi: 10.1523/jneurosci.0996-15.2015 PubMed Abstract | CrossRef Full Text | Google Scholar
32. Liu, G. J., Middleton, R. J., Hatty, C. R., Kam, W. W. Y., Chan, R., Pham, T., et al. (2014). The 18 kDa translocator protein, microglia and neuroinflammation. Brain Pathol. 24, 631–653. doi: 10.1111/bpa.12196 PubMed Abstract | CrossRef Full Text | Google Scholar
33. Maclullich, A. M., Ferguson, K. J., Miller, T., de Rooij, S. E., and Cunningham, C. (2008). Unravelling the pathophysiology of delirium: a focus on the role of aberrant stress responses. J. Psychosom. Res. 65, 229–238. doi: 10.1016/j.jpsychores.2008.05.019 PubMed Abstract | CrossRef Full Text | Google Scholar
34. Mangold, C. A., Wronowski, B., Du, M., Masser, D. R., Hadad, N., Bixler, G. V., et al. (2017). Sexually divergent induction of microglial-associated neuroinflammation with hippocampal aging. J. Neuroinflammation 14:141. doi: 10.1186/s12974-017-0920-8 PubMed Abstract | CrossRef Full Text | Google Scholar
35. Marriott, I., and Huet-Hudson, Y. M. (2006). Sexual dimorphism in innate immune responses to infectious organisms. Immunol. Res. 34, 177–192. doi: 10.1385/ir:34:3:177 PubMed Abstract | CrossRef Full Text | Google Scholar

36. Matias, I., Morgado, J., and Gomes, F. C. A. (2019). Astrocyte heterogeneity: impact to brain aging and disease. Front. Aging Neurosci. 11:59. doi: 10.3389/fnagi.2019.00059 PubMed Abstract | CrossRef Full Text | Google Scholar
37. McCarthy, M. M., Arnold, A. P., Ball, G. F., Blaustein, J. D., and De Vries, G. J. (2012). Sex differences in the brain: the not so inconvenient truth. J. Neurosci. 32, 2241–2247. doi: 10.1523/JNEUROSCI.5372-11.2012 PubMed Abstract | CrossRef Full Text | Google Scholar
38. Mecca, C., Giambanco, I., Donato, R., and Arcuri, C. (2018). Microglia and Aging: The Role of the TREM2-DAP12 and CX3CL1-CX3CR1 Axes. Int. J. Mol. Sci. 19:E318. doi: 10.3390/ijms19010318 PubMed Abstract | CrossRef Full Text | Google Scholar
39. Morandi, A., Di Santo, S. G., Zambon, A., Mazzone, A., Cherubini, A., Mossello, E., et al. (2018). Delirium, dementia, and in-hospital mortality: the results from the Italian Delirium Day 2016, a national multicenter study. J. Gerontol. A Biol. Sci. Med. Sci. 74, 910–916. doi: 10.1093/gerona/gly154 PubMed Abstract | CrossRef Full Text | Google Scholar
40. Mosconi, L., Berti, V., Quinn, C., McHugh, P., Petrongolo, G., Varsavsky, I., et al. (2017). Sex differences in Alzheimer risk: brain imaging of endocrine vs. chronologic aging. Neurology 89, 1382–1390. doi: 10.1212/WNL.0000000000004425 PubMed Abstract | CrossRef Full Text | Google Scholar
41. Norden, D. M., and Godbout, J. P. (2013). Review: microglia of the aged brain: primed to be activated and resistant to regulation. Neuropathol. Appl. Neurobiol. 39, 19–34. doi: 10.1111/j.1365-2990.2012.01306.x PubMed Abstract | CrossRef Full Text | Google Scholar
42. Perry, V. H. (2004). The influence of systemic inflammation on inflammation in the brain: implications for chronic neurodegenerative disease. Brain Behav. Immun. 18, 407–413. doi: 10.1016/j.bbi.2004.01.004 PubMed Abstract | CrossRef Full Text | Google Scholar
43. Persico, I., Cesari, M., Morandi, A., Haas, J., Mazzola, P., Zambon, A., et al. (2018). Frailty and delirium in older adults: a systematic review and meta-analysis of the literature. J. Am. Geriatr. Soc. 66, 2022–2030. doi: 10.1111/jgs.15503 PubMed Abstract | CrossRef Full Text | Google Scholar
44. Piccio, L., Buonsanti, C., Cella, M., Tassi, I., Schmidt, R. E., Fenoglio, C., et al. (2008). Identification of soluble TREM-2 in the cerebrospinal fluid and its association with multiple sclerosis and CNS inflammation. Brain 131, 3081–3091. doi: 10.1093/brain/awn217 PubMed Abstract | CrossRef Full Text | Google Scholar
45. Sandiego, C. M., Gallezot, J. D., Pittman, B., Nabulsi, N., Lim, K., Lin, S. F., et al. (2015). Imaging robust microglial activation after lipopolysaccharide administration in humans with PET. Proc. Natl. Acad. Sci. U S A 112, 12468–12473. doi: 10.1073/pnas.1511003112 PubMed Abstract | CrossRef Full Text | Google Scholar
46. Schreuder, L., Eggen, B. J., Biber, K., Schoemaker, R. G., Laman, J. D., and de Rooij, S. E. (2017). Pathophysiological and behavioral effects of systemic inflammation in aged and diseased rodents with relevance to delirium: a systematic review. Brain Behav. Immun. 62, 362–381. doi: 10.1016/j.bbi.2017.01.010 PubMed Abstract | CrossRef Full Text | Google Scholar

47. Takahashi, K., Prinz, M., Stagi, M., Chechneva, O., and Neumann, H. (2007). TREM2-transduced myeloid precursors mediate nervous tissue debris clearance and facilitate recovery in an animal model of multiple sclerosis. PLoS Med. 4:e124. doi: 10.1371/journal.pmed.0040124 PubMed Abstract | CrossRef Full Text | Google Scholar
48. Takahashi, K., Rochford, C. D., and Neumann, H. (2005). Clearance of apoptotic neurons without inflammation by microglial triggering receptor expressed on myeloid cells-2. J. Exp. Med. 201, 647–657. doi: 10.1084/jem.20041611 PubMed Abstract | CrossRef Full Text | Google Scholar
49. Tao, Q. S., Ang, T. F. A., DeCarli, C., Auerbach, S. H., Devine, S., Stein, T. D., et al. (2018). Association of chronic low-grade inflammation with risk of Alzheimer disease in ApoE4 carriers. JAMA Netw. Open 1:e183597. doi: 10.1001/jamanetworkopen.2018.3597 PubMed Abstract | CrossRef Full Text | Google Scholar
50. Teeling, J. L., and Perry, V. H. (2009). Systemic infection and inflammation in acute CNS injury and chronic neurodegeneration: underlying mechanisms. Neuroscience 158, 1062–1073. doi: 10.1016/j.neuroscience.2008.07.031 PubMed Abstract | CrossRef Full Text | Google Scholar
51. Thankam, F. G., Dilisio, M. F., Dougherty, K. A., Dietz, N. E., and Agrawal, D. K. (2016). Triggering receptor expressed on myeloid cells and 5'adenosine monophosphate-activated protein kinase in the inflammatory response: a potential therapeutic target. Expert Rev. Clin. Immunol. 12, 1239–1249. doi: 10.1080/1744666x.2016.1196138 PubMed Abstract | CrossRef Full Text | Google Scholar
52. Thomas, K. A., King, R. G., Sestero, C. M., and Justement, L. B. (2016). TREM-like transcript 2 is stored in human neutrophil primary granules and is up-regulated in response to inflammatory mediators. J. Leukoc. Biol. 100, 177–184. doi: 10.1189/jlb.3ab1115-507r PubMed Abstract | CrossRef Full Text | Google Scholar
53. Verkhratsky, A., and Nedergaard, M. (2018). Physiology of astroglia. Physiol. Rev. 98, 239–389. doi: 10.1152/physrev.00042.2016 PubMed Abstract | CrossRef Full Text | Google Scholar
54. Villa, A., Gelosa, P., Castiglioni, L., Cimino, M., Rizzi, N., Pepe, G., et al. (2018). Sex-specific features of microglia from adult mice. Cell Rep. 23, 3501–3511. doi: 10.1016/j.celrep.2018.05.048 PubMed Abstract | CrossRef Full Text | Google Scholar
55. Vom Steeg, L. G., Vermillion, M. S., Hall, O. J., Alam, O., McFarland, R., Chen, H., et al. (2016). Age and testosterone mediate influenza pathogenesis in male mice. Am. J. Physiol. Lung Cell. Mol. Physiol. 311, L1234–L1244. doi: 10.1152/ajplung.00352.2016 PubMed Abstract | CrossRef Full Text | Google Scholar
56. Wallace, L. M. K., Theou, O., Godin, J., Andrew, M. K., Bennett, D. A., and Rockwood, K. (2019). Investigation of frailty as a moderator of the relationship between neuropathology and dementia in Alzheimer's disease: a cross-sectional analysis of data from the rush memory and aging project. Lancet Neurol. 18, 177–184. doi: 10.1016/s1474-4422(18)30371-5 PubMed Abstract | CrossRef Full Text | Google Scholar
57. Wang, Y., Cella, M., Mallinson, K., Ulrich, J. D., Young, K. L., Robinette, M. L., et al. (2015). TREM2 lipid sensing sustains the microglial response in an Alzheimer's disease model. Cell 160, 1061–1071. doi: 10.1016/j.cell.2015.01.049 PubMed Abstract | CrossRef Full Text | Google Scholar

58. Ycaza Herrera, A., and Mather, M. (2015). Actions and interactions of estradiol and glucocorticoids in cognition and the brain: implications for aging women. Neurosci. Biobehav. Rev. 55, 36–52. doi: 10.1016/j.neubiorev.2015.04.005 PubMed Abstract | CrossRef Full Text | Google Scholar
59. Zhang, X. B., Yan, F., Cui, J. Z., Wu, Y., Luan, H. F., Yin, M. M., et al. (2017). Triggering receptor expressed on myeloid cells 2 overexpression inhibits proinflammatory cytokines in lipopolysaccharide-stimulated microglia. Mediators Inflamm. 2017:9340610. doi: 10.1155/2017/9340610 PubMed Abstract | CrossRef Full Text | Google Scholar
60. Zhao, Y., and Lukiw, W. J. (2015). Microbiome-generated amyloid and potential impact on amyloidogenesis in Alzheimer's disease (AD). J. Nat. Sci. 1:e138. PubMed Abstract | Google Scholar
61. Zheng, H. H., Cheng, B. Y., Li, Y. F., Li, X., Chen, X. F., and Zhang, Y. W. (2018). TREM2 in Alzheimer's disease: microglial survival and energy metabolism. Front. Aging Neurosci. 10:395. doi: 10.3389/fnagi.2018.00395 PubMed Abstract | CrossRef Full Text | Google Scholar
62. Zheng, H., Liu, C. C., Atagi, Y., Chen, X. F., Jia, L., Yang, L., et al. (2016). Opposing roles of the triggering receptor expressed on myeloid cells 2 and triggering receptor expressed on myeloid cells-like transcript 2 in microglia activation. Neurobiol. Aging 42, 132–141. doi: 10.1016/j.neurobiolaging.2016.03.004 PubMed Abstract | CrossRef Full Text | Google Scholar
63. Zhong, L., Chen, X. F., Zhang, Z. L., Wang, Z., Shi, X. Z., Xu, K., et al. (2015). DAP12 stabilizes the C-terminal fragment of the triggering receptor expressed on myeloid cells-2 (TREM2) and protects against LPS-induced pro-inflammatory response. J. Biol. Chem. 290, 15866–15877. doi: 10.1074/jbc.m115.645986 PubMed Abstract | CrossRef Full Text | Google Scholar
64. Zsido, R. G., Villringer, A., and Sacher, J. (2017). Using positron emission tomography to investigate hormone-mediated neurochemical changes across the female lifespan: implications for depression. Int. Rev. Psychiatry 29, 580–596. doi: 10.1080/09540261.2017.1397607 PubMed Abstract | CrossRef Full Text | Google Scholar